UNIVERSIDADE DE LISBOA
FACULDADE DE CIÊNCIAS
DEPARTAMENTO DE BIOLOGIA ANIMAL

Metabolomic analysis of the reconstructed epidermis cultivation protocol as a tool to improve the skin barrier properties

Sandro Filipe Silva Evaristo

Mestrado em Biologia Humana e Ambiente

Dissertação orientada por:
Doutora Sofia Leite Souza
Professora Doutora Deodália Dias

2017

Metabolomic analysis of the reconstructed epidermis cultivation protocol as a tool to improve the skin barrier properties

Sandro Filipe Silva Evaristo

Mestrado em Biologia Humana e Ambiente

This work was held in the Biomolecular Diagnostic Laboratory from ITQB NOVA - Instituto de Tecnologia Química e Biológica António Xavier, an institute of the Universidade NOVA de Lisboa.

The bibliographic references were written according to the criteria of the Journal of Biomolecular NMR.

Dissertação orientada por:
Doutora Sofia Leite Souza[1] (ssouza@itqb.unl.pt)
Professora Doutora Deodália Dias[2] (dmdias@fc.ul.pt)

[1] Biomolecular Diagnostic Laboratory, Instituto de Tecnologia Química e Biológica (ITQB NOVA) da Universidade Nova de Lisboa, Av. da República, 2780-157 Oeiras, Portugal
[2] Departamento de Biologia Animal, Faculdade de Ciências da Universidade de Lisboa, 1749-016 Lisboa, Portugal

AGRADECIMENTOS

Ao ITQB NOVA - Instituto de Tecnologia Química e Biológica António Xavier, por me ter disponibilizado as suas instalações e o equipamento necessário para realizar o trabalho experimental aqui apresentado.

À Doutora Sofia Leite Souza, minha orientadora. Estou especialmente agradecido por todo o apoio e ajuda incondicional. Não menos importante, obrigado por toda a paciência demonstrada e todo o conhecimento que me transmitiu.

À Professora Doutora Deodália Dias, minha orientadora interna, por toda a disponibilidade e apoio prestados nestes dois anos.

Ao Professor Doutor Abel Oliva e o Laboratório de Diagnóstico Biomolecular por me terem aceite e por toda a disponibilidade demonstrada sempre que necessário. Aos meus colegas de laboratório, pela entreajuda, pelas conversas nas pausas para aliviar do trabalho e pela companhia.

Ao João Sá, por toda a disponibilidade demonstrada e ajuda incondicional. Obrigado por todo o conhecimento transmitido sobre as técnicas de NMR e HPLC, entre outras coisas, que vão com certeza ser muito úteis no futuro.

À Professora Doutora Isabel Rocha pela contribuição com o seu know-how sobre análise metabolómica.

Ao CERMAX pela disponibilização das instalações e de todo o equipamento necessário. Um agradecimento especial à Helena Matias por todo o apoio demonstrado durante o tempo que "vivi" na sala do NMR.

Ao Instituto Gulbenkian da Ciência e particularmente à Unidade de Histopatologia pela ajuda preciosa no processamento das nossas amostras de tecido para análise histológica.

Aos meus colegas da FCUL pelo bom ambiente da turma e por me terem aceite tão bem no seu grupo de Biólogos. Um agradecimento especial às novas amigas, Catarina, Mariana e Patrícia, pela companhia, os risos e a amizade. Mariana e Patrícia obrigado por toda a ajuda preciosa no nosso primeiro ano de Mestrado!

À minha família e aos meus amigos de longa data, pelo apoio e desculpem por toda a ausência!

Por último, mas não menos importante, um agradecimento muito especial aos meus pais e à minha irmã, por toda a ajuda e encorajamento, sem eles nada disto teria sido possível.

SUMÁRIO

Atualmente existe uma grande procura de cosméticos e de produtos tópicos para a pele. No entanto, estes produtos podem conter substâncias que podem passar a barreira da pele, por permeabilidade, e causar efeitos tóxicos para o organismo, sendo necessário testá-los sempre, antes que estejam disponíveis comercialmente. Até recentemente, os procedimentos de teste destes produtos mais utilizados eram realizados em animais ou com recurso a pele de cadáveres humanos. Contudo, ainda que a pele de cadáver humano permita replicar com alguma fidelidade a permeabilidade da pele *in vivo*, esta não pode ser estabelecida como um procedimento padrão uma vez que existe grande variabilidade de amostra para amostra, para além de as células não estarem funcionais. Por outro lado, a pele de animais é morfologicamente diferente da pele humana. Além das implicações éticas, existem limitações legais para a utilização de animais para testes, estando o uso destes estritamente limitado na União Europeia, bem como em alguns países como os Estados Unidos da América e o Japão. Surgiu assim, nas passadas últimas três décadas um grande interesse comercial em engenharia de pele humana *in vitro* de forma a desenvolver modelos de pele adequados para a avaliação da segurança dos produtos cosméticos[1,2].

Hoje em dia já existem vários modelos de pele disponíveis no mercado, mas ainda que apresentem semelhanças morfológicas e mesmo bioquímicas à pele humana nativa, a barreira da epiderme *in vitro* é mais permeável que a da pele nativa[3]. A camada apical da epiderme é o *stratum corneum*, constituído por corneócitos (queratinócitos que já passaram por um processo de diferenciação e se tornaram células mortas, achatadas e sem núcleo, revestindo esta camada superior da pele e conferindo força estrutural)[2]. A envolver estes queratinócitos está uma matriz lipídica responsável pela barreira da pele, e se esta não é suficiente ocorrerá uma maior permeabilidade de substâncias, aumentando a toxicidade avaliada nos testes de produtos cosméticos e dermatológicos[1]. Surge assim a necessidade de melhorar a barreira da pele cultivada, tendo sido objetivos deste projeto: reconstruir e avaliar epiderme humana *in vitro* em termos de histologia e permeabilidade, utilizando três fármacos com diferentes polaridades (cafeína, uma substância hidrofílica; hidrocortisona, semi-hidrofílica; e tamoxifeno, uma substância lipofílica); fazer uma análise metabolómica do sobrenadante da cultura celular com recurso a técnicas analíticas como a ressonância magnética nuclear de protão (RMN-^{1}H) e cromatografia líquida de alta eficiência (CLAE) para determinar as taxas de consumo de nutrientes e secreção de metabolitos excretados; desenhar um novo meio de cultura com base na informação obtida com a análise metabolómica e estudar o impacto deste novo processo de cultura na função de barreira da pele.

Os queratinócitos proliferaram em cultura em monocamada em *T-flasks* e o meio de cultura foi substituído regularmente até que as células cobrissem 70-80 % do estrato disponível (confluência). Nesta fase, os queratinócitos foram submetidos a tripsinização para se soltarem da superfície do *T-flask* e ressuspendidos para serem então colocados em insertos com filtro de policarbonato para reconstrução *in vitro* de epiderme (RHE) em interface ar-líquido. Ao fim de onze dias nestas condições obteve-se uma epiderme completamente estruturada[4] e procedeu-se a uma avaliação histológica utilizando coloração H&E e avaliação da sua função de barreira com três fármacos em células de Franz. Os resultados obtidos foram comparados com estudos anteriores existentes na bibliografia[5,6] caracterizando a função de barreira de pele humana nativa e dos modelos EpiDerm™ e EpiSkin®. Verificou-se que apesar da epiderme reconstruída cultivada no Laboratório de Diagnóstico Biomolecular de acordo com o protocolo publicado pelo laboratório liderado por Yves Poumay[4] ter uma estrutura bem-diferenciada, este tecido tem uma barreira mais deficiente do que os outros modelos.

Esperando que um estudo de metabolómica do sobrenadante dos queratinócitos cultivados *in vitro* permitisse uma melhor compreensão do que está a ocorrer aos metabolitos no meio de cultura, um novo conjunto de células foi semeado para se fazer uma recolha do sobrenadante ao longo de todo o processo de cultura e reconstrução de epiderme. Com recurso a RMN-^{1}H, uma técnica analítica muito promissora no campo da metabolómica devido à simplicidade na preparação das amostras e na capacidade de identificação de metabolitos de uma forma não enviesada, vários metabolitos foram detetados e quantificados no meio de cultura, incluindo alguns produzidos pelos queratinócitos como o lactato, formato, urocanato, entre outros. Contudo, esta técnica tem uma desvantagem em relação a outras que é a baixa sensibilidade e alguns constituintes do meio de cultura não puderam ser identificados, incluindo vitaminas, quer porque poderiam estar em baixas concentrações ou mesmo porque ficavam escondidas por sinais de maior intensidade emitidos por outros metabolitos. Foi o caso particular de três aminoácidos, a asparagina, aspartato e cisteína, que ficavam escondidos por um sinal muito amplo emitido pelo tampão HEPES. Como os queratinócitos durante a fase de diferenciação são caracterizados por uma grande produção de proteínas estruturais nos diferentes estratos da epiderme, é de vital importância que tenham sempre disponibilidade de aminoácidos[7]. Como tal, era necessário determinar as concentrações dos 3 aminoácidos que não foram quantificados por RMN, recorrendo-se a CLAE para o fazer. Por sua vez, os níveis de amónia no meio foram também analisados através de um kit comercial para o efeito. A determinação dos aminoácidos por RMN e por CLAE permitiu a comparação dos resultados para verificação da confiança da técnica de RMN. Dado que por CLAE é permitida a realização de uma quantificação absoluta com recurso a soluções-padrão de aminoácidos e curvas de calibração das mesmas e que RMN é uma técnica menos sensível, e visto que o erro de medição entre ambas as técnicas era relativamente baixo (cerca de 11,5 %), utilizaram-se as medições aos aminoácidos feitas por CLAE para a análise metabolómica, à exceção do triptofano. Este apresentou um erro de medição de 181% entre as duas técnicas, sendo isto explicado pela presença de dois grupos fluorescentes (o reagente de derivatização e o próprio triptofano) que levam à redução da sensibilidade de fluorescência na técnica de CLAE. Para este aminoácido utilizaram-se então os valores obtidos com RMN-^{1}H. Após a determinação das concentrações dos metabolitos calcularam-se as taxas de consumo ou secreção destes face ao número de células em *T-flask* ou o volume de pele no inserto com filtro de policarbonato. Verificou-se que durante a fase de diferenciação dos queratinócitos em cultura na interface ar-líquido existe um grande consumo de glucose e concomitante produção de lactato até ao quinto dia, a partir do qual se parece verificar uma inversão do metabolismo para metabolismo de síntese de proteínas que requer uma maior quantidade de aminoácidos, sendo estes mais consumidos nesta fase. Devido a esta observação, um novo meio de cultura contendo uma maior concentração de aminoácidos selecionados foi desenhado e testado em nova cultura de equivalentes de epiderme. Os testes de permeabilidade com os três fármacos-modelo mostraram que a epiderme obtida era ainda mais permeável do que a obtida com o método de cultura convencional. Foi determinado o teor de proteína total em pele cultivada neste novo meio desenhado e pele cultivada em meio normal, conforme o protocolo, para verificar se o facto de se ter adicionado mais aminoácidos levava a uma maior produção de proteína. Contudo, não se observaram diferenças estatisticamente significativas ($p = 0,05$) no teor de proteína total extraído da epiderme cultivada pelos diferentes métodos.

A metabolómica tem muitas potenciais aplicações, incluindo determinação de inibidores de crescimento/diferenciação, compreensão do metabolismo de fármacos ou modelação de sistemas biológicos[8,9], e muitos outros testes e estudos podem ainda vir a ser feitos com o intuito de melhorar a barreira da pele, como nomeadamente, fazer análise metabolómica ao meio intracelular.

Este projeto poderá vir a completar estudos prévios com o intuito de descobrir formas de melhorar a função de barreira dos equivalentes de epiderme humana.

ABSTRACT

There is a trend to develop experimental approaches to replace animal testing. In which concerns the evaluation of skin toxicity induced both by cosmetics and pharmaceutical products, there are already several reconstructed skin models commercially available. However, even though they show morphological and biochemical similarities to native human skin, the skin barrier of the *in vitro* reconstructed epidermis models is considerably different and more deficient than the barrier of the native skin. A deficient barrier allows a higher permeability of substances, thus increasing the evaluated toxicity, being desirable to improve the barrier of cultivated skin.

In this work, a metabolomic analysis of the supernatant of the culture process (exometabolome) was performed by proton nuclear magnetic resonance spectroscopy (^{1}H-NMR) and high-performance liquid chromatography (HPLC). The uptake and secretion rates for both the expansion of keratinocytes in monolayer culture and the reconstructed epidermis were determined for the several metabolites observed by NMR, and for the amino acids. During the culture at the air-liquid interface, it was verified that there is a high consumption of glucose and concomitant production of lactate until the fifth day, after which an inversion of this metabolism occurs into a protein synthesis metabolism, that requires a higher amount of amino acids, thus these being more consumed at this stage.

Due to this observation, a new culture media three times more concentrated in selected amino acids was tested in the culture of a new batch of epidermis equivalents.

The morphology of the epidermis cultivated with the new culture medium evidenced a well differentiated tissue, containing the usual *strata*. The barrier function of the reconstructed epidermis was characterized by the determination of the maximum flux of three model drugs with different polarities, caffeine, hydrocortisone and tamoxifen in Franz cells. The epidermis obtained with the new culture media was more permeable than the tissue cultivated in standard conditions. Despite the cultivation with increased amount of amino acids in the culture media, the total protein content of the reconstructed epidermis did not change.

Keywords: *in vitro* epidermis; cutaneous barrier; permeability; metabolomic analysis.

RESUMO

Atualmente existe uma tendência para o desenvolvimento de métodos experimentais que venham a substituir os testes em animais. Relativamente à avaliação da toxicidade da pele induzida tanto por cosméticos como por produtos farmacêuticos, já existem vários modelos de pele reconstruída disponíveis comercialmente. Contudo, ainda que apresentem semelhanças a nível morfológico e bioquímico à pele humana nativa, a barreira dos modelos de epiderme reconstruída *in vitro* é consideravelmente diferente e menos eficiente que a barreira da pele nativa. Uma barreira deficiente permite uma maior permeabilidade das substâncias, o que leva ao aumento da toxicidade avaliada, sendo desejável melhorar a barreira da pele cultivada.

Neste projeto realizou-se análise metabolómica do sobrenadante de um processo de cultura (exometaboloma) com recurso a espectroscopia por ressonância magnética nuclear de protão (RMN-^{1}H) e cromatografia líquida de alta eficiência (CLAE). As taxas de consumo e secreção tanto para a expansão dos queratinócitos em cultura em monocamada como para a reconstrução da epiderme foram determinadas para os vários metabolitos observados por RMN e para os aminoácidos. Durante a cultura na interface ar-líquido, verificou-se que existe um elevado consumo de glucose e concomitante produção de lactato até ao quinto dia, a partir do qual uma inversão deste metabolismo ocorre para metabolismo de síntese de proteína, que requer uma maior quantidade de aminoácidos, sendo estes mais consumidos nesta fase.

Devido a esta observação, um novo meio de cultura três vezes mais concentrado em aminoácidos selecionados foi testado numa cultura com um novo conjunto de equivalentes de epiderme.

A morfologia da epiderme cultivada com o novo meio de cultura mostrou um tecido bem diferenciado, contendo os estratos normais. A função de barreira da epiderme reconstruída foi caracterizada pela determinação do fluxo máximo de três fármacos-modelo com três diferentes polaridades, cafeína, hidrocortisona e tamoxifeno, em células de Franz. A epiderme obtida com o novo meio de cultura foi mais permeável do que o tecido cultivado em condições padrão. Apesar do cultivo com uma maior quantidade de aminoácidos no meio de cultura, o teor de proteína total na epiderme reconstruída não se alterou.

Palavras-chave: epiderme *in vitro*; barreira cutânea; permeabilidade; análise metabolómica.

TABLE OF CONTENTS

LIST OF TABLES

LIST OF FIGURES

APPENDICES INDEX

NOMENCLATURE

°C – Celsius (SI Unit)
µ- (unit prefix) – micro-
^{13}C – Carbon-13
^{1}H – Hydrogen
^{31}P – Phosphorus-31
AABA - α-Aminobutyric acid
AQC – 6-aminoquinolyl-N-hydroxysuccinimidyl carbamate
ATP – Adenosine triphosphate
BC – Before Christ
BCA – Bicinchoninic Acid
Brij-58® – Polyoxyethylene (20) cetyl ether
BSA – Bovine Serum Albumin
c- (unit prefix) – centi-
Ca^{2+} – Calcium
CO^2 – Carbon Dioxide
D_2O – Deuterium Oxide / ^2H_2O / heavy water
Da – Dalton
DFBS – Dialyzed Fetal Bovine Serum
DMSO – Dimethyl sulfoxide
DNA – Deoxyribonucleic Acid
DSS-d_6 – 3-(Trimethylsilyl)-1-propanesulfonic acid-d_6 sodium salt
ECVAM –European Centre for the Validation of Alternative Methods
EDTA – Ethylenediaminetetraacetic Acid
FGF-7 – Fibroblast Growth Factor-7
FT – Full-Thickness Skin
g – gram (SI Unit)
GC-MS – Gas Chromatography-Mass Spectrometry
GS – Glutamine Synthetase
h – hour
H&E – Hematoxylin and Eosin stain
H_2O – Water
HEKn – neonatal Human Epidermal Keratinocytes
HEPES – 4-(2-Hydroxyethyl)piperazine-1-ethanesulfonic Acid
HKGS – Human Keratinocyte Growth Supplement
HPLC – High-Performance Liquid Chromatography
HPPR – High Performance Preamplifier
Jmax – Maximum Flux
KBM – Keratinocyte Basal Media
KCl – Potassium Chloride
KGF – recombinant human Keratinocyte Growth Factor
L – Litre (SI Unit)
LC-MS - Liquid Chromatography-Mass Spectrometry

m – metre (SI Unit)
M – Molar (SI Unit)
m- (unit prefix) – milli-
MDH II – Malate Dehydrogenase II
MFA – Metabolomic Flux Analysis
Milli-Q® – "ultrapure" water
min – minute
mol – mole (SI Unit)
mRNA – Messenger RNA
n- (unit prefix) – nano-
$Na_2HPO_4 \cdot 7H_2O$ - Disodium Hydrogen Phosphate Heptahydrate
NaCl – Sodium Chloride
NAD^+ – oxidized form of Nicotinamide Adenine Dinucleotide (NAD)
NADH – reduced form of Nicotinamide Adenine Dinucleotide (NAD)
$NAHCO_3$ – Sodium Bicarbonate
NMF – Natural Moisturizing Factor
NMR – Nuclear Magnetic Resonance
O_2 – Oxygen
OECD –Organisation for Economic Co-operation and Development
ppm – parts per million
PBS – Phosphate Buffered Saline
PF – Polycarbonate Filter
PG – Propylene Glycol
pH – potential of Hydrogen
Q_{24} – Cumulative Corrected Amount of substance that passed to the receiver compartment per unit area of skin in 24 hours
R^2 – Coefficient of Determination (R squared)
RH – Relative Humidity
RHE – Reconstructed Human Epidermis
RNA – Ribonucleic Acid
s – second (SI Unit)
SB – *Stratum* Basale
SC – *Stratum Corneum*
SD – Standard Deviation
SDS – Sodium Dodecyl Sulfate
SG – *Stratum Granulosum*
SL – *Stratum Lucidum*
SS – *Stratum Spinosum*
T25 – 25 cm^2 T-flask
TCA – Tricarboxylic Acid Cycle
UK – United Kingdom
USA – United States of America
UV – Ultraviolet radiation
v/v % – volume/volume percent
λ – wavelength

1. INTRODUCTION

The human skin portrays an important aesthetic role, being not only a motive but also a consequence of it the high demand in the use of cosmetics seen nowadays[10]. In fact, cosmetics have been part of the lives of people since ancient times – beauty and skin-care applications were already used as early as in 3000 BC, in Egypt, where it was common to prepare ointments by grounding incense, wax, fresh olive oil and cypress bark to remove facial wrinkles or mixtures of ostrich eggs with milk and bile from bullock to treat acne. Thanks to the continuous progress of medical and cosmetic technologies, today it is possible not only to change the appearance of the skin through the use of cosmetics[11], but also to prevent skin from aging or to treat dermatologic diseases with remedies derived from natural compounds, by applying topically substances like antioxidants, that reduce oxidative damage to the skin[12]. For example, in cases of atopic dermatitis (eczema), a chronic inflammatory skin disease that affects mostly children, it is common to prescribe the application of skin moisturizing creams in order to minimize the aggravation of the disease[13]. Atopic dermatitis is characterized by cutaneous hyperreactivity to (usually) common environmental elements and one of the reasons for its occurrence is a defect in the skin barrier function that leads to transepidermal water loss and consequently dry skin, causing eczema. Many emollients with different applications can be used to reduce this dryness: from simply forming a protective layer on top of the skin to increase its hydration (reduction of evaporation) to restoring the lipid contents of the external layers of the skin (reduction of fissures)[14]. Apart from vanity purposes, cosmetics also have other utilities because, in addition to physical discomfort, skin problems cause a big impact in terms of quality of life (both personal and social), with studies reporting that patients with these types of problems may experience feelings of embarrassment, lack of confidence and even depression[15], being very common to resort to cosmetics or certain topical applications to hide or mitigate a skin problem in order to get some relief.

Many topical products are commercially available, either for cosmetics or pharmaceutical application, but before their placement in the market tests have been performed to verify if their constituting active substances have hazardous effects to the organism, independently if they are intended for topical delivery (transported to the skin) or transdermal (transported through the skin and into the body itself). Therefore, companies working in these fields must do toxicological tests to assess the safety of the components of cosmetic formulations. Until recently these tests were most commonly performed on animals or by using human skin (mainly obtained from biopsies or cadavers). However, even though native human skin can replicate *in vivo* permeability performance to some extent, it cannot be established as a standard procedure as there is a limited source of these specimens. On the other hand, animal skin is morphologically different from human skin and due to legal and ethical demands, animal testing has become strictly limited in the European Union, as well as in other countries like Japan and the United States of America (USA). This led to an increase in the demand for alternative testing methods and in these last three decades a lot of effort has been applied to the field of *in vitro* engineering of human skin developing suitable skin models for testing of cosmetics, as well as pharmaceutical and chemical compounds[1,2].

EpiDerm™ (MatTek Corporation, Ashland, MA, USA) and EpiSkin™ (EPISKIN, Lyon, France) were the first human skin equivalents to be validated by the ECVAM (European Centre for the Validation of Alternative Methods) as predictive models for skin corrosion, in 1998. In 2004, with the publishing of the "OECD (Organisation for Economic Co-operation and Development) Guidelines for the Testing of Chemicals", they were internationally accepted and more models have been developed since then[1]. Bioengineered skin is also of interest for the field of regenerative medicine in clinical skin replacements and grafts. The creation of implantable or *in situ* forming tissues may help overcome some

difficulties associated with organ transplantation like a donor not having enough skin to graft, risk of rejection of foreign tissue, and the patients having to take immunosuppressive drugs for the rest of their lives associated with risk of tumour growth[2,16].

1.1. Human Skin

The skin is the largest organ of the human body. It forms the integumentary system, along with the accessory structures hair, glands and nails, carrying many important functions such as[15,17,18]:

- Protection – serves as a barrier against environmental insults
    - By covering the whole body, the skin can guard all underneath structures from physical damage, prevent the entrance of external agents (microorganisms or other types of substances) and act as a barrier to water diffusion, preventing the loss of essential body fluids and consequent dehydration;

- Sensation – Sensory receptors located in the integumentary system allow the capacity to feel at touch, as well as the detection of heat, cold, pressure and pain;

- Regulation of temperature;

- Production of vitamin D, which portrays an important role in the regulation of the metabolism of calcium and phosphorus;

- Excretion – small amounts of waste products resulting from protein metabolism (urea, uric acid and ammonia) and anaerobic respiration (lactic acid), along with water and salts, are excreted through the skin by the sweat;

- The appearance of the skin may also help with the diagnosis of some disorders, from allergic reactions that cause skin rashes to heart attacks, where the reduction of the blood flow through the skin results in a pale appearance.

This multitude of functions is only possible due to the complex organization and the interaction between the various elements that constitute the skin[1]. It is composed of three layers: subcutaneous tissue (also known as subcutis or hypodermis), dermis and epidermis.

1.1.1. Hypodermis

It is not considered by many authors as part of the skin but it is, nevertheless, its innermost and supporting layer. It works as a connection between the skin and the muscles or bones and is a supplier of blood vessels and nerves. It contains a great abundance of adipocytes, cells that have the functions of storing energy, thermal insulation and shock-absorption, as well as macrophages and fibroblasts[15,17,19].

1.1.2. Dermis

The dermis accounts for around 90 % of the weight of the skin[15]. It is responsible for its structural strength and for preventing it from tearing[17].

1.1.3.Epidermis

The epidermis is the outermost and thinnest layer of the skin, composed primarily of keratinocytes. It is a continually renewing structure attached to the dermis by means of a basement membrane, a specialized type of extracellular material secreted by both tissues. Since blood vessels do not penetrate it, the delivery of gases and nutrients, as well as excretion of waste products, between the epidermis and the capillaries of the dermis is made through diffusion across this membrane; in the case of the outermost layers of this tissue the diffusion is made across cells, which results in the most metabolically active cells being the ones from the innermost layers due to their proximity to the basement membrane[17,20].

Keratinocytes are producers of keratin, a protein mixture that adds strength to the skin, as well as to the hair and nails, increasing their durability. Keratins have mainly a structural role in the cells and belong to the family of the intermediate filaments (cytoskeletal components). They can be divided in two types: acidic (labelled as type I and numbered from K9 – K19) or basic-to-neutral (type II, K1 – K8) forming filaments that contain both an acidic and a basic keratin gene[17,20].

It is responsible for the reduction of water loss from the organism and protection against microorganisms and abrasion on the surface of the skin. The keratinocytes have very important functions contributing with the components responsible for this barrier structure and regulating nutrient and gas interchange across the epidermis[20]. The stratified squamous epithelium that characterizes the epidermis is a result of keratinocyte differentiation (keratinization), a complex genetic program where the cube-shaped keratinocytes from the basal layer (the deepest layer) progressively differentiate and flatten towards the most superficial layer (apical layer). As these cells move towards the surface their cytoplasm is gradually replaced by keratin until the cells lose their nucleus and die, becoming terminally differentiated corneocytes. This results in the formation of a keratinized surface composed of dead squamous cells, the outermost part of the epidermis that acts as a barrier of the skin (the *stratum corneum*)[15,17,20]. The cell layers of the epidermis are divided into 4 – 5 *strata*, depending on their location in the body (see figure 1.1 for a representation of the epidermis).

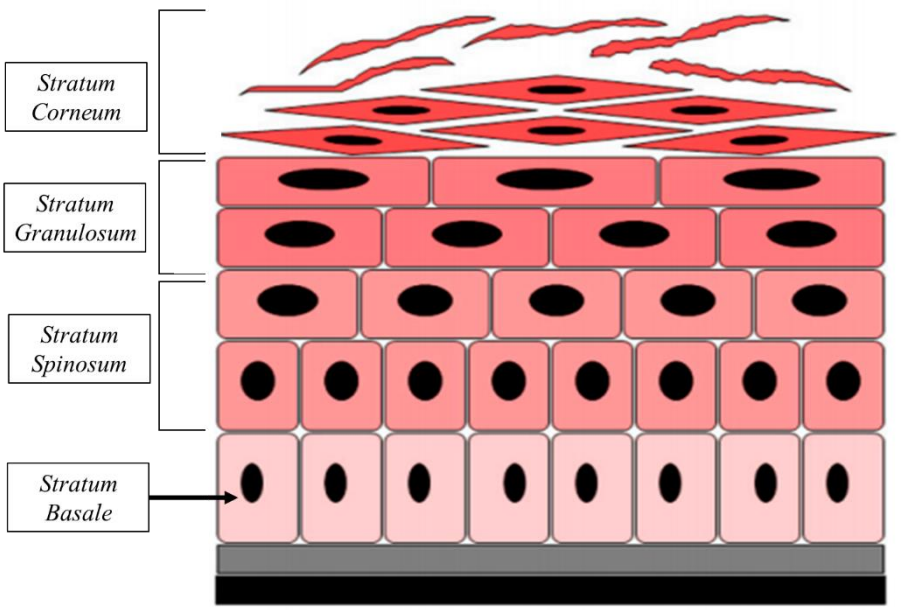

Figure 1.1 - Schematic picture of the epidermis with representation of the main *strata*. *Adapted from ref.*[21].

The *strata* of the epidermis are arranged in the following order[17,20]:

- *Stratum basale* (SB)
    - Also called as *stratum germinativum*, it is the innermost *stratum* of the epidermis and consists of a single layer of cuboidal mitotically active keratinocytes, linked together by the desmosomes and to the basement membrane by the hemidesmosomes. Desmosomes are calcium-dependent modifications of the cell surface that contribute to cell adhesion and resistance to mechanical stress, having an important role in intercellular adhesion, since the loss of this structure results in the rounding and separation of keratinocytes. Calcium is an important mediator of adhesion, as observed in diseases caused by mutations in genes that regulate calcium transport, like Darier disease and Hailey-Hailey disease;

- *Stratum spinosum* (SS)[22]
    - Composed of 8 – 10 layers of cells. As they move from the SB, they start to flatten and old desmosomes break apart only for new desmosomes to be formed. Despite retaining the K5/K14 keratins produced in the SB, spinous cells do not synthesize anymore mRNA for these proteins. Instead, a new keratin pair is synthesized in this *stratum*, the differentiation-specific K1/K10 pair (for this reason, this pair is also viewed as an epidermal pattern of differentiation). In addition, these cells produce lamellar bodies, secretory organelles, also known as Odland bodies, keratinosomes or membrane-coating granules. These granules contain precursors of the *stratum corneum* extracellular lipids, including glycoproteins, glycolipids, phospholipids, free sterols, acid hydrolases and glucosylceramides as well as their corresponding enzymes, and constitute another marker of differentiation;

    - During histologic preparations, the cells from this layer shrink, except at the sites with desmosomes attached, resulting in a spiny appearance of the keratinocytes and the reason for the "*spinosum*" designation.

- *Stratum granulosum* (SG)[7,22,23]
    - The SG is constituted of 2 – 5 layers of flattened cells and its name comes from the keratohyalin granules that are very prominent in the interior of the cells. At this point the cells have interrupted the generation of keratins and envelope proteins and form these protein granules, mainly constituted by keratins, profilaggrin (a histidine-rich protein precursor of filaggrin that interacts with the keratins by assembling them into aggregates) and loricrin (a cysteine-rich protein that reinforces the cornified envelope of the corneocytes, being their main component and accounting for more than 70 % of their mass);

    - The spaces between the uppermost cells of the SG are sealed by tight junctions, suggested by some authors as having also a role in the barrier function of the epidermis. They appear exclusively between these cells and provide an additional barrier that regulates the flux of water and some molecules and ions in the intercellular space.

- *Stratum lucidum* (SL)
    - SL is only present in thick skin which is, in turn, found only in areas prone to suffer pressure or friction like the palms of the hands, the soles of the feet and the fingertips. Consists of 3 – 5 layers of dead cells above the SG with a transparent appearance. In this *stratum*, keratins and keratohyalin can be found dispersed in the cytoplasm (instead of being accumulated in granules, like in SG).

- *Stratum corneum* (SC)[2,3,7,24–28]
    - The outermost *stratum* of the epidermis, constituted of 25 or more layers of dead squamous cells, corneocytes, the ending point of the keratinization process. Corneocytes are held together by corneodesmosomes (modified desmosomes), and when these break apart, the cells slough off from the surface of the skin. This is a naturally occurring event even after the simple act of rubbing the skin while washing them or wearing clothes, for example. The process from the time new cells are produced in the SB to when older cells are pushed to the surface and slough off takes approximately 40-56 days. It is a continuous cycle where the outermost cells protect the ones beneath them while the innermost cells keep on replicating to replace the others that were lost from the surface;

    - When the cells from the SG reach the transition layer to *stratum corneum*, the lamellar bodies in the interior of the cells move to the plasma membrane to release their lipid contents into the extracellular space. Simultaneously the cells die, as can be observed by the degeneration of their nucleus and all other cellular contents, except keratins and keratohyalin granules, which start to release their contents. Upon release, loricrin is cross-linked to the plasma membrane, together with other proteins like involucrin, cystatin A, small proline-rich proteins (SPR1, SPR2, and cornifin), elafin and envoplakin, forming a hard protein (cornified) envelope. This envelope and the keratin content of the corneocytes confer structural strength to the SC, UV protection and hydration of the skin. The permeability barrier function is the result of the embedment of the corneocytes in a lipid matrix, composed of ceramides, cholesterol, cholesterol esters and free fatty acids, products of the precursor lipids released from the lamellar bodies;

    - Through a series of processes, the profilaggrin released from the keratohyalin granules forms filaggrin which, in turn, releases histidine and glutamic acid, along with other proteolysis products. The deamination of histidine by a histidase in the SC leads to the formation of *trans*-urocanic acid that can act as a natural sunscreen by absorbing the ultraviolet B (UVB) radiation, preventing the penetration of the rays into the lower areas of the epidermis. After being exposed to UVB this molecule is converted into *cis*-urocanic acid, a natural immunosuppressant. Glutamic acid is, in its turn, converted to pyrrolidone carboxylic acid (pyroglutamate) which, together with the other proteolysis products, constitute the natural moisturizing factor (NMF), small molecules capable of retaining small amounts of water that work as natural humectants of the skin, localized in the interior of the corneocytes;

- While the viable epidermis (all *strata* below SC) has a pH value of around 7.35 – 7.45 (physiological pH), a more acidic environment is found in the SC, where the pH value may range between 4.5 – 5.5. This happens due to a variety of reasons:
    - Studies show that the acidity of the SC is mainly influenced by endogenous mechanisms including a sodium/proton antiporter (transporter NHE1) responsible for the acidification of the SG – SC interface and the conversion of phospholipids to free fatty acids during cornification by a secretory phospholipase A2 ($sPLA_2$). *In vitro* studies have shown that urocanic acid generation from histidine may also have a role in acidification;

    - The formation of an efficient permeability barrier is only possible due to the extracellular lipid matrix existent in the SC. Here, β-glucocerebrosidase and acidic sphingomyelinase metabolize, respectively, glucosylceramides and sphingomyelin to ceramides, the main constituent of this matrix, and for their optimal enzymatic activity an acidic environment is required. Consequently, an increase in the pH of the SC would interfere with the metabolism of ceramides and a less efficient permeability barrier would be formed;

    - Serine proteases located in the SC have an important role in the desquamation process, cleaving the cadherins and corneodesmosin that constitute the corneodesmosomes. They have a better enzymatic activity with an increase of the pH level and, therefore, an acidic environment is necessary to inhibit their activity to maintain the integrity of the SC (homeostatic desquamation);

    - The acidification of the surface of the skin is considered a means of defence against infection since it inhibits the growth of pathogenic microorganisms like *Staphylococcus aureus* and *Streptococcus pyogenes*.

1.1.3.1. Permeability Pathways through the Skin

The SC has undoubtedly an important protective role and it is the first barrier that external agents find when trying to invade the human body. Likewise, topically applied drugs and other compounds must also permeate through this layer of the epidermis before they are able to affect any viable cells underneath it. It is generally accepted that there are two possible pathways that may allow the penetration of these substances (see figure 1.2)[2,29,30]:

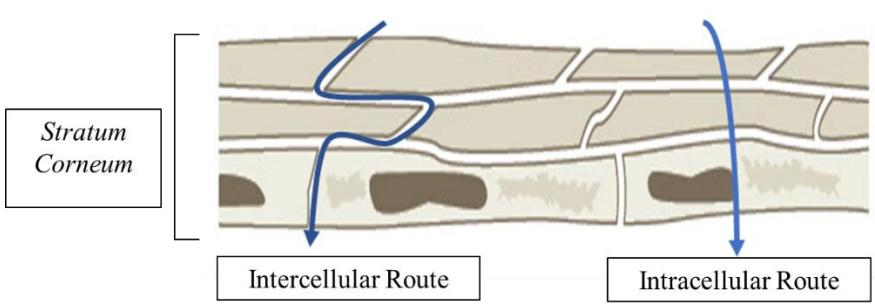

Figure 1.2 – Representation of the transepidermal pathways through the skin (showing the *stratum corneum*, the outermost layer of the epidermis). *Adapted from*[31].

- Transepidermal pathway – permeability of the molecule through the SC by diffusion across the cell layers (the main route of permeability for most compounds)

    - Intracellular route – the substance traverses the intercalated layers of corneocytes and extracellular matrix, alternating between a more hydrophilic domain (interior of the cell) and a lipophilic domain;

    - Intercellular route – the substance progresses through the extracellular matrix pathway, without passing through the cells;

    - Hydrophilic (polar) molecules encounter greater energy barriers while diffusing through the SC than compared to lipophilic (non-polar) molecules due to its lipidic nature, and thus they generally use the intracellular route instead of intercellular, being the latter the preferred route for lipophilic compounds;

- Appendageal pathway – permeability through hair follicles or sweat ducts

    - The follicular route is a topic of interest as a means for drug administration. Due to the architectural structure of the hair follicle, it can provide a faster delivery of certain molecules into the systemic circulation, depending if it is possible to perform transfollicular penetration (substance penetrates transfollicularly into deeper skin layers). In cases where transfollicular penetration does not occur, it can work instead as a long-term intrafollicular storage.

1.2. *In vitro* Reconstruction of Human Skin

The high demand for alternative testing methods to the use of animals in the cosmetics and pharmaceutics industry led to the need of development of 3D human skin models. An example is the epidermal model, with morphological and functional properties similar to native skin. Initially, keratinocytes were cultivated in immersed conditions, either as a monolayer or as stratifying layers. However, under these conditions keratohyalin granules do not appear and cornification does not occur. Consequently, *in vitro* studies regarding the SG or SC layers or the epidermis as a whole tissue were impossible to perform, being only possible to do basic research on cell biology. A study in 1983 led to the finding that exposing the cells to an air–liquid interface would stimulate the synthesis of profilaggrin which, in turn, resulted in the development of these granules and, consequently, the appearance of the SG[32]. Also, this allowed the cornification of the cells (SC) resulting in the reconstruction of an epidermis with 3D organization and well-differentiated. With this discovery, it was finally possible to develop *in vitro* models of reconstructed human epidermis (RHE): from a skin biopsy, the epidermis can be separated from the dermis and then be dissociated into keratinocytes that cultivated under optimal conditions at the air-liquid interface form a stratified and well-differentiated epithelium during the time course of around 11 days[1,2,4,33]. Currently, a wide variety of *in vitro* skin models can be found.

According to the demands of the researcher or the company, the models may have different levels of biological complexity, even containing other cell types like melanocytes or Langerhans cells, and can be divided into three major categories[1,2,4,5,34]:

- Epidermal models (RHE)

- Dermal models
    - Fibroblasts are seeded into a collagen I matrix to mimic native dermis. As it develops, the dermal layer contracts uniformly while the fibroblasts and collagen fibrils interact with each other, resulting in a gel that mimics the strength and flexibility of the human dermis;

- Full-Thickness (FT) models
    - These models are generated by seeding human keratinocytes on a collagen matrix seeded with human fibroblasts, forming a bilayer structure composed of both epidermal and dermal layers.

Skin equivalents consisting of one cell type can only be used typically for tests of toxicity, corrosion and irritation, while FT models allow for more complex research on skin diseases, dermal-epidermal interactions and effect of external stimuli and chemical insults on the skin[1,34]. However, the reproducibility of these skin models must be guaranteed by fulfilling certain functional conditions established in the OECD Test Guideline No. 439 (2010), including[1,35]:

- The SC and its lipid content should be sufficient to resist the rapid penetration of toxic chemicals (barrier function). This evaluation can be performed by determining the concentration at which the viability of the tissues is reduced by 50 % (IC_{50}) after a fixed exposure time to the chemical, or by applying the chemical at a known, fixed concentration to determine the exposure time required to reduce cell viability by 50 % (ET_{50});

- The epidermal layer structure must be confirmed by histological analysis.

Although simple 3D systems like RHE exhibit a high reproducibility, the demands of the barrier function of these *in vitro* skin models do not entirely meet the requirements for permeability studies of drugs and substances, since their barrier function is reduced compared to native skin, even though having morphological similarities[1,3]. On the other hand, complex models do generally mimic native skin more reliably than the other simpler systems, even though they present also a higher permeability[36], but they are harder to standardize and more costly to maintain due to their complexity of creation. It is, therefore, of commercial interest to develop simpler skin models like *in vitro* human epidermis, even though some authors do not support their use as alternative methods for permeability studies due to their high permeability[37].

1.2.1. Attempts to Improve the Barrier Function of the Skin

Many attempts have been made in order to improve the quality of the barrier function of the SC, being the ultimate goal the creation of a human epidermal model with the same barrier properties found in native skin[3]. As mentioned before, the barrier is affected by the lipid composition of the SC, and analysis of the lipid content of epidermal equivalents revealed that their composition is different than from native skin: *in vitro* skin models contain a much lower number of glucosylceramides, ceramides (C4 – C7, especially C6 and C7, the most polar ceramides) and free fatty acids[27], and a higher content of triglycerides[5,38]. It has been suggested that the improvements should be focused on the lipid composition of the SC[39].

There have already been identified several parameters that may enhance and accelerate barrier formation and homeostasis in skin models. In the case of ceramides C6 and C7, these are composed of hydroxylated sphingoid bases and/or fatty acids, and it has been found that the addition of vitamin C to the media, which is an antioxidant and an important cofactor in lipid hydroxylation, improved the characteristics of the *in vitro* epidermis[6,40]. The addition of choline, myo-inositol and phosphoethanolamine also may help in maintaining the integrity of the SC, since this also influences the barrier properties of this layer. These nutrients are basic building blocks for the synthesis of phospholipids, which in turn, are used to generate free fatty acids, a phenomenon that is said to be related to the acidity of the SC[28,41]. Other modifications to the culture media have been tested, and all had positive outcomes in terms of improvement of the lipid composition[16,40,42–44]:

- Supplementation with lipids and/or essential fatty acids (arachidonic, palmitic, oleic and linoleic, along with alpha-tocopherol acetate, an antioxidant) helped the production of lamellar lipids and to get a better lipid organization of the *stratum corneum*;

- Lowering the relative humidity (RH)
    - On the contrary to what happens in incubation conditions, where the RH is almost 100 %, native human skin grows in an environment with a lower RH. Based on the premise that if the permeability barrier is improved with the existence of a water activity gradient across the membrane (reason why submerged keratinocytes do not develop SC), lowering the RH outside of the membrane would improve the barrier properties and, indeed, it was found that lowering it to 50 – 75 % lead to an increase in the number of SC layers, higher density of corneodesmosomes and a decrease in water diffusion through the skin;

    - In a test with preterm infants, the ones raised at more humid environments of 75 % RH manifested higher levels of transepidermal water loss than those at 50 % RH, meaning that the former had a less efficient skin barrier[44];

- Other modifications, including use of serum-free media, lowering the incubation temperature, adding vitamin D_3, …

However, despite these additions to the culture media, human epidermal equivalents are still lacking in terms of lipid profile and, consequently, have a higher permeability than native skin. As of yet, no reconstructed skin model has been able to fully mimic the barrier properties of human skin[2,3].

1.3. Cell Culture Optimization

The metabolism of mammalian cell culture is typically inefficient, with a production of large quantities of growth inhibiting products like lactate and ammonia due to a high consumption of glucose and glutamine[45].

Lactate production (a process also known as lactate fermentation) occurs due to an incomplete oxidation of glucose during glycolysis (glycolytic pathway). This pathway involves a sequence of reactions that lead to the metabolism of one molecule of glucose into two molecules of pyruvate with the additional production of two molecules of ATP (and two of NADH). It can occur anaerobically in the absence of oxygen, where pyruvate is further transformed to lactate to recover the oxidized form of NADH, NAD^+ (to maintain the redox balance). However, it can be a much more energy efficient process if it occurs under aerobic conditions, with pyruvate being completely oxidized to CO_2 which leads to the generation of much more ATP (36 molecules)[45–47]. Lactate formation is very common in aerobic cells undergoing very high rates of glycolysis and several studies reported that it can affect hybridoma cell growth, metabolism, and antibody production by means of culture medium acidification occurring at concentrations above 20 mM[48].

In animal cell culture, ammonia can be released by chemical decomposition of glutamine as well as by metabolic deamination of glutamine to glutamate and the conversion of the latter to α-ketoglutarate. It is a central metabolite at low levels: the nitrogen needed to synthesize amino acids and other nitrogenous compounds is assimilated from ammonia via reactions that lead to the production of glutamine and glutamate (amino nitrogen of glutamate and amide nitrogen of glutamine)[46], with the excess ammonia being transported to the liver for its conversion and excretion as urea (in the case of most mammals)[47]. However, in cell culture ammonia tends to accumulate and reach toxic levels: cell growth inhibition occurrence has been reported at ammonia concentrations as low as 2 – 3 mM[49], depending on the cell line and culture conditions, being shown to affect strain L mouse cells, chorioallantoic tissue, mouse asitics tumor cells, and hybridoma cells, as well as interferon production from human fibroblast cells and virus production.

Examples of procedures to improve cell culture performance include improving the culture mode (e.g. continuous vs intermittent perfusion culture[50]) and/or the cell line (e.g. enhanced gene expression by means of strong promoters[51]), and doing a rational design of the media which leads to the need to understand the nutrient consumption and metabolite accumulation in the culture medium over time[52]. Traditionally these optimizations have been achieved by simulations or in an empirical way (by trial-and-error, for example trying different media with different metabolite concentrations and then, with multivariate analysis[9], identifying patterns and/or relationships from the amount of data obtained)[53]. However, medical needs where the use of the traditional small molecule drugs is not enough have led to an increased interest in therapeutics based on proteins or nucleic acids, manufactured through expression in genetically modified cells (mammalian or bacterial)[54]. The importance of improving the production of therapeutic proteins lead to the development and application of new strategies with recourse to the "omics" studies comprising genomics (genes), transcriptomics (mRNA), proteomics (proteins) and metabolomics (metabolites)[55].

1.3.1. Metabolomics

The purpose of metabolomics is to identify and quantify as many small molecule components in a biological system (cell, tissue or organism) as possible, under a given set of conditions[56].

Around the 1980s, initial approaches in this area aimed to better understand the systems biology in human health (e.g. identification of urinary organic acids as a means of diagnostic[57]) or plant science (e.g. metabolic profiling of plant material[58]), focusing on the metabolic profile of the entire organism. Information about specific cell types was lacking which is of vital importance when developing novel drugs or markers for specific cellular phenotypes[8].

Subsequently in drug research, with the necessity to understand drug metabolism and toxicity to produce safe and efficient therapeutics came the need to develop laboratory based testing models such as the *in vitro* slice assay. Here, thin slices of liver treated with drug are suspended in defined culture medium and analysed over time (the slices or the media) to verify the effect of the drug on the liver slice, as well as its metabolism[54].

The analysis of the metabolites in the cell culture presents many advantages, one of them being that the concentration of the metabolites acts as a marker of changes at the phenotype level. With this came the comprehension of the many potential applications of metabolic analysis of cell cultures, including determining cell stresses, understanding the metabolism of drugs or modelling of biological systems[8,9], as well as the possibility to improve the energy metabolism or protein production by genetic engineering[59]. In fact, some positive results have already been obtained by applying metabolomic analysis to the cell culture[54,60,61]. Two examples can be referred:

- The HEK293 cells, derived from human kidney fibroblasts, are used for the production of adenovirus vectors to be used in the potential treatment of alcoholism using a gene therapy strategy[62]. The metabolic states of these cells during growth and adenovirus production were compared by measuring the intra- and extracellular fluxes of the cells to perform a Metabolomic Flux Analysis (MFA) study. The objective was to minimize the production of metabolites that have inhibitory effects on cell growth. MFA resorts to an assemblage of the metabolic network representing the cell metabolism which allows to obtain a picture of the metabolic pathways in the cellular metabolism[60]. In this manner, by determining the fluxes the authors were able to optimise the culture medium according to the demand of the cells in terms of glucose and glutamine concentrations and obtained higher values of maximum cell concentration and increased adenovirus production;

- For CHO cells, Chinese hamster ovary cells that are used for the production of therapeutic proteins[63], the analysis of the extracellular metabolites identified an accumulation of malate due to an enzymatic bottleneck at malate dehydrogenase II (MDH II) in the tricarboxylic acid cycle (TCA) due to the presence of aspartate in the media. Subsequent overexpression of MDH II by metabolic engineering resulted in higher levels of intracellular ATP and NADH, as well as viable cell number.

Metabolomic analysis can be of two types[64]:

- Targeted – Used when it is intended to measure only a specific metabolite (for example in the TCA cycle);
- Untargeted – used when a more global view of the metabolites in different samples is intended, having a broader coverage of the metabolites in the sample.

1.3.1.1. Nuclear Magnetic Resonance

In metabolomics studies, advanced analytical tools like nuclear magnetic resonance (NMR) spectroscopy and mass spectrometry (MS) are used for quantitative analysis of complex biological samples[65]. These instruments are highly sensitive, may handle a large range of concentrations and allow easy identification of all measurable metabolites[66]. It is required to have a metabolite extraction procedure that guarantees that every class of compound is recovered. Also the analysis is associated with the help of computational tools that can analyse complex and large amounts of data[8].

From the many techniques available, NMR has had a very prominent role in the application of metabolomics to cell culture. The working principle of this technique is that if a sample is submitted to a static magnetic field and its nuclei excited with a radio frequency pulse, it is possible to measure the frequency of the signals they emit (NMR spectrum), which allows to obtain information about the bonding and arrangement of the atoms in the analysed sample[67]. Thus, a 1D NMR spectrum is no more than a plot containing the resonance frequencies of the nuclei (usually referred to as chemical shifts in ppm units) at different chemical environments, in the sample, against the intensity of the signal[68].

A wide variety of NMR spectrometers operating at different frequencies, from 270 – 900 MHz (ultra-high-field NMR), can be found nowadays, depending on the application[69]. In figure 1.3 is represented a 500 MHz NMR Spectrometer.

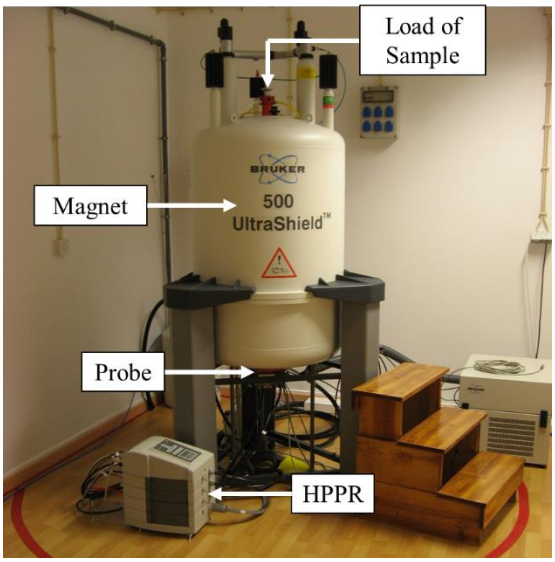

Figure 1.3 – Photograph of a Bruker AVANCE II+ 500 MHz Spectrometer in the CERMAX facilities with representation of the different parts of the equipment. The HPPR (High Performance Preamplifier) is used to amplify the NMR signal. *Adapted from*[67,70].

Unlike mass spectrometry or traditional high-performance liquid chromatography (HPLC), NMR does not require excessive sample preparation, avoiding the risk of loss of volatile compounds. This technique is less costly and allows to save time[52,54]. In addition, it is possible to obtain a

multidimensional spectrum with two-dimensional NMR (2D NMR) experiments to determine the structure of a given molecule[71].

The sensitivity of NMR is dependent on the natural abundance of the atoms studied according with the capacity of the probe to observe proton (^{1}H), phosphorus (^{31}P), carbon (^{13}C), or others[66]. This is because not all isotopes are NMR active and react to radio frequency pulses. In the case of hydrogen, three isotopes are found in nature and all of them are NMR active, but the isotope commonly excited to analyse a sample for hydrogen is the ^{1}H since it is the most abundant (99.98 %). Thus 1D ^{1}H-NMR is the method of choice for metabolomic analysis. The natural abundance of the proton confers versatility to this technique, being possible to use it to identify many different molecular classes like amino acids, alcohols, organic acids, to more complex structures like proteins, lipids[72] and even nanoparticles[73]. However, this technique also has its drawbacks. A sample from cell culture contains, in general, water solvent ($^{1}H_2O$) and the resonance of its ^{1}H nuclei dominates the ^{1}H-NMR spectrum of the sample, making it impossible to detect the minimal signals emitted from the nuclei of other compounds. The most common solution is to do a selective saturation of the excitation of $^{1}H_2O$, by irradiating the sample so that the water nuclei equalize the ^{1}H spin populations in both upper- and lower- energy states. By eliminating the excess of spins in the low-energy state the net macroscopic excitation is neutralized[74]. An additional problem in the case of mammalian cell culture is the presence of proteins in the culture media either as a supplement (for example fetal bovine serum) or as a product of the cells. These molecules cause broad signals in the NMR spectrum that may hide compounds located in that region (the "protein envelope")[52,54]. The sensitivity of the probes, and the cryogenic probes in particular, can also be affected by the electrical noise generated by conductive samples (containing metal ions), being once again a drawback to cell culture samples, since the media used is, generally, a complex commercial formulation containing, along other essential compounds, salts[75,76].

Additional disadvantages of the NMR in comparison with other instruments include the necessity to have large sample volumes (at least 500 µL vs 10 - 50 µL for MS techniques) and low sensitivity (micromolar concentrations vs pico- to femtomolar concentrations for MS techniques)[66]. In fact, this low sensitivity is responsible for a detection bias in NMR-based metabolomics, since these usually do not include low abundance metabolites with concentrations below 5 µM (for example neurotransmitters) neither hydrophobic molecules with higher abundance (including lipids, fatty acids, etc.), being Gas Chromatography-Mass Spectrometry (GC-MS) and Liquid Chromatography-Mass Spectrometry (LC-MS) the best methods to detect and quantify hydrophobic molecules, in general[77].

Nevertheless, NMR alone is a very popular analytical tool applied to mammalian cell cultures, namely 1D ^{1}H-NMR followed by multivariate analysis methods (e.g. principal component analysis or partial least-squares discriminate analysis) for metabolic profiling and ^{13}C for monitorization of the physiology and metabolic pathways of the cells[52,71].

2. OBJECTIVES

The aim of this work is:

- To grow human keratinocytes in monolayer in serum-free conditions and subsequently reconstruct a stratified epidermis on polycarbonate filter at air-liquid interface;

- To evaluate the reconstructed epidermis in terms of histology and drug permeability using different model drugs;

- To do untargeted metabolomic analysis of the supernatant of the cultivated keratinocytes (exometabolome) with 1D-^{1}H NMR to identify and measure the depletion of nutrients and accumulation of excreted metabolites;

- To design a new culture media based on the information obtained with metabolomic analysis and study its impact in the barrier function of the skin.

This project may give a contribution to previous studies, reinforcing the know-how, with the purpose of finding ways to improve the barrier function of human epidermis equivalents.

3. MATERIALS AND METHODS

3.1. *In vitro* Reconstruction of Human Epidermis

Primary human epidermal keratinocytes isolated from neonatal foreskin (HEKn) were purchased from Cascade Biologics (Portland, OR, USA) and stored in a liquid nitrogen tank for cryopreservation until further use. Since the cells were frozen, their proliferative potential had first to be reactivated by culturing them in monolayer, before seeding the polycarbonate filters to reconstruct epidermis[4].

For the inoculation and cell culture maintenance steps it was followed the protocol recommended by Cascade Biologics, while the preparation of solutions (e.g. culture media and fetal bovine serum dialysis), trypsinization and reconstruction of human epidermis on polycarbonate filter followed what was described in the literature[4].

3.1.1. Preparation of Solutions for Cell Culture

Before starting with the cell culture some solutions, necessary for this work, had to be prepared, including a washing solution, the media for cell culture and dialysis of fetal bovine serum (FBS) (Biowest, Riverside, MO, USA).

For the washing solution for tissues and cells (solution A), an aqueous solution containing 10 mM glucose, 3 mM KCl, 130 mM NaCl, 1 mM $Na_2HPO_4 \cdot 7H_2O$, 0.0033 mM phenol red and 30 mM HEPES, was prepared, its pH adjusted to 7.4 and stored at 4 °C. Solution A is used as a solvent to prepare other essential solutions: solution A containing 0.01 % ethylenediaminetetraacetic acid (EDTA) is used to prepare 0.025 % trypsin solution, while the blocking solution is composed of solution A with 2% dialyzed fetal bovine serum (DFBS)[4]. All these reagents were purchased from Sigma-Aldrich Corp. (St. Louis, MO, USA).

FBS was dialysed to remove calcium that interferes with the proliferation of the keratinocytes. For this effect, it was used Visking Dialysis Tubing membranes (Medicell Membranes Ltd, UK) with inflated diameter 4.5 mm and retention of proteins with molecular weight > 12000 Da. Glycerin was removed from the membranes as recommended by the manufacturer, by incubating them in a solution containing 2 % $NAHCO_3$ and 1 mM EDTA at 80 °C for 30 min, and then, washing 5 times with distilled H_2O for 3 min each. They were left to dry for 1 day and then 20 mL of FBS were put into the dialysis tubing, which followed a protocol already described in the literature[4]. After sealing the dialysis bag, it was stirred at 4 °C in 2 L of PBS, pH = 7.4, which was changed 4 times during 12h. In the end, the serum was sterilized with a Filtropur S plus 0.2 µm filter (Sarstedt AG & Co, Nümbrecht, Germany) and stored in aliquots at -20°C.

Two different commercial formulations were used for keratinocyte culture:

- Keratinocyte Basal Medium KBM™-2 (Clonetics) supplemented with KGM™-2 SingleQuots™ (Clonetics) (La Jolla, CA, USA);

- EpiLife® Calcium-Free (Cascade Biologics) supplemented with 0.06 mM $CaCl_2$ (Cascade Biologics) and human keratinocyte growth supplement HKGS (Cascade Biologics) (Portland, OR, USA).

Both media are modifications of the defined serum-free media MCDB 153[78] (the formulation of EpiLife® can be found in Appendix A). For the entire course of keratinocyte proliferation in monolayer and epidermis reconstruction, 4 different types of media were used, based on these two formulations[4]. One of the main differences in each media is their calcium composition. As studies with mouse keratinocytes have shown, calcium is a regulator of the growth of keratinocytes and, as such, the levels of calcium must be regulated according to the type of culture: while the cells can be grown as a monolayer and repeatedly subcultivated at a calcium concentration of 0.05 – 0.1 mM, the terminal differentiation of keratinocytes can be induced by increasing the levels of Ca^{2+} to the physiological concentration (1.0 – 1.5 mM). Thus, during the initial proliferation of keratinocytes in T-flask two different media are used[79]:

- Medium for culture setting, consisting of KBM™-2 supplemented with KGM™-2 SingleQuots™. It already contains in its composition 0.15 mM of Ca^{2+}, and it is used with frozen primary keratinocytes due to the high efficacy it demonstrates when seeding and starting the formation of colonies from this type of cells;

- Medium for culture growth, consisting in EpiLife® supplemented with 0.06 mM $CaCl_2$ and HKGS. This media is more efficient for further proliferation of keratinocytes and for subcultures.

During the phase of epidermis reconstruction on polycarbonate filter, the calcium in medium for culture growth is increased from 0.06 mM to 1.5 mM, to induce terminal differentiation of the keratinocytes, and two other different media are prepared:

- Medium for culture growth containing 1.5 mM calcium, used to seed the polycarbonate filter;

- Medium for epidermis reconstruction at air-liquid interface (RHE media) consisting of medium for culture growth with 1.5 mM Ca^{2+}, 50 µg/mL of vitamin C (Sigma-Aldrich Corp., St. Louis, MO, USA) and 10 ng/mL of recombinant human keratinocyte growth factor KGF/FGF-7 (R&D Systems, Minneapolis, MN, USA)
    - Prior to adding it to the RHE media, KGF was reconstituted at 100 µg/mL in sterile PBS containing 0.1 % bovine serum albumin (BSA), according to the instructions of the manufacturer;
    - Keratinocyte growth factor KGF (or FGF-7) is a protein that plays a key role in wound healing[80], and vitamin C, an antioxidant and an important cofactor in lipid hydroxylation[27].

All culture media were also supplemented with antibiotics, as recommended in the protocol for reconstruction of human epidermis: 50 U/mL of Penicillin G and 50 µg/mL of Streptomycin (Sigma-Aldrich Corp., St. Louis, MO, USA).

3.1.2. Cell Culture in Monolayer

First, after thawing the cells a 1:2 dilution of 20 µL of cell suspension in trypan blue (Sigma-Aldrich Corp., St. Louis, MO, USA) was prepared to count the number of viable keratinocytes in the cryovial. Trypan blue can penetrate cells with compromised membranes and stain them blue, by binding to intracellular proteins, being useful to identify and quantify live (unstained) and dead (blue) cells. The rest of the cell suspension in the cryovial was immediately transferred to a falcon containing 4 mL of

fresh medium for culture setting, in order to reduce the cell exposure to the dimethyl sulfoxide (DMSO) present in the freezing solution.

Keratinocytes were counted in a Bürker Counting Chamber (hemocytometer) (LO – Laboroptik Ltd, Lancing, UK) using an inverted microscope ECLIPSE TE2000-S (Nikon Instruments Inc., Melville, NY, USA) at magnification 200x. To ensure precision of the counting method, more than 10 cells needed to be counted in each of the 4 large squares in the corners of the hemocytometer, with a total of more than 100 cells counted per chamber. First the number of cells in one square (C_v) is calculated, as in equation 3.1:

$$(3.1)\ C_v(\text{cells/square}) = \frac{\text{number of live cells in 4 squares}}{\text{4 squares}}$$

Each of the large squares of the hemocytometer have a dimension of 1 mm x 1 mm x 0.1 mm (volume of 0.1 mm^3)[81], being possible to obtain the number of cells per mL of diluted sample (C_D) by multiplying C_v by 10^4, as in equation 3.2:

$$(3.2)\ C_D(\text{cells/mL}) = C_v \times \text{Dilution Factor} \times 10^4$$

By counting the number of live and dead cells, it is also possible to evaluate the viability of the cells in a cryovial, as in equation 3.3[82]:

$$(3.3)\ \text{Viability (\%)} = \frac{\text{Live cell count}}{\text{Live+Dead cell count}} \times 100$$

After counting, the cells were diluted to a seeding concentration of 1.25 x 10^4 viable cells/mL with medium for culture setting. The inoculation was performed in 75 cm^2 T-flasks with 15 mL of media. For subsequent days and subcultures this media was replaced with medium for culture growth. Cultures were incubated in a 37°C, 5 % CO_2/95 % air, humidified cell culture incubator with their media being changed every other day until the keratinocytes covered approximately 50 % of the available substrate (confluence). The control of the cell growth was performed by observing the cell culture at the inverted microscope using phase-contrast, a type of light microscopy that reveals cellular structures otherwise difficult to observe (or not visible at all) with an ordinary bright-field microscope, without the need to stain the cells (and consequently kill them). When the keratinocytes covered 50 % of the T-flask surface, the medium was changed every day until they reached 70 - 80 % confluence. The cells were then detached from the surface of the flask 8 minutes after adding 3 mL of a solution containing 0.025% trypsin, and re-suspended in 12 mL of blocking solution containing 2 % DFBS, which acts by blocking the action of trypsin on the cells to avoid damaging them. Subsequently the cells were centrifuged for 5 minutes at 335 g and 4 °C in a Heraeus Sepatech Centrifuge Biofuge 28RS (Heraeus, Hanau, Germany). The supernatant was removed and a pellet containing 2nd passage keratinocytes was obtained. The cells were then submitted to subcultures until the desired passage of keratinocytes was reached and they were ready to be used for epidermis reconstruction.

The remaining keratinocytes not used to inoculate T-flasks were cryopreserved following the protocol: first, the cells were suspended at 2x10^6 cells/mL with medium for culture growth; then, the cell suspension was diluted in an equivalent volume of freezing solution that consisted of 60 % medium for culture growth, 20 % DFBS and 20 % dimethyl sulfoxide (DMSO) (Sigma-Aldrich Corp., St. Louis, MO, USA, catalogue no. D2650) to obtain half of the initial concentration (1x10^6 cells/mL). During cryopreservation, DMSO is used to prevent the crystallization of water which would damage the cells. Aliquots of the cell suspension were then transferred to -80 °C in cryopreservation vials for at least 24h and in the end stored in liquid nitrogen tank for cryopreservation[83].

3.1.3. Reconstruction of Human Epidermis on Polycarbonate Filter

The pellet of keratinocytes previously obtained was dissolved in medium for culture growth containing 1.5 mM calcium chloride (Sigma-Aldrich Corp., St. Louis, MO, USA) and diluted to obtain a cell density of $3x10^5$ cells/mL. After placing Millicell® cell culture inserts with polycarbonate filter with inner diameter 10 mm and pore size of 0.4 µm (Merck Millipore, Billerica, MA, USA, catalogue no. PIHP01250) inside 6-well culture microplates, 500 µL of cell suspension were added to the upper compartment of the inserts and 2.5 mL of medium for culture growth containing 1.5 mM Ca^{2+} into the wells (under the polycarbonate filter, avoiding formation of air bubbles). Cultures were then left to incubate in a 37°C, 5 % CO_2/95 % air, humidified cell culture incubator for 24h, after which cells were exposed to the air-liquid interface by aspiration of the media in the upper chamber of the insert. The culture medium inside the well (under the polycarbonate filter) was replaced by 1.5 mL of medium for epidermis reconstruction at air-liquid interface (RHE media) consisting of medium for culture growth containing 1.5 mM calcium, 50 µg/mL of vitamin C and 10 ng/mL of recombinant human keratinocyte growth factor KGF/FGF-7. Media inside the well was renewed every other day and a morphologically fully differentiated epidermis was obtained after 11 days at the air-liquid interface.

3.1.4. Histological Analysis

The preparation and processing steps (until the wax infiltration inside the tissue) were performed according to what is described in the literature[4]. The sectioning of the tissue and the staining were performed by the Histopathology Unit (HU) of the Instituto Gulbenkian de Ciência (IGC).

First, the inserts containing skin were transferred to flasks filled with formalin 10 %, buffered (VWR International BVBA, Leuven, Belgium), which is a fixative and helps preserving the tissue, for at least 24h at room temperature. Then, the tissue was dehydrated in four successive baths of methanol to completely remove water from inside the tissue and subsequently submerged in toluene to detach the filter from the insert. The skin samples were placed in embedding cassettes properly labelled and incubated in pure toluene four times for 10 minutes, a clearing agent that replaces the alcohol trapped inside the tissues. This is because toluene is a miscible solvent with wax and will allow its infiltration into the tissue to eventually solidify it. Therefore, after the toluene baths the samples were dipped in a glass containing hot paraffin (60°C) to replace as much toluene in the skin as possible by liquid paraffin and then incubated for 1h at 60°C in another glass containing hot paraffin to allow its infiltration. After 1h, the glasses were brought to room temperature to allow the wax to solidify, after which the blocks of paraffin were sent to Histopathology Unit of IGC for further processing for microscopy. Following a protocol already established in that facility, the tissue samples were sectioned with a microtome and stained with Hematoxylin and Eosin (H&E) to allow a morphological analysis of the epidermis.

3.2. Skin Barrier Function

All diffusion experiments were performed as described in the literature[5,84] using 3 model drugs with different lipophilicities: caffeine (Alfa Aesar, Lancashire, UK), a highly hydrophilic drug; tamoxifen (Alfa Aesar, Lancashire, UK), highly lipophilic; and hydrocortisone (Sigma-Aldrich Corp., St. Louis, MO, USA), vastly used as a model drug for transdermal studies. For this experiment, 5 replicates of 3rd passage human reconstructed epidermis were used for each model drug. Both the Franz cells and the

water bath reservoir were manufactured at ITQB NOVA, and are represented in figure 3.1. The dimensions of the Franz cells are described in Appendix B.

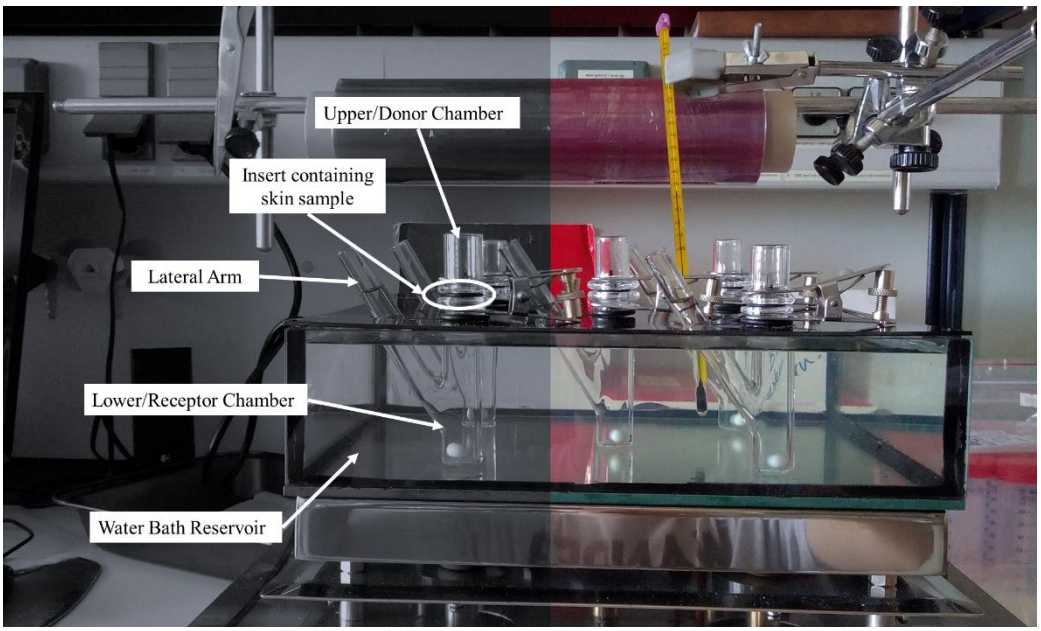

Figure 3.1 – Photograph of the assembly designed for the diffusion experiments.

Due to the available equipment, the model drug permeability tests could not be performed all at once, in a single day. Therefore, they were distributed in 3 consecutive days, in the following manner:

- Day 11 – caffeine permeability study;
- Day 12 – hydrocortisone permeability study;
- Day 13 – tamoxifen permeability study.

3.2.1. Diffusion Experiments

The water bath reservoir was kept at a temperature of 37 ± 0.5 °C. The Franz cells were mounted on top of the water reservoir and the receptor compartment was filled with phosphate buffered saline (PBS) with pH = 7.2. In the case of the penetration study with tamoxifen, 1 % of polyoxyethylene (20) cetyl ether (Brij-58®) (Sigma-Aldrich Corp., St. Louis, MO, USA) was added to the PBS solution since it is a solubilizer and helps overcome the low solubility of this drug. The flux of the substance in the donor chamber is dependent of the temperature and, as such, a thermostatic bath was used. A magnet was placed inside each Franz cell to allow a constant stirring to ensure homogenization of the solution in the lower chamber. Cell culture inserts containing reconstructed epidermis were carefully mounted on top of the Franz diffusion cells to avoid formation of air bubbles and left to hydrate for 1h.

Saturated suspensions of each model drug were prepared with propylene glycol (PG) (Sigma-Aldrich Corp., St. Louis, MO, USA), by adding as much of drug to a specific volume of PG as possible, until a thick suspension was obtained. Subsequently, 500 µL of the suspension were added to the donor chamber, after which all orifices of the Franz cells were covered with Parafilm®. The saturated suspensions were added to ensure a maximum thermodynamic activity[85] and to guarantee that the concentration of penetrant (model drug) in the upper chamber does not reduce during the test (remaining more or less constant during the whole experiment). As for the receptor phase, the amount of drug in

this chamber increases insignificantly during the experiment (sink conditions). To respect this condition, it was established that the concentration of drug in the receptor chamber should not exceed 10 % of the initial concentration in the donor phase[86]. At predetermined times (every 1h until 6h inclusive, then after 10h, 12h and on the next day after 24h) 300 µL samples were taken from the lateral arm of the receiver chamber (a micropipette with the aid of long capillary tips for gel loading was used so that the sample could be removed as near the magnet as possible) and immediately replaced by the same volume of fresh PBS solution to maintain a constant volume. The samples were kept at -20 °C prior to analysis by UV spectrophotometry.

3.2.2.NanoDrop

The samples were analysed using the UV-Vis application of the NanoDrop™ 2000c spectrophotometer (Thermo Fisher Scientific, Waltham, MA, USA). This application allows the equipment to work as a conventional spectrophotometer, displaying the absorbance of the sample from 190 - 840 nm[87]. The highest absorbance peak of each model drug was then identified: the detection of hydrocortisone was performed at 244 nm, caffeine 273 nm and tamoxifen 278 nm. The blank used was PBS.

In the case of hydrocortisone and tamoxifen, and specially the latter, these are hydrophobic substances quite difficult to dissolve in an aqueous solution. Therefore to prepare the standard solutions of these substances 1 % and 10 % of Brij-58® were added to hydrocortisone and tamoxifen solutions, respectively[5]. To make sure that the addition of the solubilizer would not interfere with the absorbance measurement of the drug, solutions of PBS with 1 % of Brij-58® and another with 10 % were also prepared and measured with the NanoDrop™. Their absorbance spectra were then analysed with the absorbance spectrum of PBS and the drug in question (see Appendix B).

It was verified that both PBS and PBS with 1 % of solubilizer do not absorb at all, which means that the use of this quantity of Brij-58® will not interfere with the absorbance of the drug. As for PBS with 10 % of solubilizer, which was used only for the standard solutions of tamoxifen, its absorbance is not significant, especially at 278 nm (wavelength where tamoxifen has its maximum peak of absorbance). The absorbance spectrum of each model drug was also obtained to confirm the reliability of the substances used by checking if their absorbance agreed with what is found in the literature (see Appendix B). By constructing calibration curves for the model drugs, it was possible to determine their concentrations in the samples.

3.2.3.Diffusion Experiments Data Analysis

To determine the cumulative corrected amount of substance that passed to the receiver compartment per unit area of skin in 24 hours (Q_{24}) it is first necessary to calculate the amount (mass) of model drug present in the solution of the receptor compartment at time = 24 (h) by multiplying the sample concentration with the volume. For this, it is necessary to do a correction of the amount of drug withdrawn from the receiver solution since every time a sample was taken part of the substance in that solution is removed, being the total mass that crossed the epidermis at a certain time given by equation 3.4[5,86]:

$$(3.4)\ Mass_{total}\ (\mu g) = V_s \left(\sum_{n=1}^{n} C_{n-1} \right) + C_n \times V_r$$

where C_n corresponds to the sample concentration in sample number "n". V_s and V_r are, respectively, the volume of the sample and volume of the receiver solution (volume of the Franz cell). The cumulative corrected amount could then be calculated using equation 3.5:

$$(3.5)\ \text{Cumulative Corrected Amount } (\mu g/cm^2) = \frac{\text{Mass}_{\text{total}}}{\text{Cross-sectional area of tissue}}$$

By plotting the cumulative corrected amounts ($\mu g/cm^2$) of drug permeated through the skin as a function of time (hours) it was possible to obtain the permeability parameters of the model drugs. The maximum flux values (Jmax) at steady state ($\mu g/cm^2/h$) were given by the linear portion of the graph with the maximum slope. By extrapolating that linear portion to the X-axis (time) it was obtained the lag time, which is the time it takes for the model drug applied to the skin to diffuse through it and finally be detected on its other side[88].

3.3. Metabolomic Analysis

3.3.1. Design of Experiment

3rd passage keratinocytes were used to inoculate T-flasks (25 and 75 cm^2) and proliferated in monolayer culture until they reached the desired confluence to seed the inserts. During this time, samples of media were collected for exometabolome analysis in the following manner:

- Before changing media;
- Middle time point between every change of media;
- After changing media.

After medium sample collection, the samples were immediately stored at -20°C. An additional 25 cm^2 T-flask (T25) was trypsinized to count the number of cells. Nine samples of media representative of the cell culture in T-flask over time (days) were obtained, as well as the corresponding cell number for that time point. Subsequently, inserts were seeded with keratinocytes and 4th passage skin was obtained.

During this period, samples of media were once again collected in the following manner:

- Before changing media;
- Middle time point between every change of media;
- After changing media.

Every time a sample of media was collected, one insert would be placed in fixative (formalin) to be further processed for histological analysis. Histological analysis allowed the determination of the thickness (µm) of the different *strata* of the epidermis, as well as its total thickness, by performing 10 measurements along two slices of skin (20 measurements in total for each timepoint). This information was used to normalize the rates of secretion and uptake to the number of cells and to the volume of the tissue. A biological replicate was performed, and the spectra acquisition and the metabolite quantification were performed in triplicate.

3.3.2. Quantification of Extracellular Metabolites

For the metabolomic analysis of the samples ^{1}H-NMR was used to quantify the extracellular metabolites in the culture. HPLC was used to quantify the amino acids. Ammonia was determined using K-AMIAR Ammonia Assay Kit (Megazyme, USA).

3.3.2.1. ^{1}H-NMR Methodology

3.3.2.1.1. Sample Preparation for NMR Analysis

The preparation of the samples for the ^{1}H-NMR and the acquisition of the spectra were performed as described in the literature[89].

First, a phosphate buffer prepared in D_2O and containing 5 mM of 3-(Trimethylsilyl)-1-propanesulfonic acid-d_6 sodium salt (DSS-d_6) (Sigma-Aldrich Corp., St. Louis, MO, USA) was prepared, as well as solutions of HCl and NaOH in D_2O. DSS is an internal standard that must be added to the samples in order to calibrate the ppm scale of the NMR spectra, being recommended by Chenomx NMR Suit (software used to integrate the exometabolome spectra) due to having a lower sensitivity to pH changes when compared to other standards (e.g. 3-trimethylsilylpropionate TSP)[90]. The addition of phosphate buffer to the samples helps minimizing the occurrence of shifts of NMR peaks due to pH changes that may have occurred during cell culture. Therefore, 110 µL of phosphate buffer supplemented with 5 mM DSS-d_6 were added to 500 µL of samples. When needed pH was adjusted to 7.4 with HCl or NaOH solutions. The use of deuterium oxide (D_2O) is because it has a different magnetic moment when compared to light water (H_2O) and, as opposed to it, does not interfere with the signal from the other molecules in the solution when performing ^{1}H-NMR. After centrifugation at 1000 g for 1 min, 500 µL were added to 5 mm NMR sample tubes and stored at 4 °C until analysis.

3.3.2.1.2. Spectrum Acquisition

The NMR data was acquired at CERMAX (Centro de Ressonância Magnética António Xavier), using an Avance II+ 500 MHz equipped with a 5 mm CryoProbe Prodigy TCI H/C/N (Bruker BioSpin Corporation, Billerica, MA, USA) that contains cold preamplifiers for ^{1}H, ^{2}H and ^{13}C which allow an increase of the signal to noise (vertical resolution) when compared to other probes and consequently improve the sensitivity of the spectrometer[67,70].

For the acquisition, the parameters of the equipment were set as recommended by Chenomx:

- Spectral (Sweep) width = 12 ppm
- Acquisition time: 4s
- Relaxation time (delay): 1s
- Working temperature: 25 °C

For each spectrum, 256 scans of the samples were collected.

3.3.2.1.3. NMR Spectra Integration

The integration of the obtained spectra and quantification of the metabolites was done with Chenomx NMR Suite software (Chenomx Inc., Alberta, Canada). It allows the reconstruction of the spectrum of the sample by doing a linear sum of spectra from pure compounds that are included in the software database[89,90]. As for the quantification, the total area under the resonance of a metabolite is directly proportional to its concentration[91] and, as soon as the peak is fitted, Chenomx immediately provides the concentration value of that metabolite (in mM).

3.3.2.2. Determination of Amino Acids by HPLC

3.3.2.2.1. Sample Preparation

For the preparation of the samples it was followed an already established protocol by the Animal Cell Technology Unit from ITQB-UNL/IBET. First, to ensure the detector limit of the HPLC was not reached due to a very high concentration, a 1:4 dilution of the samples with Milli-Q® (Merck Millipore, Billerica, MA, USA) and 20 µL of AABA (internal standard) (Sigma-Aldrich Corp., St. Louis, MO, USA) was made. Subsequently a deproteinization step was performed where a dilution of 1:2 was made by adding acetonitrile to the samples to precipitate any protein. After centrifugation at 19900 g for 15 min at 4 °C the supernatant was filtered and transferred to another vial. The derivatization agent AccQ-Fluor™ (6-aminoquinolyl-N-hydroxysuccinimidyl carbamate, AQC) (Waters Corporation, Milford, MA, USA), was reactivated, according to the protocol of the manufacturer, and left at room temperature[92]. It was used to derivatize the amino acids in the samples in a way that the derivatives could be separated by reverse-phase HPLC and quantified by fluorescence detection. This way, 70 µL of borate buffer and 20 µL of AccQ-Fluor™ reagent (AQC) were added to 10 µL of sample, mixed and left for incubate at room temperature for 1 minute. The samples were heated at 55 °C for 10 mins.

3.3.2.2.2. Data Acquisition with HPLC

The HPLC data was acquired with a Waters 2695 Separations module/Waters multi λ 2475 fluorescence detector (Waters Corporation, Milford, MA, USA) using an AccQ-Tag column 3.9 x 150 mm (Waters Corporation, Milford, MA, USA) for hydrolysate amino acid analysis by separation of the amino acid derivatives produced by the AccQ-Fluor™ derivatization reaction.

Two mobile phases were used, one containing 50 mM Sodium Acetate with 5 mM Triethylamine at pH = 5.5, and the other containing 100 mM Sodium Acetate with 5 mM Triethylamine at pH = 6.8. The standards were prepared from Pierce™ Amino Acid Standard H (Thermo Fisher Scientific, Waltham, MA, USA) and glutamine, asparagine and tryptophan.

3.3.2.3. Quantification of Ammonia

For the quantification of ammonia in the samples a K-AMIAR Ammonia Assay Kit was used. The working principle is that starting from a sample containing ammonia, 2-oxoglutarate and reduced nicotinamide-adenine dinucleotide phosphate (NADPH), the addition of glutamate dehydrogenase (GIDH) will trigger a reaction where ammonium ions (NH^{4+}) react with 2-oxoglutarate to form L-glutamic acid and $NADP^+$, as in equation 3.7:

$$(3.7)\ \text{2-Oxoglutarate}+\text{NADPH}+NH_4^+ \xrightarrow{(\text{GIDH})} \text{L-glutamic acid}+NADP^+ + H_2O$$

The amount of $NADP^+$ formed is directly proportional to the amount of ammonia, and the consumption of NADPH can be measured with a spectrophotometer at 340 nm.

3.3.3.Metabolomic Data Analysis

Through the use of Chenomx and by constructing calibration curves for the analysed compounds in HPLC and the ammonia kit, it was possible to determine the metabolite concentrations (mM) in the media. The rates were obtained through a linear regression method between the number of moles of the compound (mmol) in the media against the duration of the latter (days). This was done for each 3 points (after adding media, middle time point, and before adding media) and the slope of the line represented the value of uptake/secretion rate. After this, the rates were normalized according to the number of cells (mmol/days/10^4 cells) during the proliferation phase in T-flask, and to the skin volume (mmol/days/μm^3) during epidermis reconstruction phase in inserts.

3.4. Total Protein Quantification of Reconstructed Human Epidermis

3 samples of skin grown in normal conditions and 3 of skin in an improved media containing 3 times the concentration of selected amino acids were used to quantify the total protein in the tissues.

3.4.1.Protein Extraction from Skin

A lysis buffer containing 1 % v/v Triton X-100, 2 % v/v Sodium Dodecyl Sulfate (SDS) and twice concentrated cOmplete™ Protease Inhibitor Cocktail (Sigma-Aldrich Corp., St. Louis, MO, USA) was used. The filter containing epidermis was removed from the insert with the help of a scalpel. Subsequently, the homogenization of the skin was performed by grinding with liquid nitrogen in a mortar[93]. The homogenized skin was transferred to a vial and 200 µL of lysis buffer were added. The samples were boiled at 99 °C for 7 min and centrifuged at 9300 g for 5 min to pellet all the cellular debris and the filter that were not dissolved in the lysis buffer. The supernatant was transferred to a different vial and the pellet (again submitted to 200 µL of lysis buffer) was submitted to sonication, using a Sonicator/cell disruptor Branson 450 CE (Branson Ultrasonics, Danbury, USA) with the following parameters: 12 pulses, 2s ON, 5s OFF, amplitude 10 %. Both the supernatant and the pellet were placed in a thermomixer at 75 °C and 350 rpm for 15 min. If the protein had eventually precipitated during the homogenization with liquid nitrogen or during boiling at 99 °C, the sonication and the incubation at 75 °C would cause its denaturation and make it easier to dissolve in lysis buffer. After incubation, the pellet was centrifuged at 1000 g for 2 min and the resulting supernatant transferred to a different vial. The pellet was stored at -20 °C. This process was repeated two additional times for each

pellet, so that, in the end, 4 protein extractions had been done for each skin (4 supernatants containing extracted protein for each replicate of skin).

3.4.2. Total Protein Quantification

For the quantification of total protein in the supernatants obtained a Micro BCA™ Protein Assay Kit (Thermo Fisher Scientific, Waltham, MA, USA) was used, which is a detergent-compatible bicinchoninic acid (BCA) formulation.

4. RESULTS & DISCUSSION

4.1. Morphology of *in vitro* Reconstruction of Human Epidermis

Human epidermal keratinocytes isolated from neonatal foreskin (HEKn) were successfully seeded to recreate an *in vitro* equivalent of the epidermis. The reason to choose this type of keratinocytes was because these present a greater growth potential than adult cells, having a more regular and consistent growth. Furthermore, foreskin keratinocytes express higher levels of stem cell markers than from other tissue sites (e.g. auricular keratinocytes), having a higher capacity for epidermal reconstruction[33,94].

After 11 days of culture of 3rd passage keratinocytes at air-liquid interface a fully differentiated epidermis similar to the native was obtained, containing all the 4 *strata*: *stratum basale* anchored on the polycarbonate filter, *stratum spinosum*, *stratum granulosum* (containing keratohyalin granules) and *stratum corneum* (see figure 4.1).

Figure 4.1 - Histology of the reconstructed human epidermis (approx. 77 µm thick) at 11 days at air-liquid interface. Magnification 400x. PF – Polycarbonate Filter; SB – *Stratum* Basale; SS – *Stratum Spinosum*; SG – *Stratum Granulosum*; SC – *Stratum Corneum*.

The use of H&E stain is very helpful for the histological analysis of tissues like the epidermis, since it allows to distinguish many cytoplasmic, nuclear, and extracellular matrix structures. Hematoxylin is the name of a complex formed from aluminium ions and oxidized hematoxylin, and when it is applied to the sample it confers the purple/blue colour to any basophilic (acidic) components of the cells. Then, by applying eosin (an acidic dye), it reacts with the eosinophilic (acidophilic/ basic) components of the cells and stains them in various shades of red and pink. Thus, hematoxylin binds to the nucleus (contains DNA), as well as some parts of the cytoplasm that also contain nucleic acids (RNA in ribosomes and in the endoplasmic reticulum), and other structures (including keratohyalin granules), because they are acidic, staining them purple. On the other hand, eosin binds to the proteins present in the cytoplasm, since most of them are basic, as well as to the corneocytes in the *stratum corneum*, since they lack nuclei, and stains them pink[95].

Not only the morphology of the skin was evaluated but also its thickness. According to what was found in the literature, the commercially available skin equivalents vary very much in thickness, with the penetration models EpiDerm™ and Episkin™ ranging from around 30 – 50 µm, when comparing to the native epidermis that ranges around 80 – 90 µm[6]. During this study it was observed that the RHE showed much variability from batch to batch, but, on average the thickness of the skin was around 70 µm.

4.2. Evaluation of the Barrier Properties of *in vitro* Skin

After obtaining a fully differentiated epidermis *in vitro* it was then necessary to evaluate the barrier properties of this skin model. To achieve this objective, three model drugs with different lipophilicities were selected for the diffusion tests: caffeine, hydrocortisone and tamoxifen. In figure 4.2 is represented a H&E staining of a sample of the batch of 3rd passage skin used for these diffusion studies. Interestingly, in this figure it is possible to see layers of corneocytes that seem to be detaching, which may be due to the desquamation phenomenon.

Figure 4.2 – 3rd passage RHE (approx. 100 µm thick) at 11 days at air-liquid interface used in permeability study. Magnification 400x.

Given that the skin culture was prolonged two more days than the usual (11 days, with the last renovation of media at the 10th day), another renovation of the media was done at day 12, to ensure that the skins had all the nutrients available. The results of the diffusion tests were expressed as average ± standard deviation (SD) and compared to data from other skin models available in the literature, namely native skin excised from human cadaver (Female, Caucasian abdominal, 500 µm thick) and a commercial model used specifically in permeability studies EpiDerm™ (MatTek Corporation, USA)[5]. These results can be found in table 4.1 and the permeability profiles for each model drug (through the skin) can also be viewed in figures 4.3 to 4.5.

Table 4.1 – Comparison of model drug permeability of reconstructed human epidermis (RHE) with commercial model EpiDerm™ and native skin from human cadaver (n=5, average ± SD)[5]

Drugs	Permeability Parameters	RHE	EpiDerm™	Human Cadaver
Hydrocortisone	Lag time (h)	3.9 ± 0.7	0	2.5 ± 0.3
	Q_{24} (µg/cm^2)	298.7 ± 253.3	93.0 ± 18.4	27.4 ± 7.2
	Jmax (µg/cm^2/h)	14.2 ± 12.1	4.8 ± 0.8	1.8 ± 0.2
Caffeine	Lag time (h)	1.6 ± 0.3	0	5.5 ± 0.3
	Q_{24} (µg/cm^2)	28437.8 ± 4120.3	210.2 ± 78.6	11.0 ± 0.9
	Jmax (µg/cm^2/h)	1222.0 ± 185.0	11.0 ± 1.7	0.7 ± 0.1
Tamoxifen	Lag time (h)	3.5 ± 1.0	2.1 ± 1.4	5.2 ± 2.7
	Q_{24} (µg/cm^2)	140.3 ± 31.5	69.4 ± 5.2	49.1 ± 7.8
	Jmax (µg/cm^2/h)	8.8 ± 2.0	6.3 ± 2.4	2.8 ± 0.8

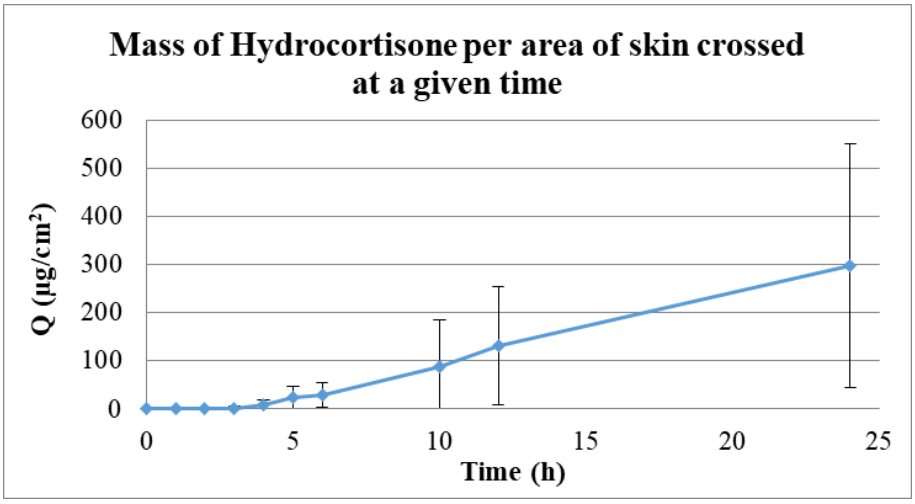

Figure 4.3 – Permeability profile of hydrocortisone in RHE during 24h (n=5, average ± SD).

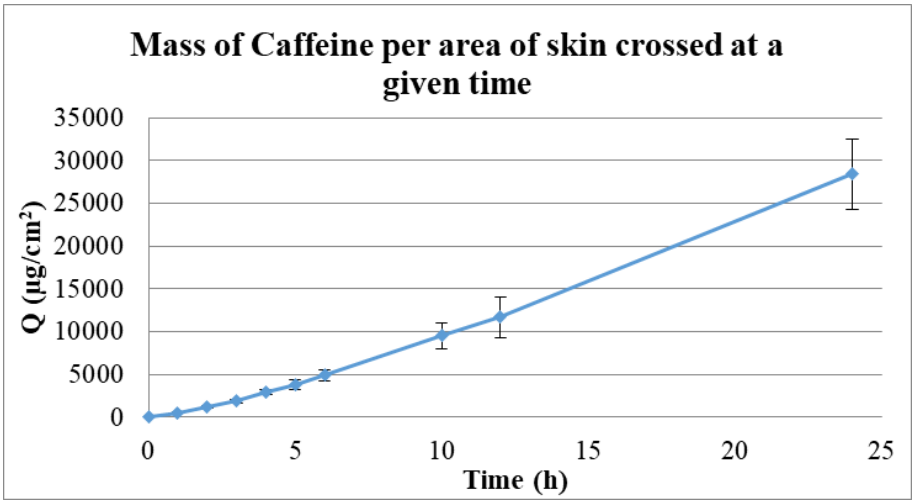

Figure 4.4 – Permeability profile of caffeine in RHE during 24h (n=5, average ± SD).

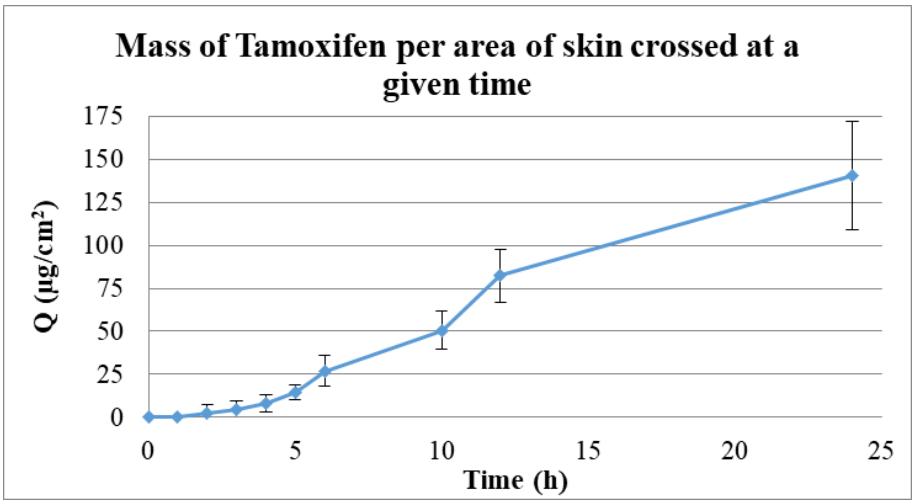

Figure 4.5 – Permeability profile of tamoxifen in RHE during 24h (n=5, average ± SD).

The diffusion tests were always performed under infinite dose conditions, with the amount of model drug in the receptor chamber being always below the permitted range of 10 % of the initial concentration in the donor phase. From the obtained results, it is possible to see that the skin is much more permeable than both the EpiDerm™ model and human cadaver skin. In fact, according to the Q_{24}, which is the cumulative corrected amount of substance that passed to the receptor compartment in the Franz cell per unit area of skin in 24 hours, when comparing to the EpiDerm™ model the RHE demonstrated to be 100 times more permeable to caffeine, 3 times more permeable to hydrocortisone and 2 times more permeable to tamoxifen. Concomitantly, the maximum flux values (Jmax) of the model drugs diffusion are also higher than the EpiDerm™ equivalent. As for the lag time, it is an indicator of the time taken for the drug to diffuse through the skin, and in this case, it would be expected, by checking the permeability profiles of the drugs, that caffeine took less time to pass through the skin, while tamoxifen and hydrocortisone took more time. Since this parameter is dependent on the calculation of the flux, it is not possible to use it as a comparison to the other models.

As said before, the main barrier of the skin against drug diffusion is the *stratum corneum* (SC), more specifically, the lipid matrix embedding the corneocytes. Due to the hydrophobic nature of this matrix, polar and non-polar substances travel through different diffusional pathways, being easier for more lipophilic drugs to be transported through the skin[5,20,29]. In the case of the permeability parameters for native skin, it is possible to see that there really was a more facilitated passage to tamoxifen, the most lipophilic drug, followed by hydrocortisone (semi-polar) and caffeine, the most polar substance. However, the totally opposite occurs to the cultivated RHE and to the EpiDerm™ model. While RHE was seen as being much more permeable than the latter, both showed a higher permeability to caffeine than the other substances, being tamoxifen the model drug that penetrated the less.

4.3. Metabolomic Analysis

4.3.1. Metabolomic Analysis Study

During the stage of keratinocyte proliferation, one T25 was trypsinized every time a sample of media was collected so that a relation could be established between the number of cells with the uptake/secretion rates of the metabolites in the culture media. For that, 3 technical replicates of the cell

count were performed for each timepoint. In figure 4.6 is represented the exponential growth of the keratinocytes, expressed mathematically by the equation 4.1:

$$(4.1)\ y=0.1844e^{0.4681x}$$

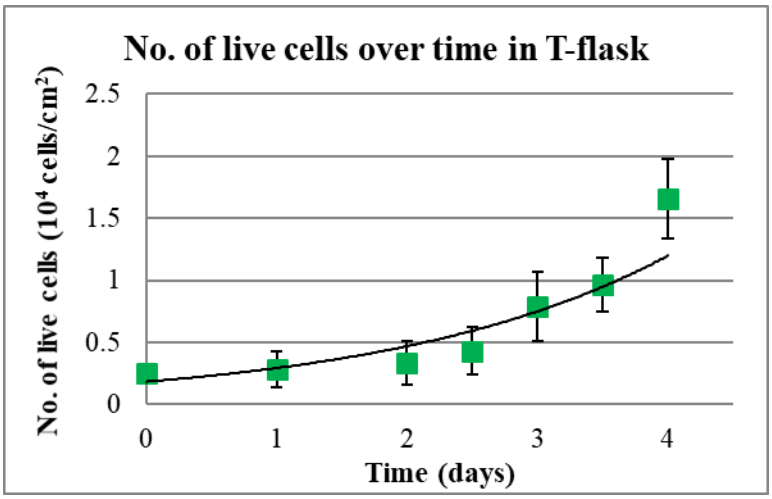

Figure 4.6 – Number of keratinocytes over time during monolayer culture in T-flask (n=3, average ± SD).

Based on figure 4.6 it is possible to see that the cells experience a greater increase in their numbers from day 3 to 4 (see also Appendix C). This is something that has already been observed during other batches of HEKn culture, since the cells usually take the first 3 days to occupy around 50 % of the T-flask. Then, only one day after (at day 4) the keratinocytes already occupy 70 – 80 % of the available substrate. In figures 4.7 – 4.9 are represented the different growth stages of the keratinocytes.

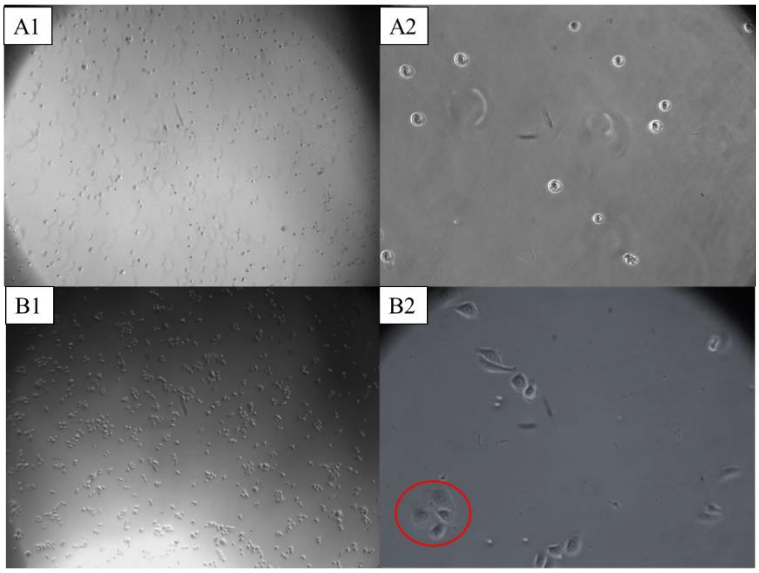

Figure 4.7 – Cell Culture: (A1-A2) Keratinocytes at day 0, after inoculation of culture flasks containing medium for culture growth. (B1-B2) Keratinocytes at day 1, already attached to the surface of the T-flask and started to form small colonies (highlighted in red). There were, however, still a lot of empty spaces between these colonies, with a cell confluence of around 20 %. It is also possible to find many cells floating, which meant that these were probably dead cells that eventually disappear with the renovation of the media. (A1/B1) Magnification: 40x. (A2/B2) Magnification: 200x.

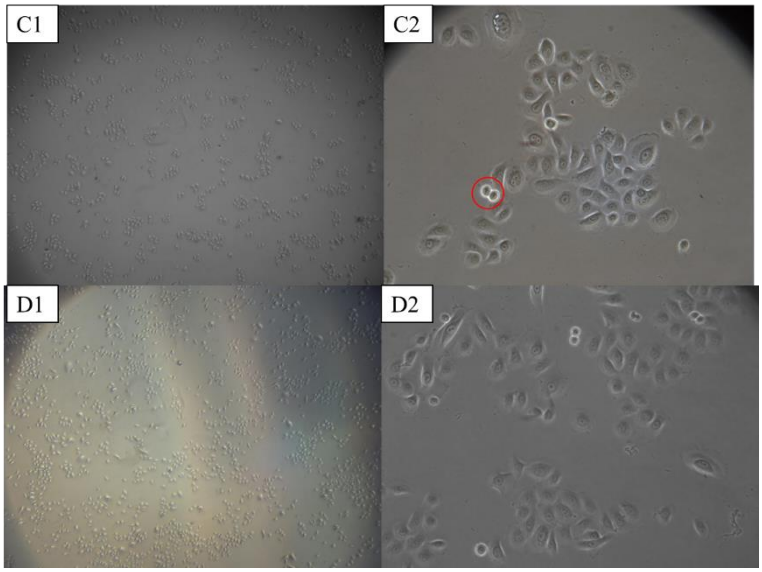

Figure 4.8 – Cell Culture: (C1-C2) Keratinocytes at day 2, with formation of bigger colonies. It is easier to find mitotic figures since their number started to increase (highlighted in red). At this point the confluence has not changed much from the past day, being around 25 %. (D1-D2) Keratinocytes at day 2.5, yet with more colonies and more mitotic figures. (C1/D1) Magnification: 40x. (C2/D2) Magnification: 200x.

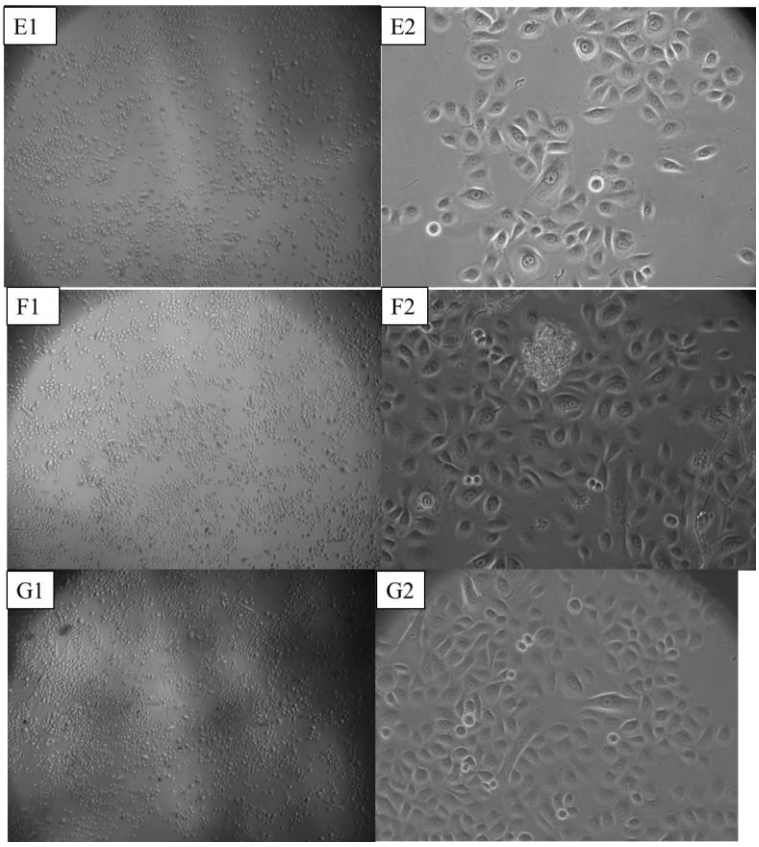

Figure 4.9 – Cell Culture: (E1-E2) Keratinocytes at day 3, already reached a confluence of 50 %; (F1-F2) Keratinocytes at day 3.5, with a big alteration of cell confluence, being already at around 60 %, with fewer empty spaces on the surface of the flask as there was previously. This was already expected since it was observed a high number of mitotic figures. The keratinocytes colonies are now very extensive and still a high number of mitotic figures are visible. (G1-G2) Keratinocytes at day 4, the cells had already achieved a confluence of around 70-75 %. Keratinocytes cannot be grown up to more than 80 % to the risk of losing the proliferative capacity of these cells, and as such, they are now ready to be seeded in inserts. (E1/F1/G1) Magnification: 40x. (E2/F2/G2) Magnification: 200x.

Then, in the stage of reconstruction of human epidermis in polycarbonate filter, one insert was prepared for histological analysis every time a sample of media was collected so that a relation could be established between the volume of skin (by measuring its thickness on the microscope) with the uptake/secretion rates of the metabolites in the culture media. In figure 4.10 it is possible to see the increase in thickness over time (see also Appendix C), which is expressed mathematically by the equation 4.2:

$$(4.2)\ y = 8.0812x + 3.1849$$

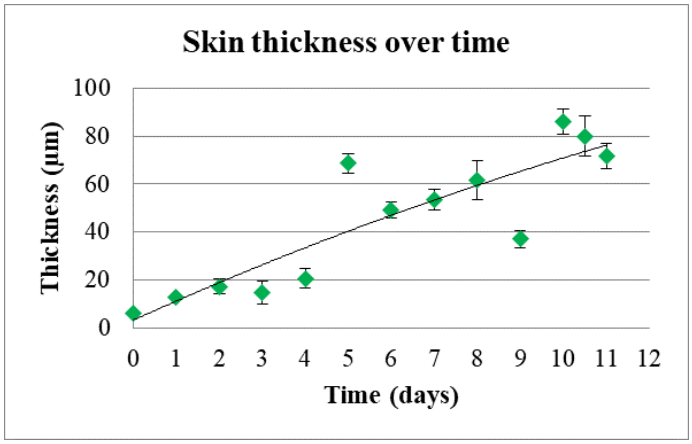

Figure 4.10 – Increase of epidermis thickness over time at air-liquid interface (n=20, average ± SD).

The development of the skin *strata* during the time of culture is represented in figure 4.11, being possible to see that at the first day at air-liquid interface only SB exists, with SS appearing at day 2 and the rest of the *strata* (SG and SC) at day 3. Then, their thickness keeps increasing (opposed to SB, which keeps decreasing, with the basal cells becoming more compact and squared) until they reach an equilibrium at around days 8-9. It is important to refer that no information could be obtained regarding skin thickness during the time the cells are still submerged in media (before changing to air-liquid interface). During the preparation of those skin samples for histological analysis, the filter holding the skin/cells dissolved completely in the bath with toluene. This means that no skin, or a very much thin skin, was created at that time, or else the filter would not have been dissolved so easily, as was verified with the skin samples at more advanced stages of development.

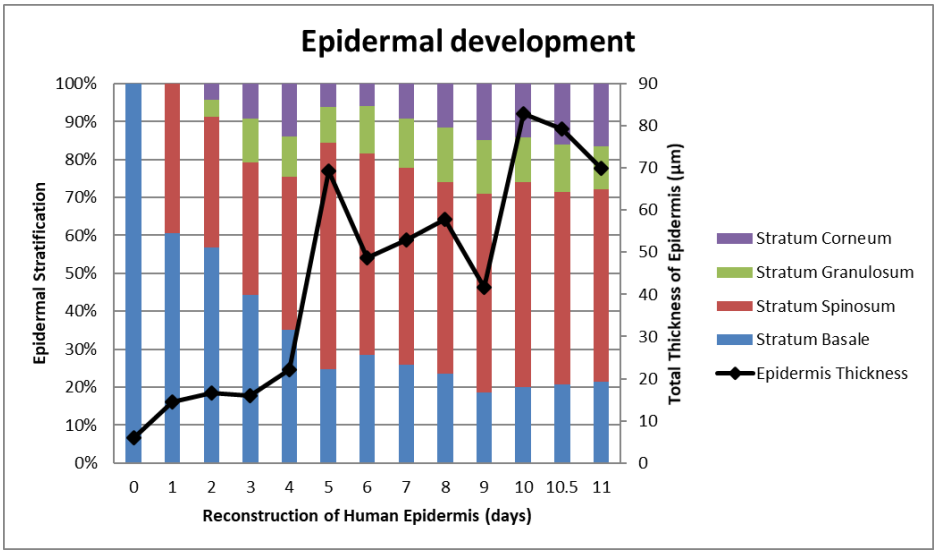

Figure 4.11 – Epidermal development with *strata* differentiation over time at air-liquid interface (average ± SD).

After analysing the obtained ^{1}H-NMR spectra for each sample, there was still a significant number of metabolites that were not possible to quantify with this technique, namely:

- Amino Acids
  - Asparagine
  - Aspartic acid (Aspartate)
  - Cysteine

- Vitamins
  - Biotin
  - D-Pantothenic acid (Pantothenate)
  - Folic acid
  - Niacinamide
  - Pyridoxal (Pyridoxine)
  - Riboflavin
  - Thiamine
  - Vitamin B12

- Other components
  - DL-alpha-Lipoic acid
  - Ethanolamine
  - Phosphoethanolamine
  - Putrescine
  - Thymidine

At around 2.5 – 4.0 ppm a broad signal caused by the HEPES buffer masked the amino acids asparagine, aspartate and methionine, as well as ethanolamine. Cysteine, on the other hand, was located in a region crowded by other metabolites, being very difficult to identify as well. As for the rest of the metabolites they are probably in very low concentrations (as seen in MCDB 153 formulation[78] and in Appendix A) and, as such, they did not even appear in the spectra.

Due to the somewhat large number and variety of metabolites that needed to be measured, a decision was taken to quantify the amino acids based on the premise that keratinocytes, during the differentiation stage, need to produce many structural proteins and, as such, it is vital to have all the building blocks available, the amino acids. In fact, besides being composed of keratin (composed, in turn, by many amino acids including glycine, serine, glutamate and glutamine), keratinocytes do produce many different types of proteins along their process of keratinization: in the SS they produce envelope proteins (like filaggrin, involucrin and small proline-rich proteins) constituted of glycine, serine, lysine, glutamine and proline; and in the SG, where the keratohyalin granules are composed of profilaggrin and loricrin rich in, respectively, histidine and cysteine[22]. Thus, the composition in amino acids was of the most interest. Since by ^{1}H-NMR some amino acids could not be quantified, namely aspartate, asparagine and cysteine, the analysis was then complemented with their determination by HPLC. In addition, the ammonia concentration was also determined since animal cell cultures produce ammonia which can be toxic to the culture process. The concentrations of the metabolites are represented in figures 4.12 – 4.44.

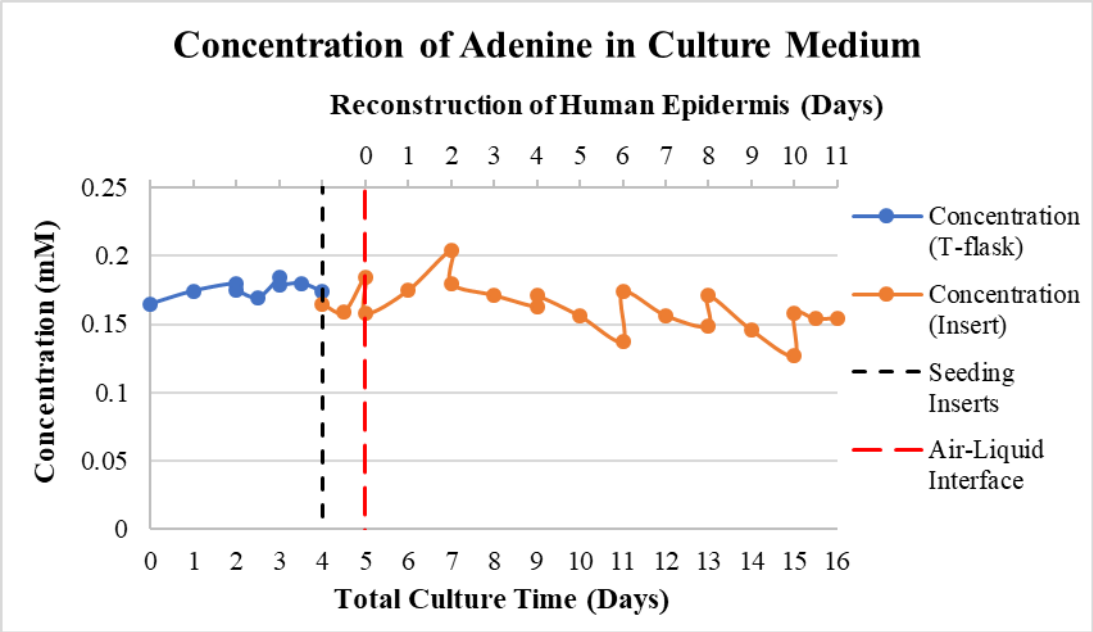

Figure 4.12 – Concentration of Adenine in culture medium over time.

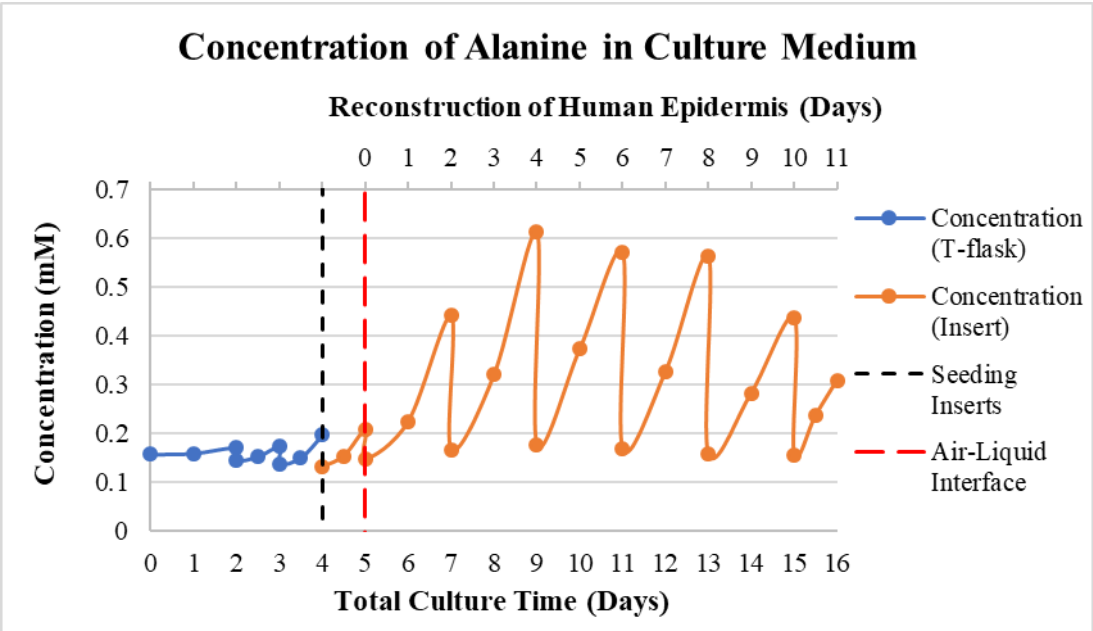

Figure 4.13 – Concentration of Alanine in culture medium over time.

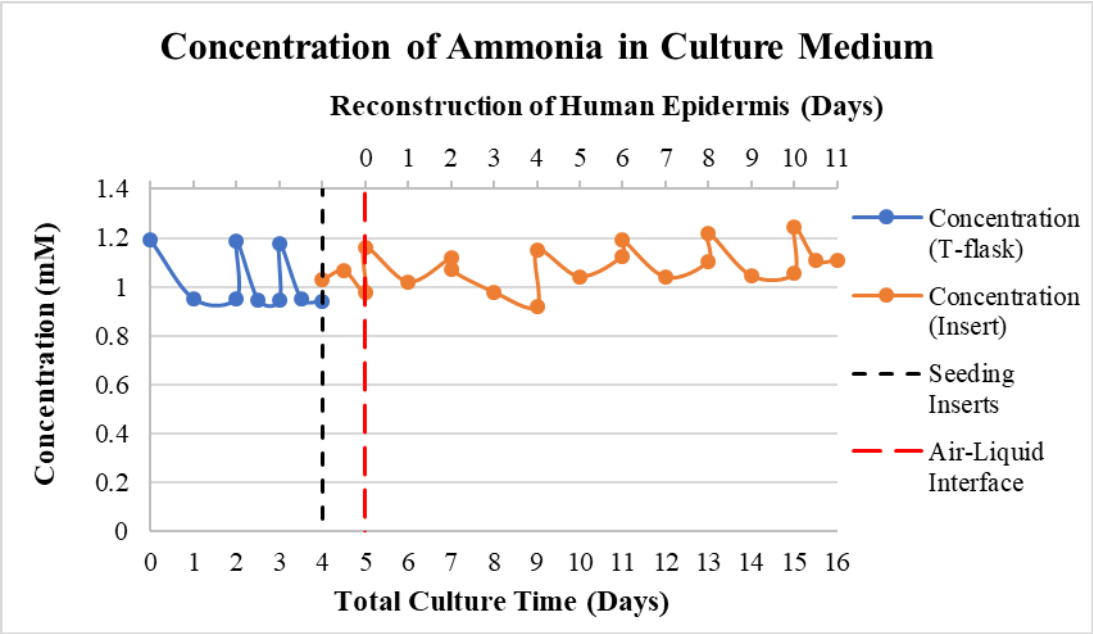

Figure 4.14 – Concentration of Ammonia in culture medium over time.

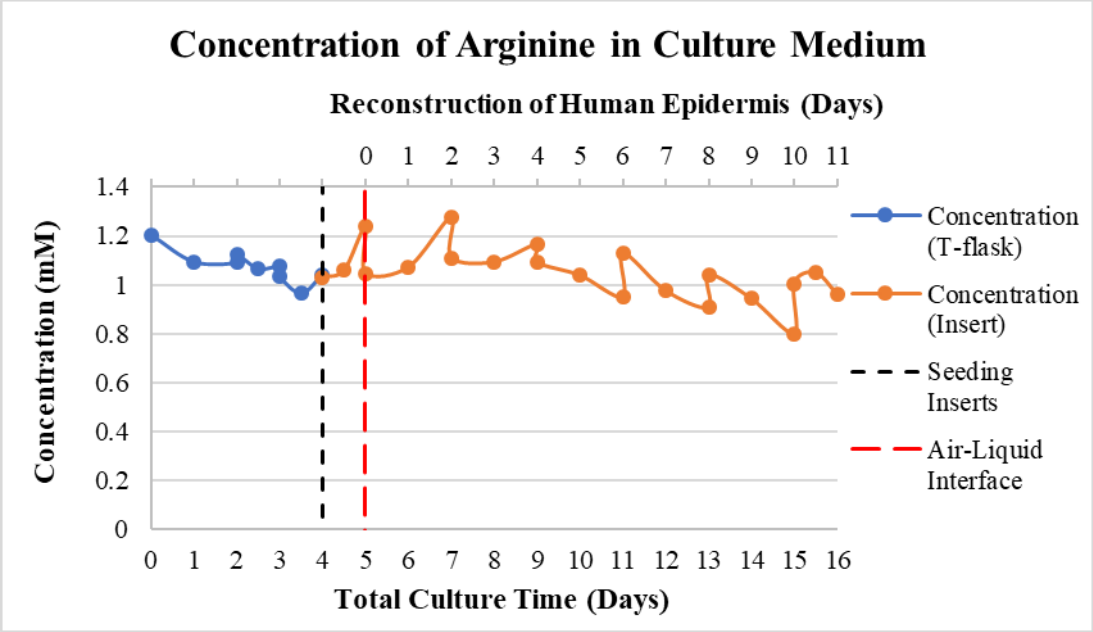

Figure 4.15 – Concentration of Arginine in culture medium over time.

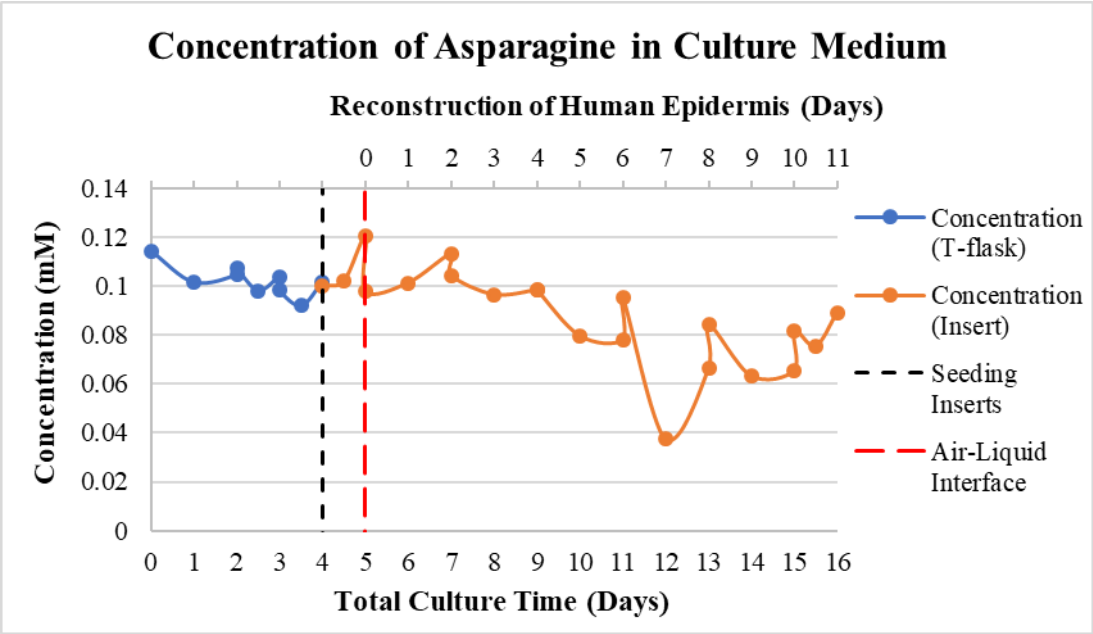

Figure 4.16 – Concentration of Asparagine in culture medium over time.

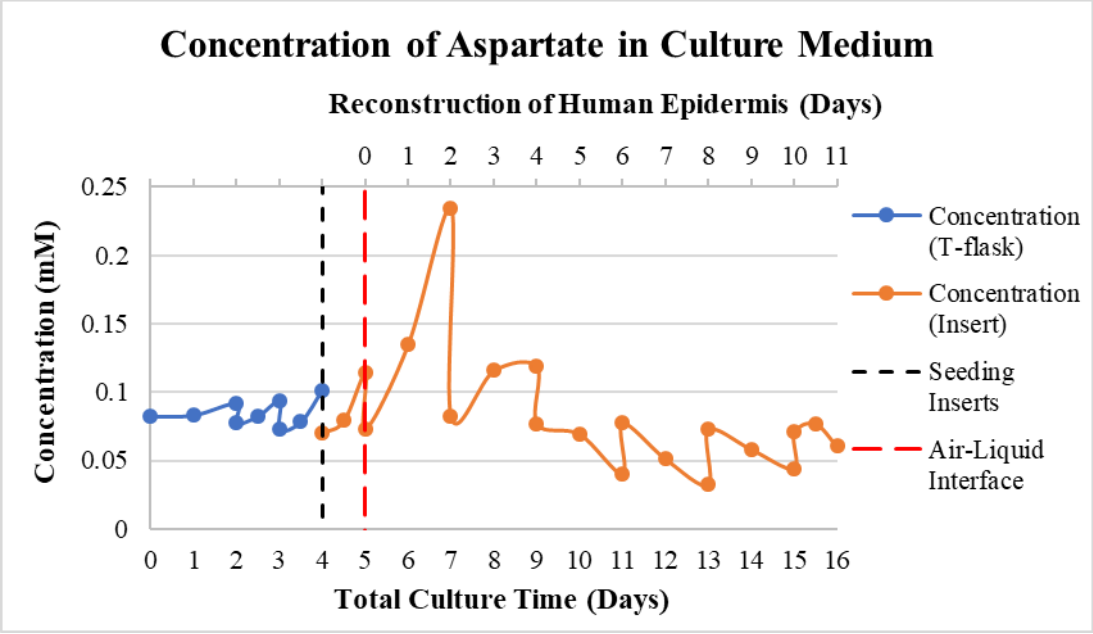

Figure 4.17 – Concentration of Aspartate in culture medium over time.

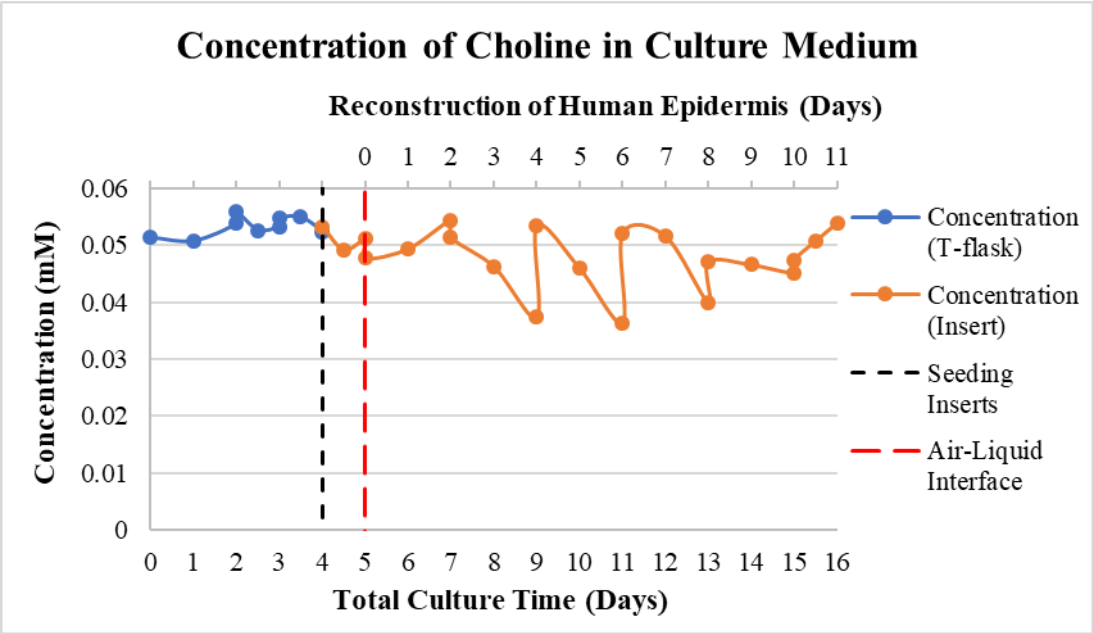

Figure 4.18 – Concentration of Choline in culture medium over time.

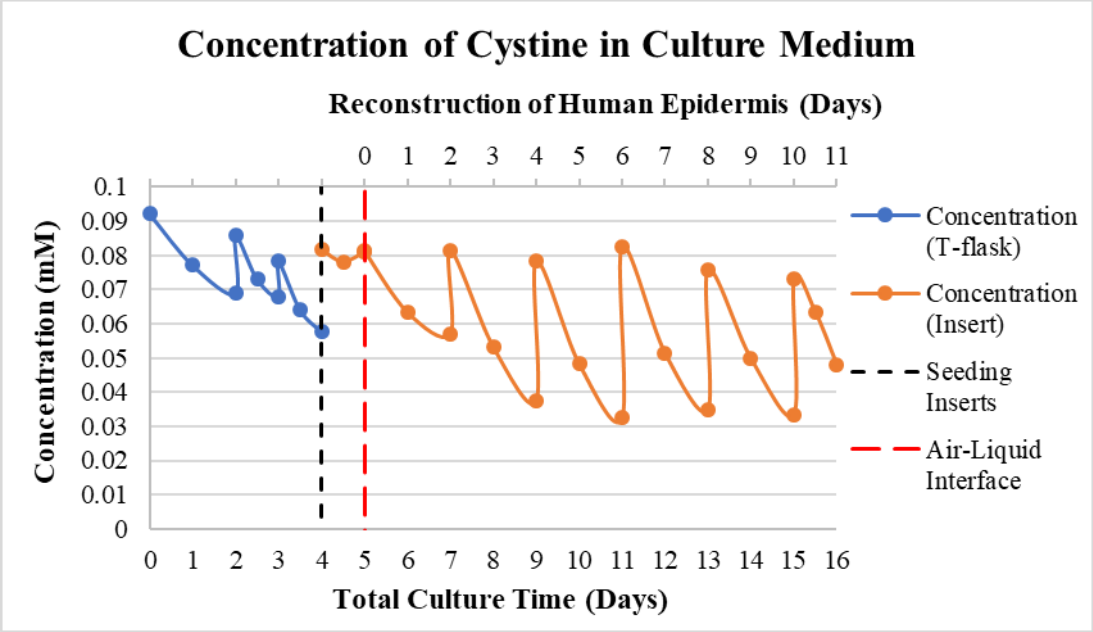

Figure 4.19 – Concentration of Cystine in culture medium over time.

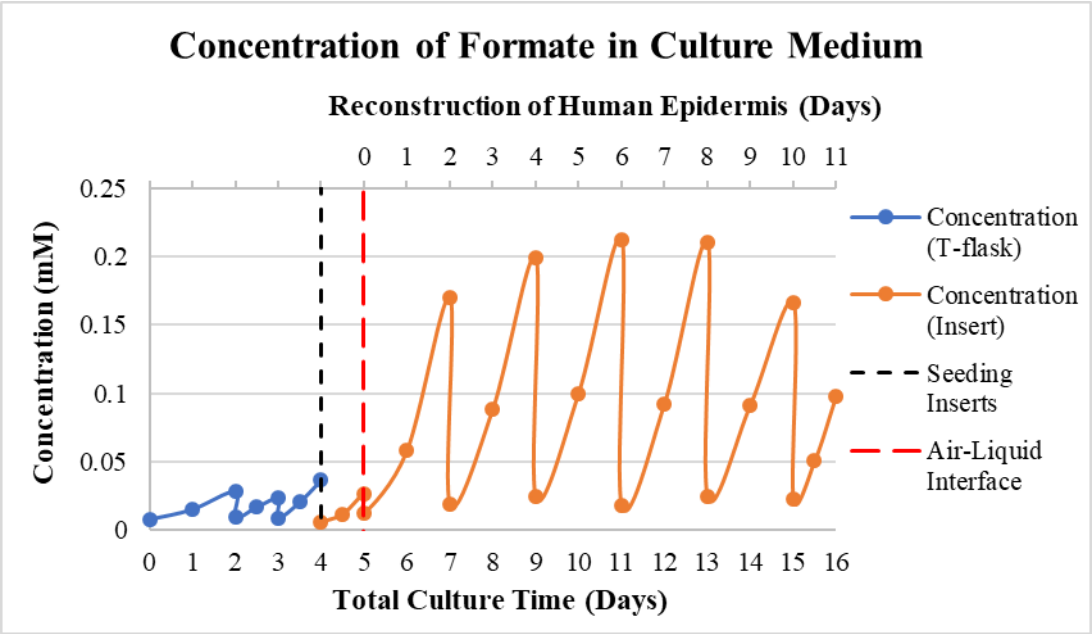

Figure 4.20 – Concentration of Formate in culture medium over time.

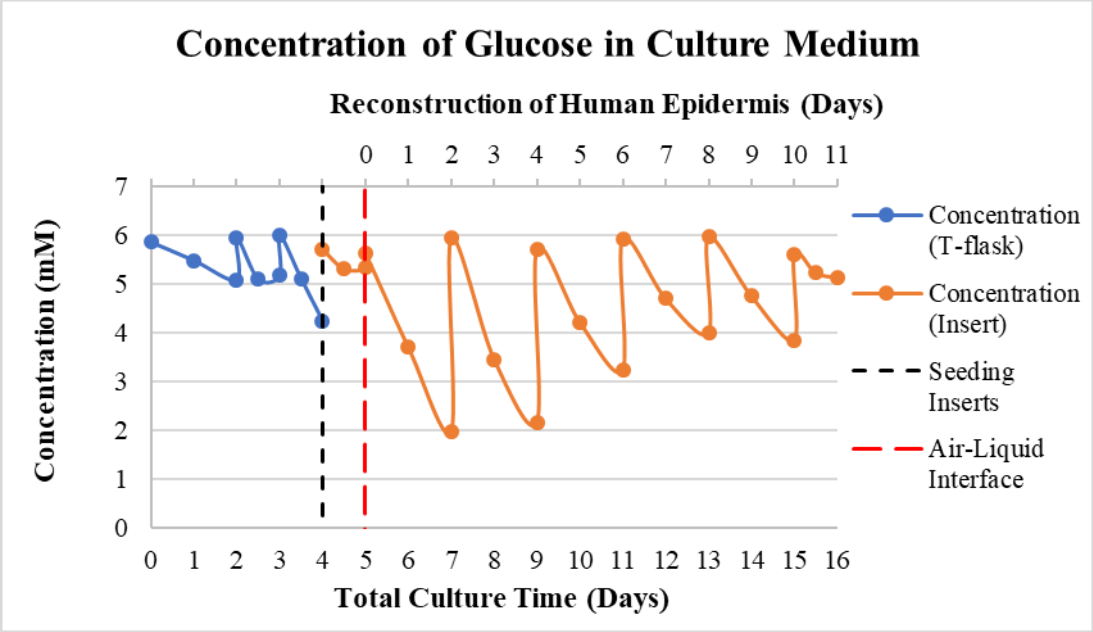

Figure 4.21 – Concentration of Glucose in culture medium over time.

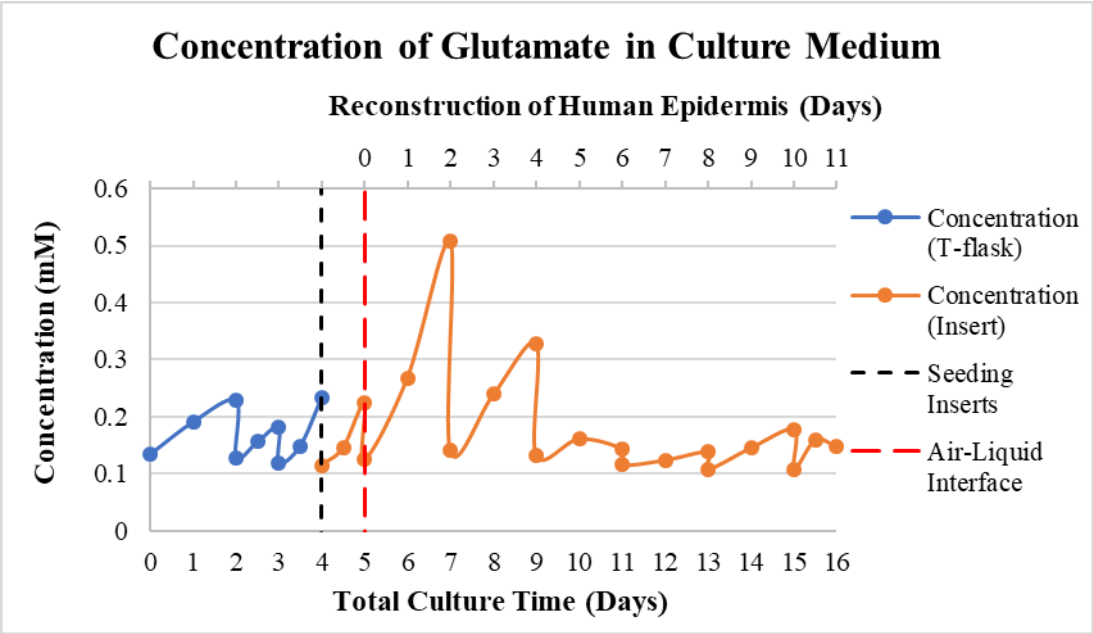

Figure 4.22 – Concentration of Glutamate in culture medium over time.

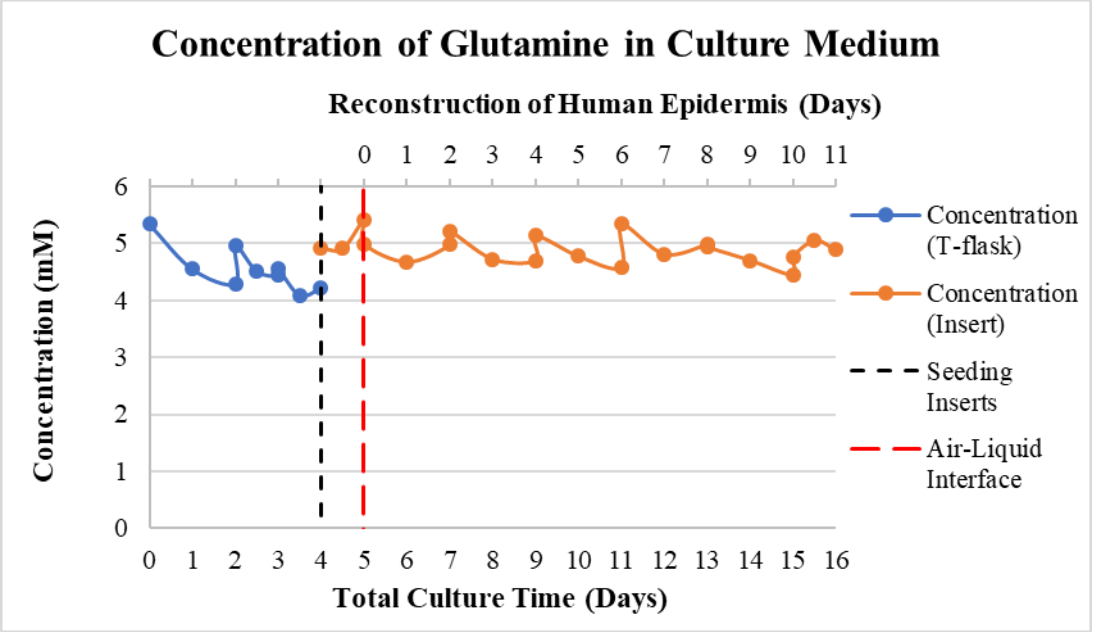

Figure 4.23 – Concentration of Glutamine in culture medium over time.

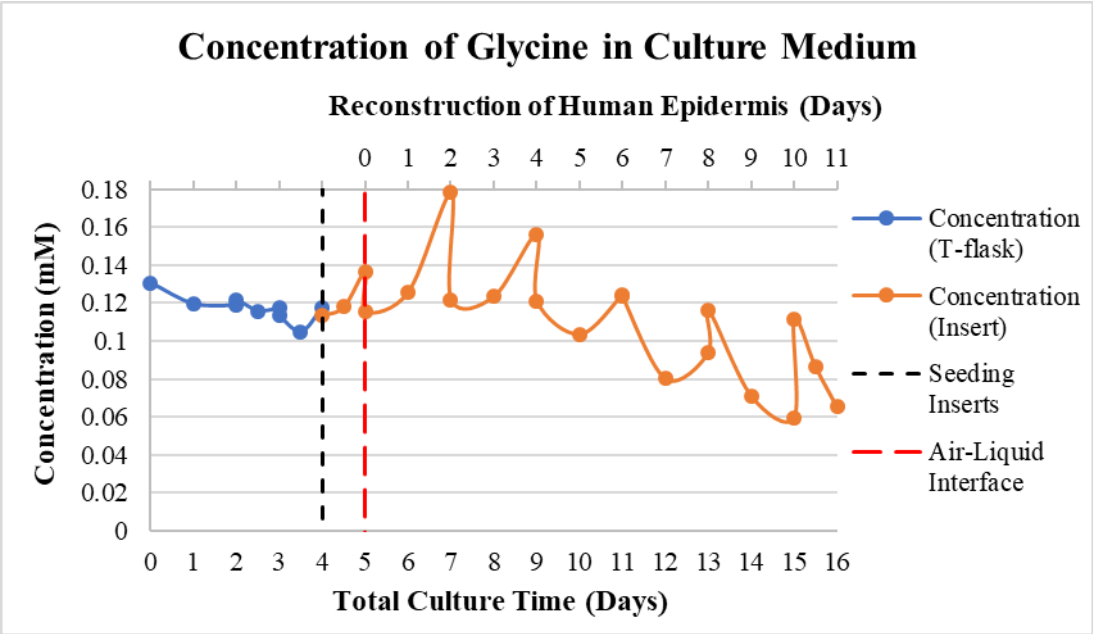

Figure 4.24 – Concentration of Glycine in culture medium over time.

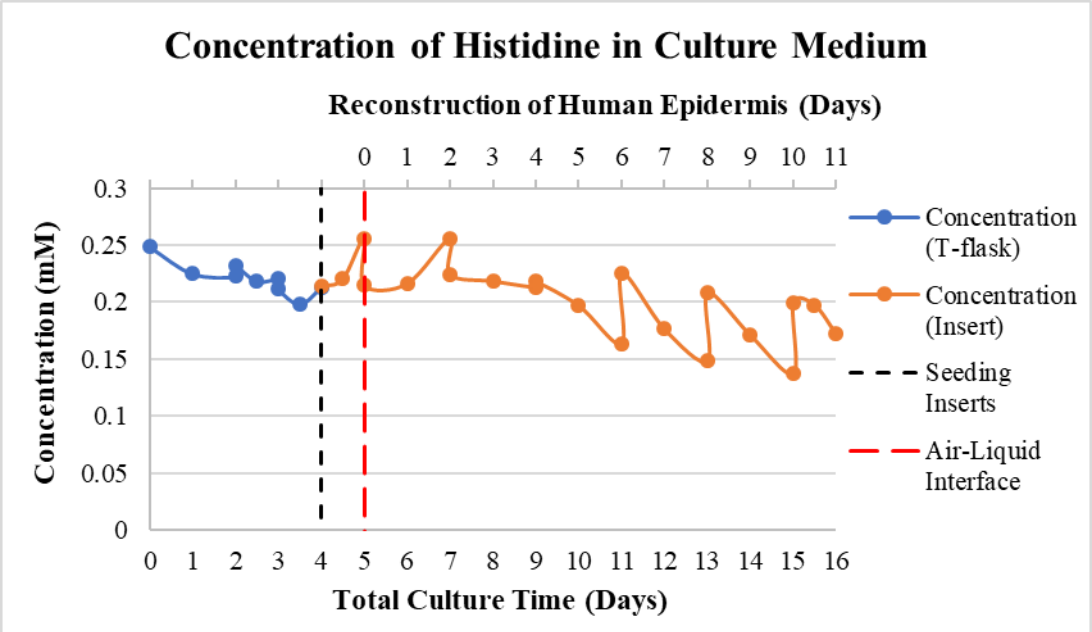

Figure 4.25 – Concentration of Histidine in culture medium over time.

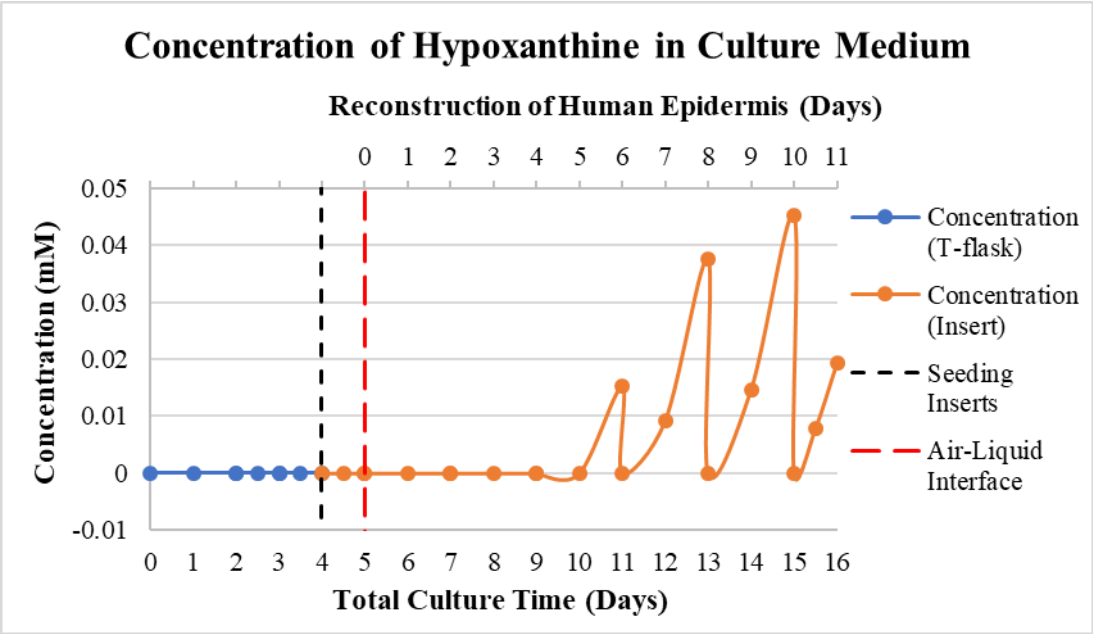

Figure 4.26 – Concentration of Hypoxanthine in culture medium over time.

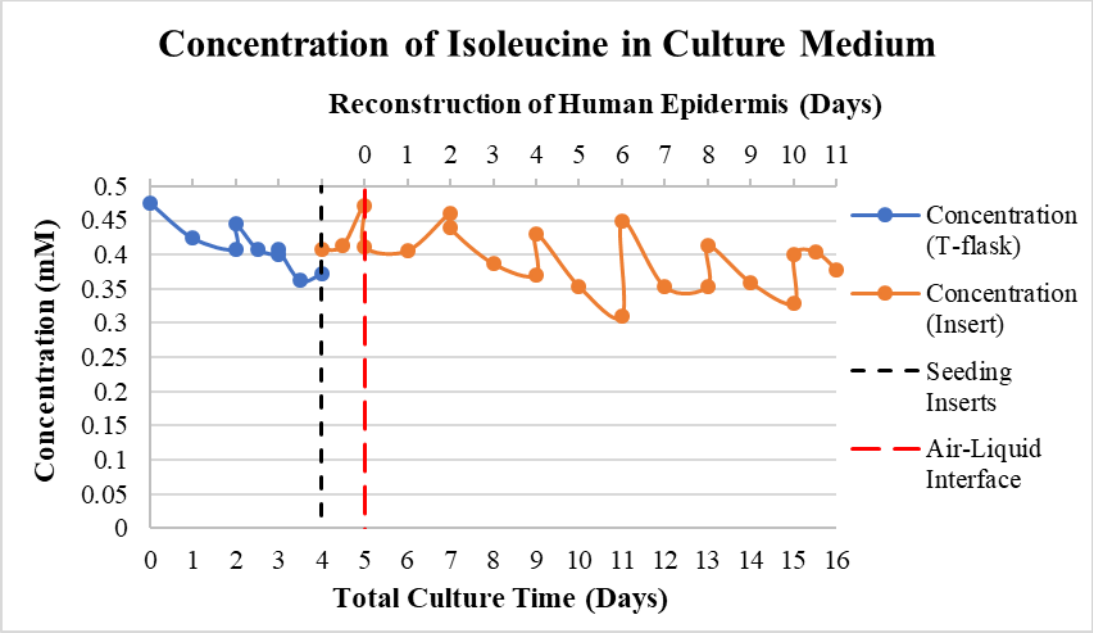

Figure 4.27 – Concentration of Isoleucine in culture medium over time.

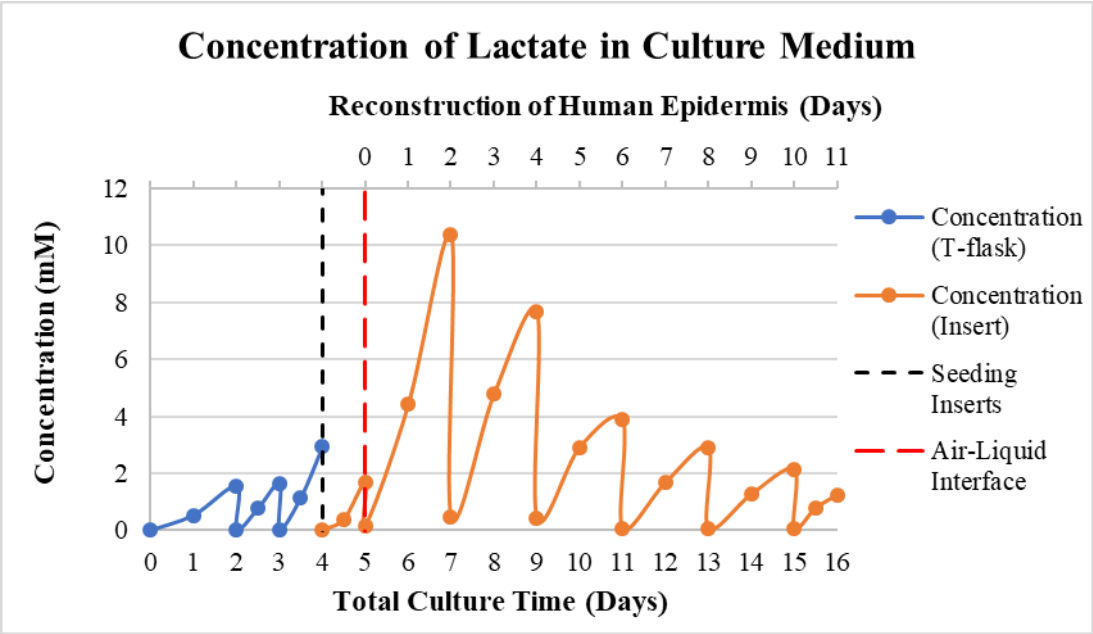

Figure 4.28 – Concentration of Lactate in culture medium over time.

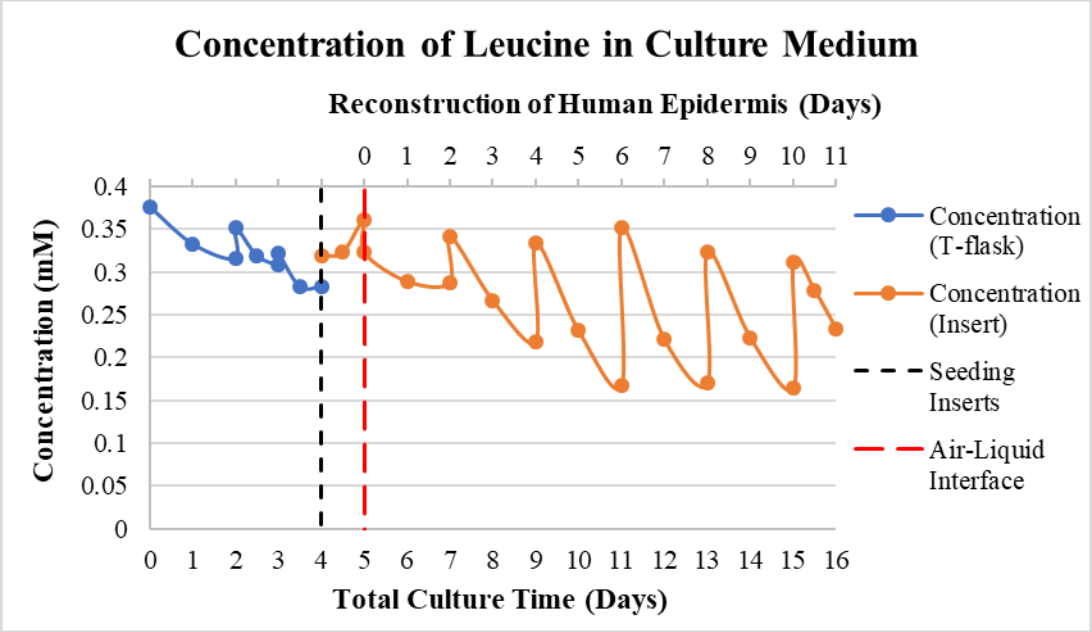

Figure 4.29 – Concentration of Leucine in culture medium over time.

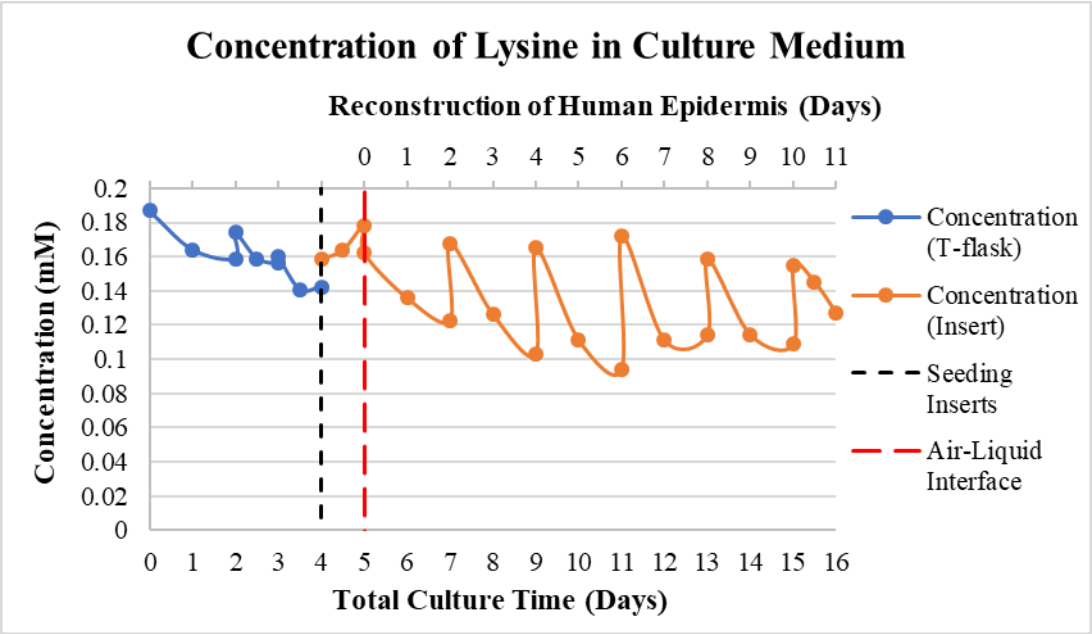

Figure 4.30 – Concentration of Lysine in culture medium over time.

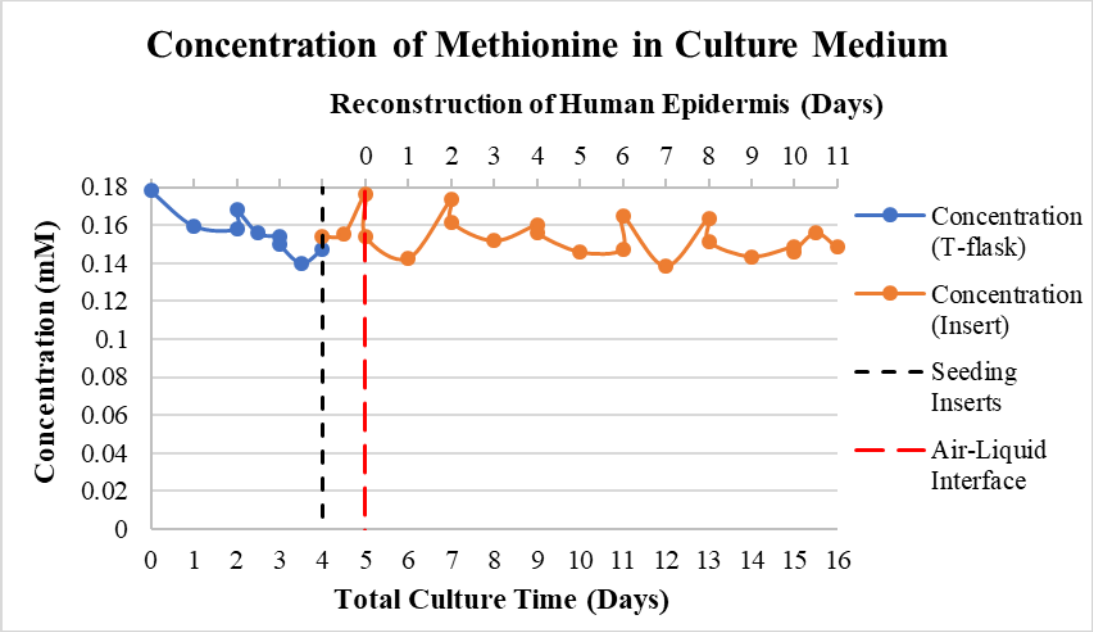

Figure 4.31 – Concentration of Methionine in culture medium over time.

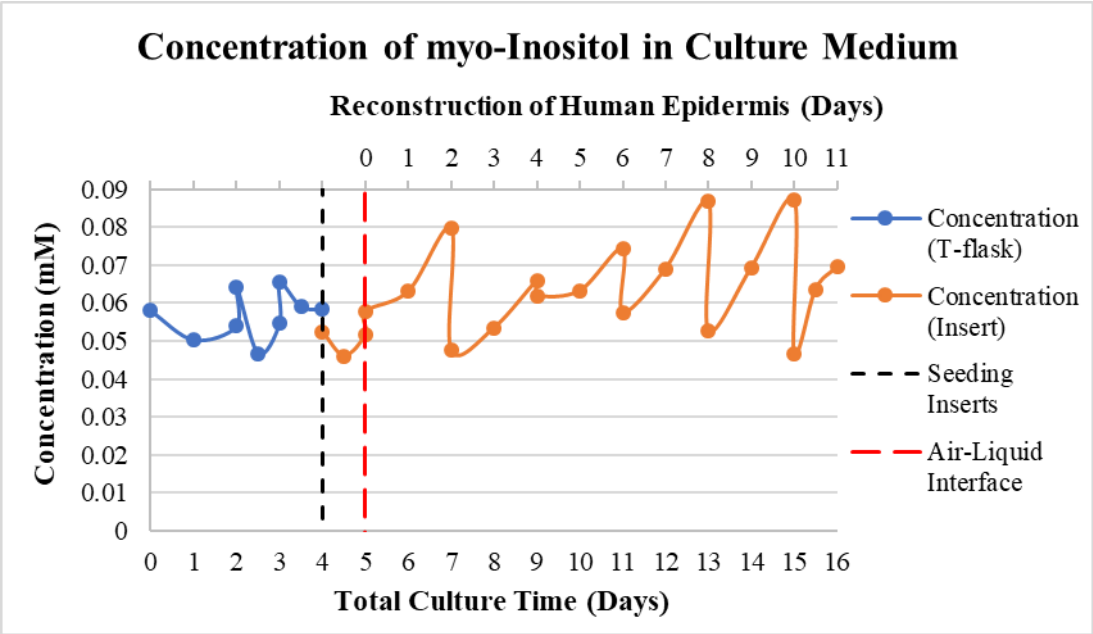

Figure 4.32 – Concentration of myo-Inositol in culture medium over time.

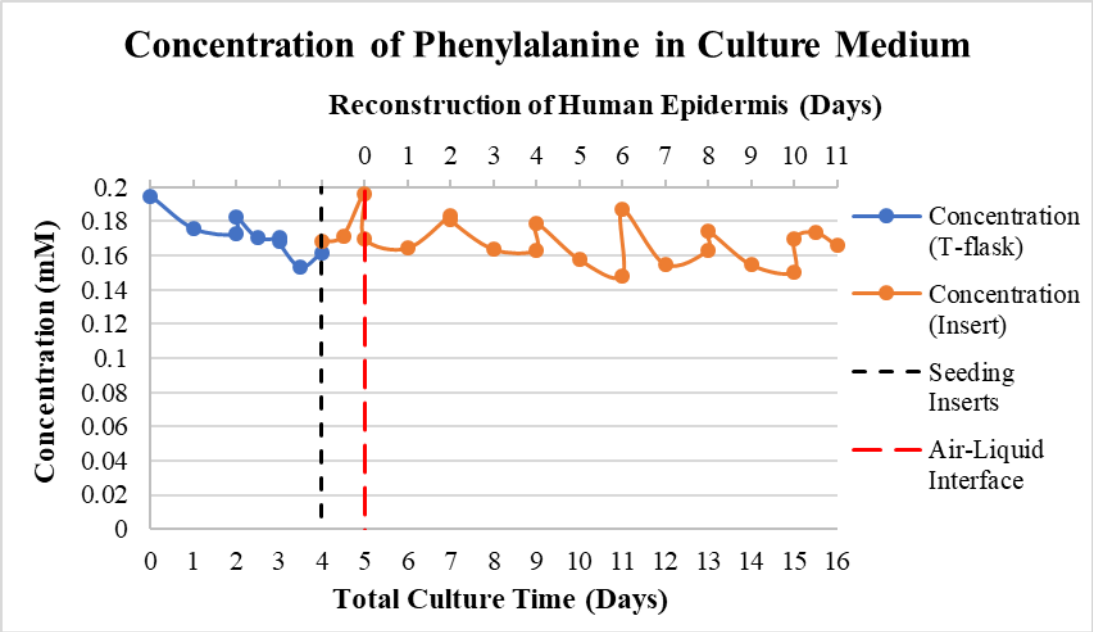

Figure 4.33 – Concentration of Phenylalanine in culture medium over time.

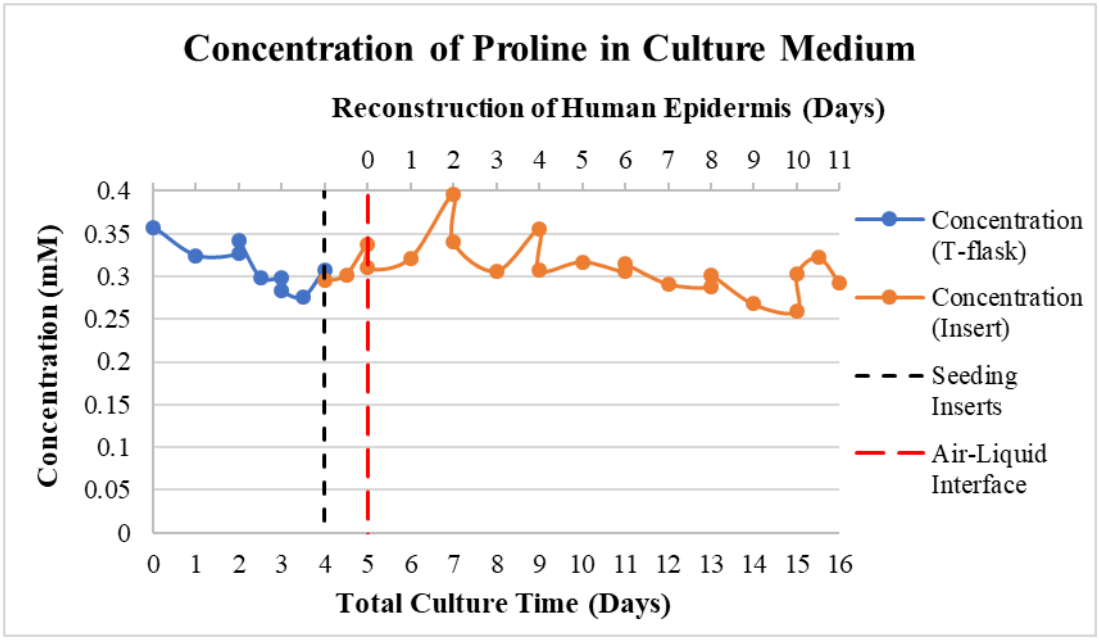

Figure 4.34 – Concentration of Proline in culture medium over time.

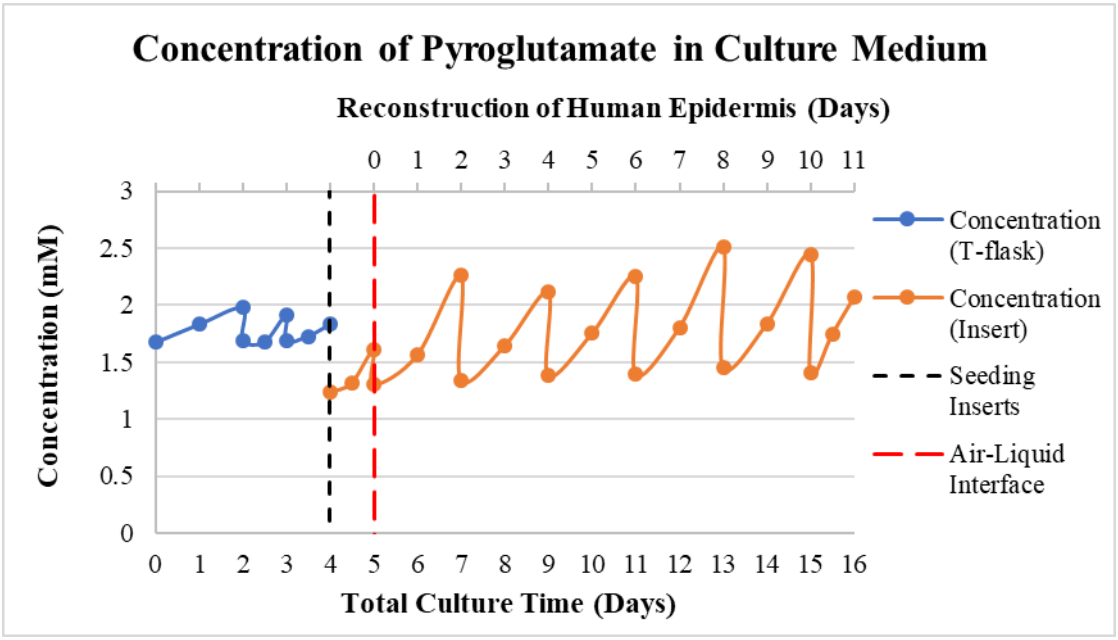

Figure 4.35 – Concentration of Pyroglutamate in culture medium over time.

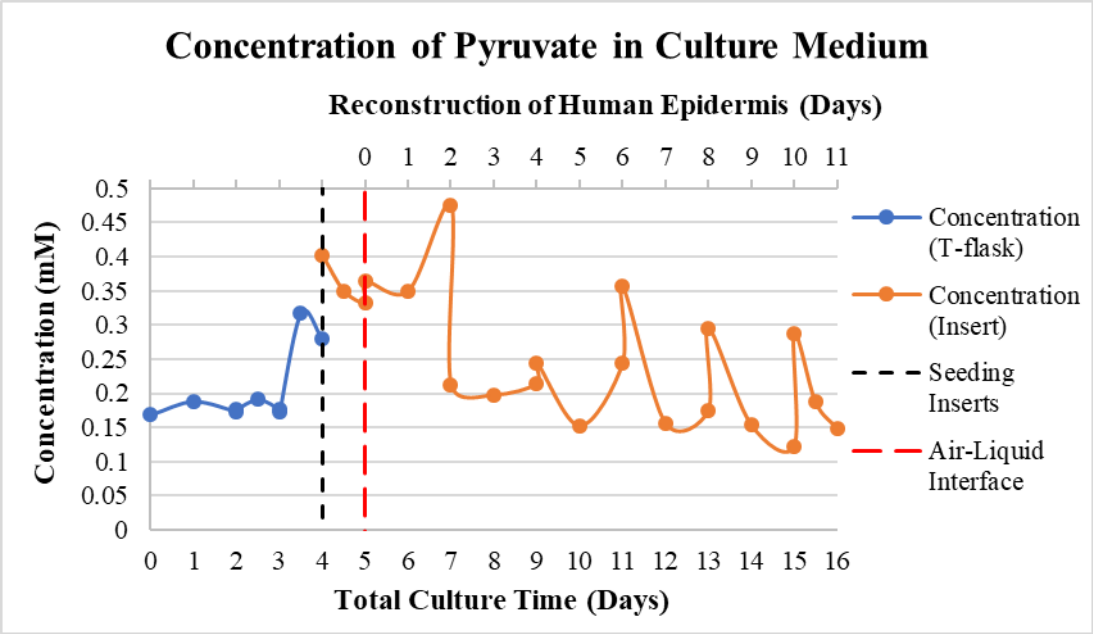

Figure 4.36 – Concentration of Pyruvate in culture medium over time.

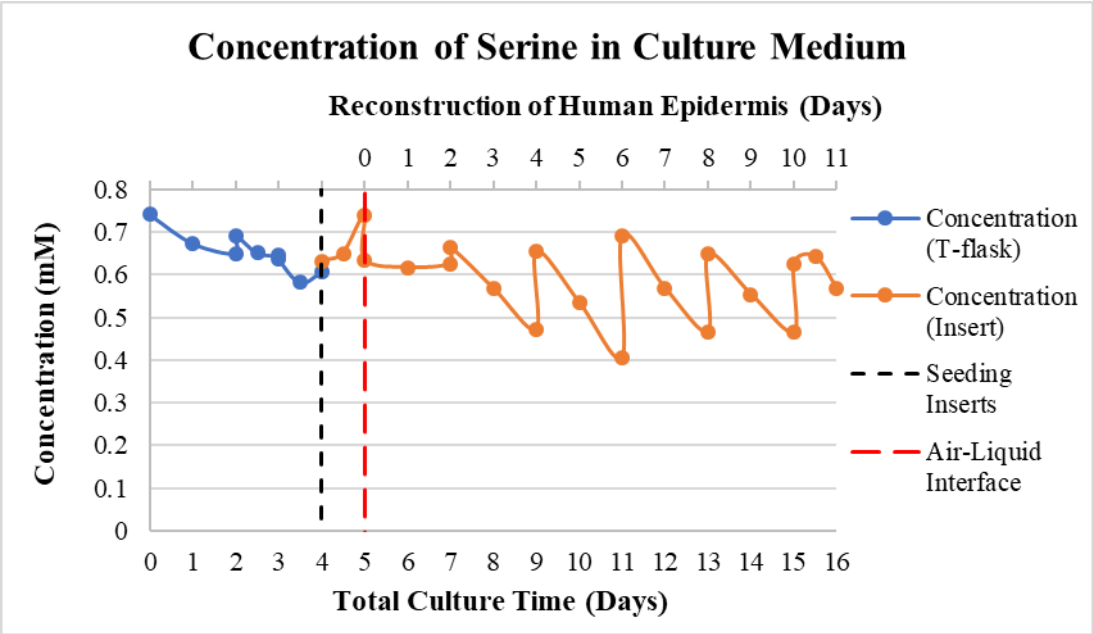

Figure 4.37 – Concentration of Serine in culture medium over time.

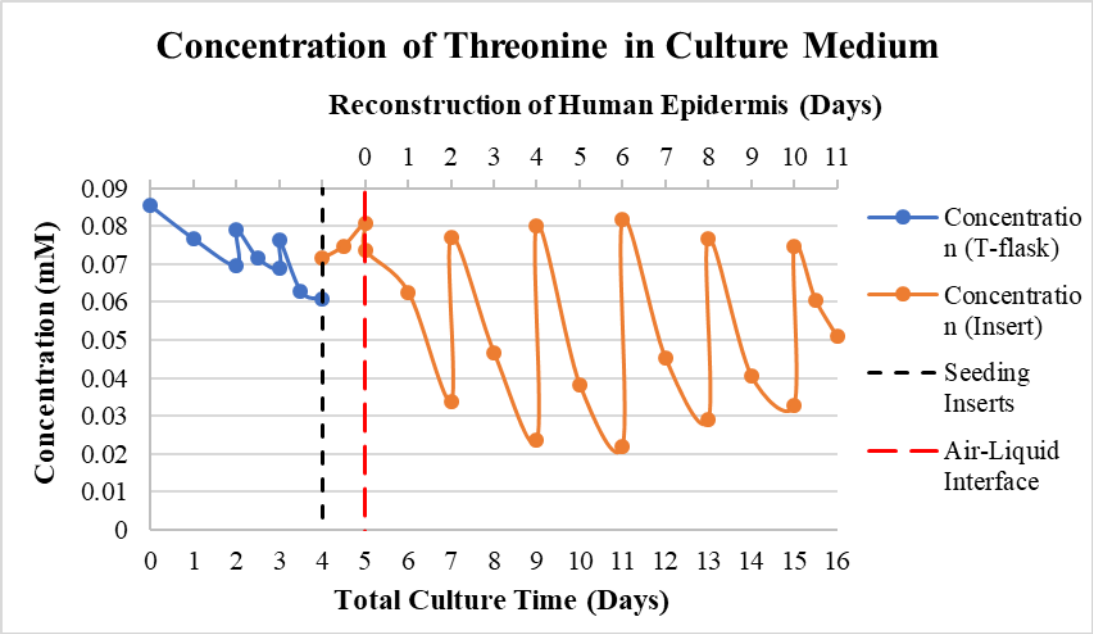

Figure 4.38 – Concentration of Threonine in culture medium over time.

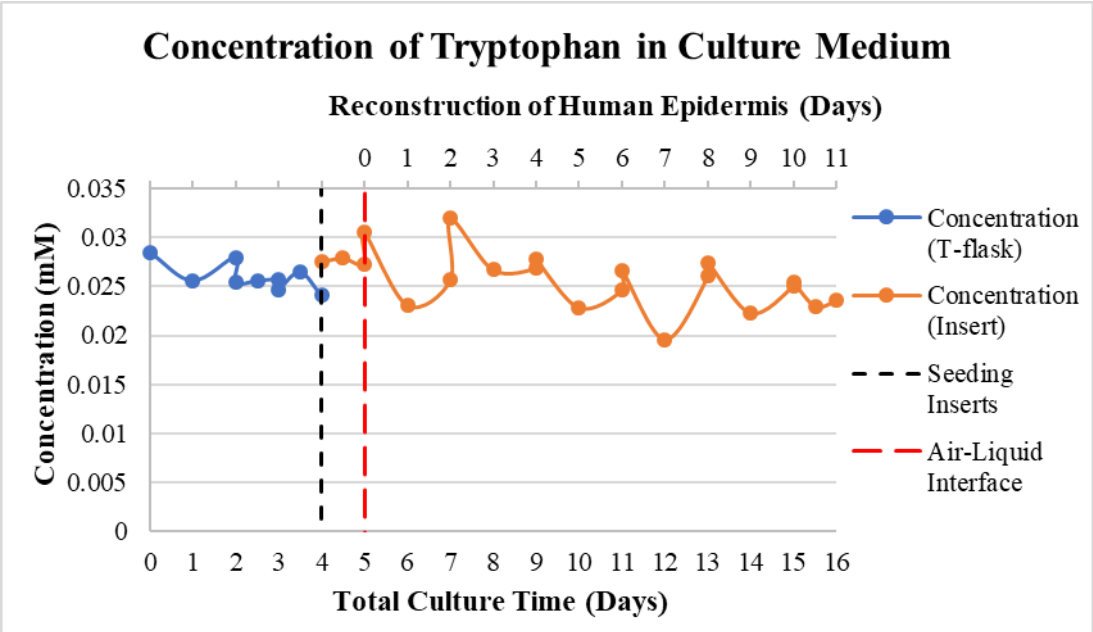

Figure 4.39 – Concentration of Tryptophan in culture medium over time.

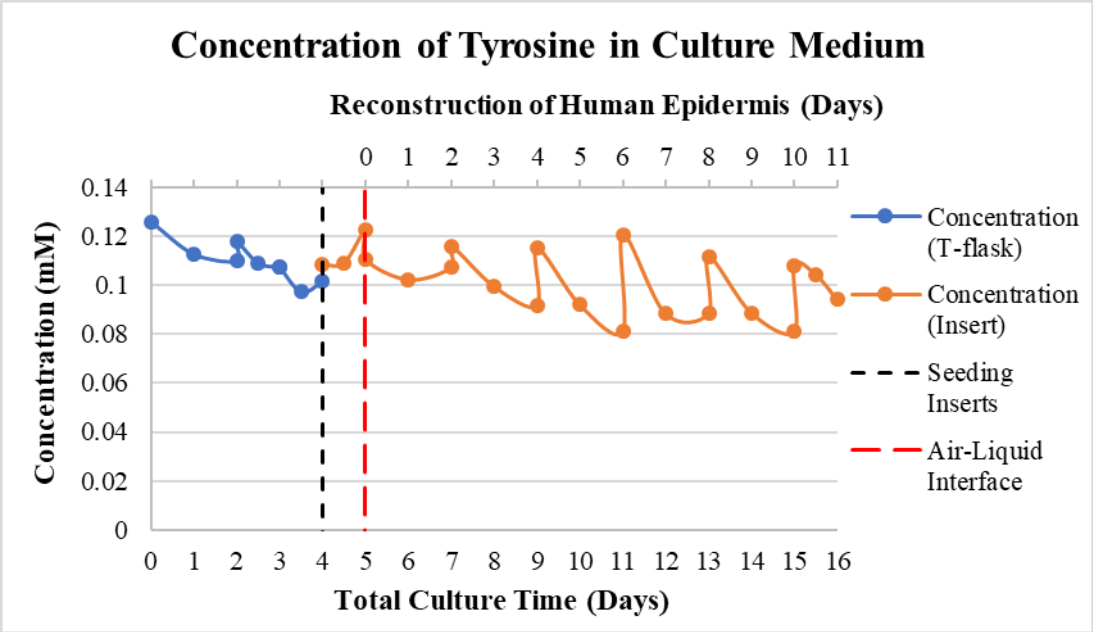

Figure 4.40 – Concentration of Tyrosine in culture medium over time.

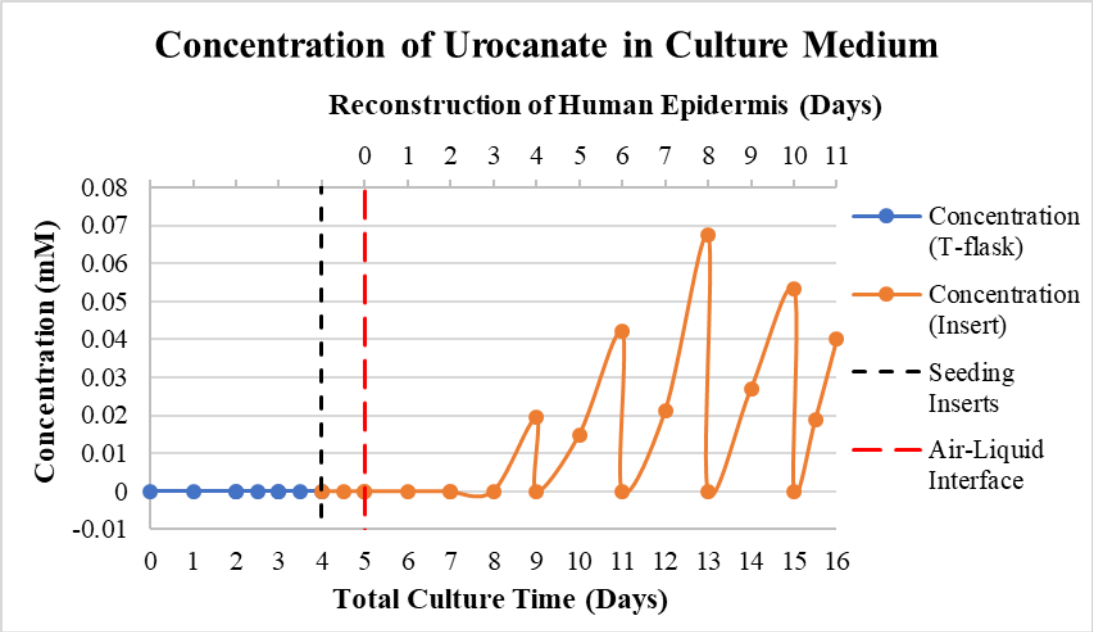

Figure 4.41 – Concentration of Urocanate in culture medium over time.

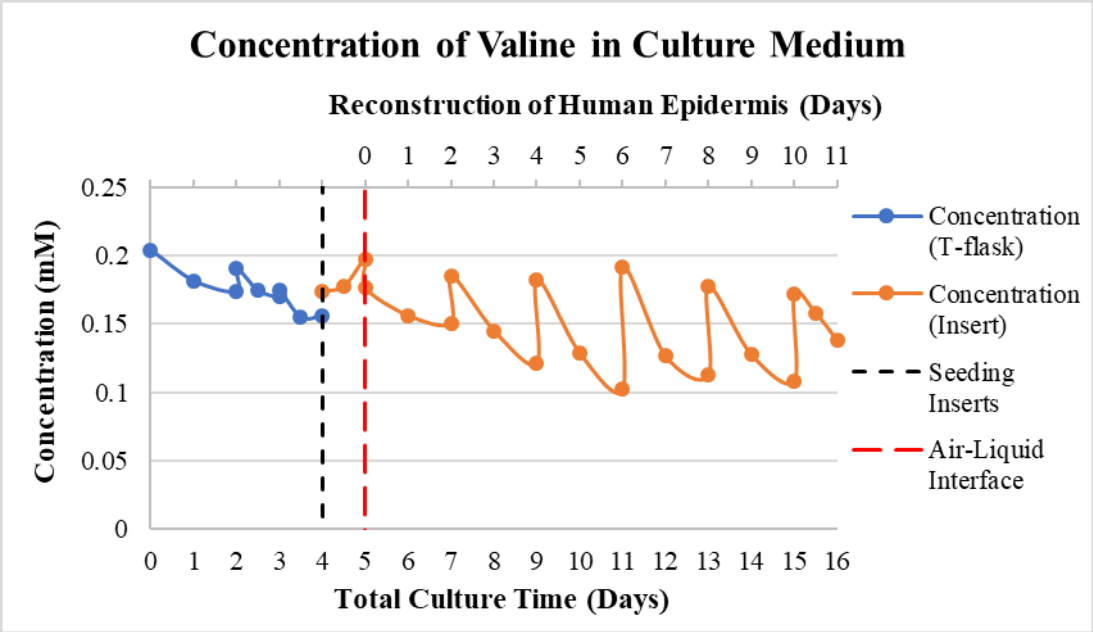

Figure 4.42 – Concentration of Valine in culture medium over time.

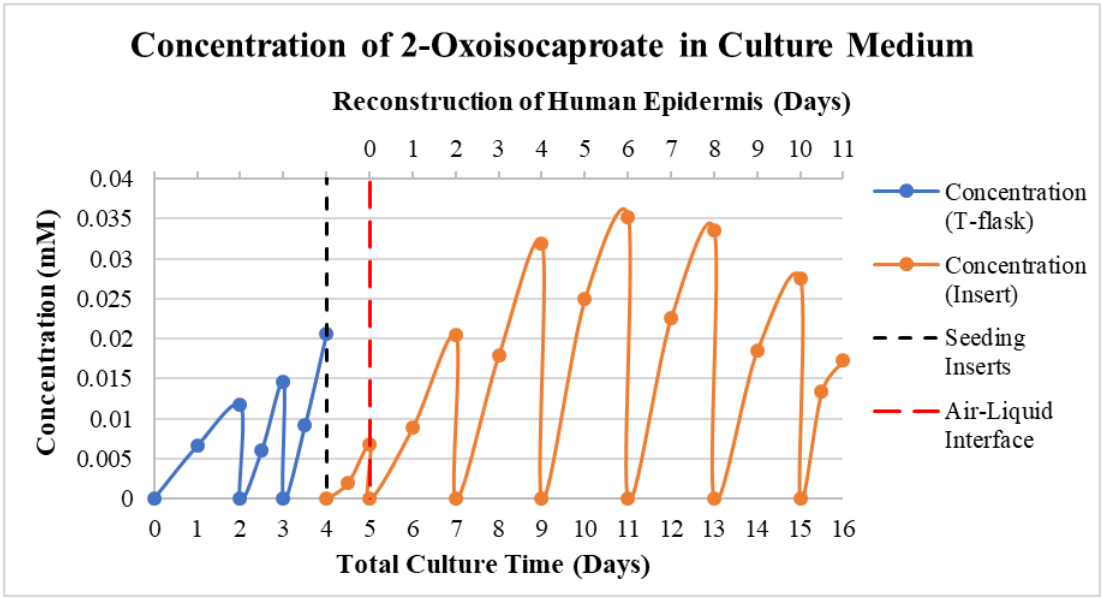

Figure 4.43 – Concentration of 2-Oxoisocaproate in culture medium over time.

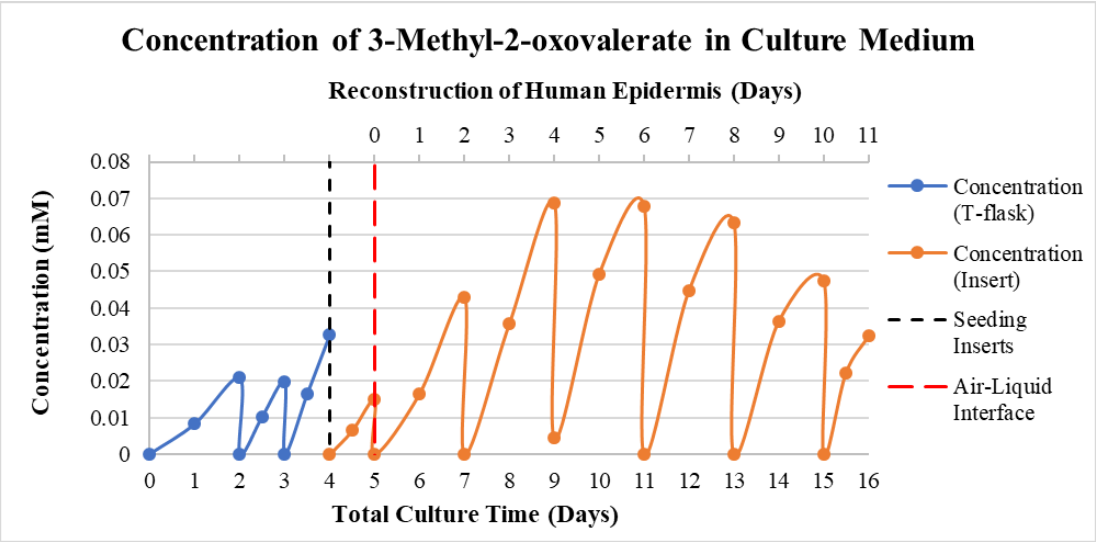

Figure 4.44 – Concentration of 3-Methyl-2-oxovalerate in culture medium over time.

Even though only 3 amino acids were missing, the standard solutions used for the HPLC were prepared with all the amino acids so that an absolute quantification of all these metabolites could be done. This allowed to compare the results obtained between the NMR and HPLC, to see how much reliable was ^{1}H-NMR. In fact, it was verified that the difference was, in average, of 11.5 %, which is acceptable since NMR is not as sensitive as HPLC. In addition, only a relative quantification is done in ^{1}H-NMR. For this reason, it was decided that the concentrations used for the amino acids would be those obtained by HPLC. The only exception was tryptophan, which showed a difference of around 181 %. This deviation may be due to the presence of two fluorescent groups (in this case the AccQ-Fluor™ and tryptophan itself) which is known to reduce fluorescence sensitivity (internal quenching)[96]. As for cysteine, which is a constituent of EpiLife®, its thiol group is very susceptible to oxidation. This leads to the formation of a disulphide bond between two cysteine molecules forming, subsequently, cystine. This oxidized dimer form of cysteine is very prone to appear during the process of preparation of samples for HPLC and/or during the injection of the samples in the mobile phases. Therefore, the quantification of this amino acid by HPLC was done in the form of cystine[97,98].

When performing metabolomic analysis, the first steps to take are:

- To verify if any nutrient is depleted throughout the time of culture and, if so, the first procedure to attempt consists in increasing the concentration of that nutrient and observe if any improvements occur in the culture process;
- To determine if there is any metabolite accumulating in the culture media that may have growth or differentiation inhibitory effects on the cells.

This can be done by analysing the concentration of the metabolites over culture time, as well as the uptake/secretion rates of the metabolites, that are represented in figures 4.45 – 4.77.

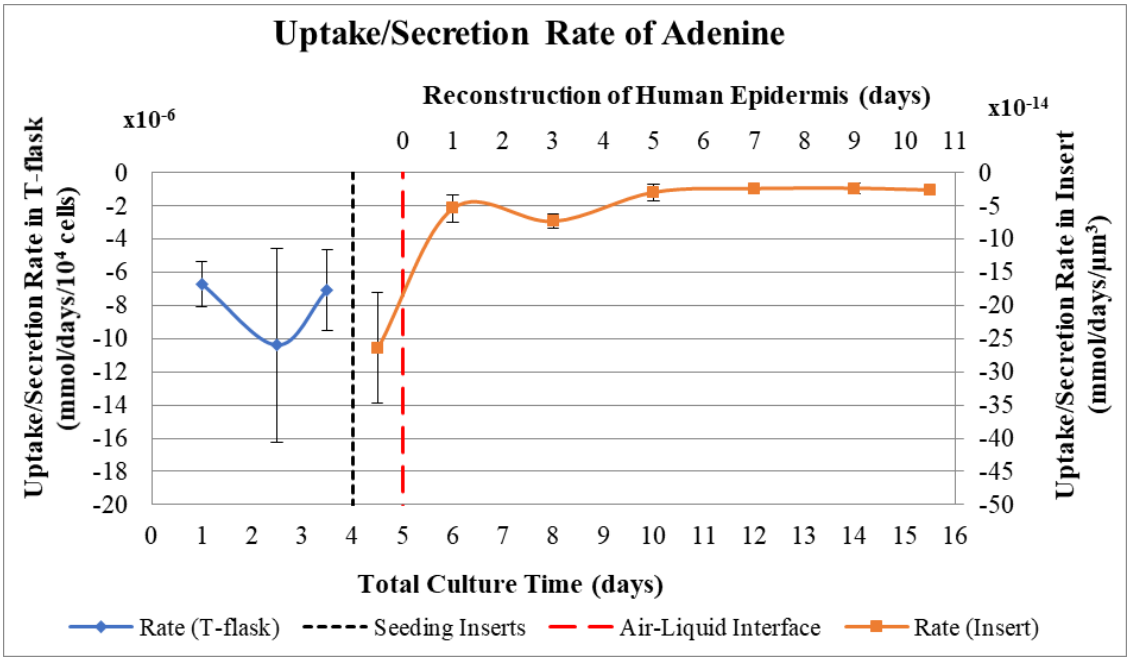

Figure 4.45 – Uptake/secretion rate of Adenine during the keratinocyte culture in monolayer and reconstruction of human epidermis in polycarbonate filter.

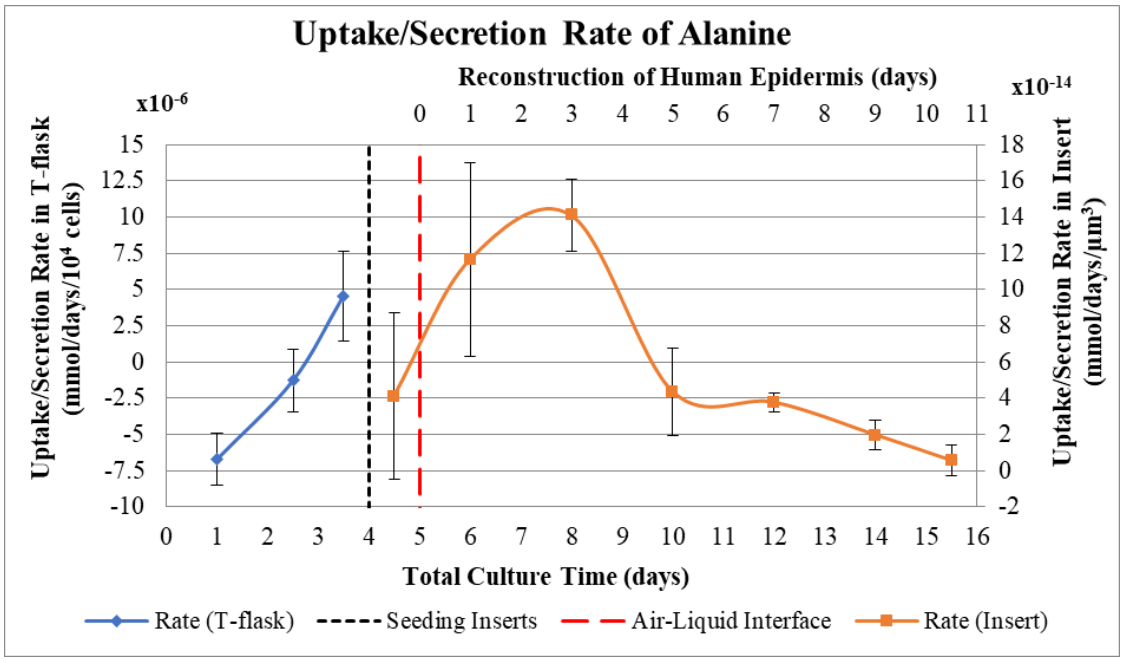

Figure 4.46 – Uptake/secretion rate of Alanine during the keratinocyte culture in monolayer and reconstruction of human epidermis in polycarbonate filter.

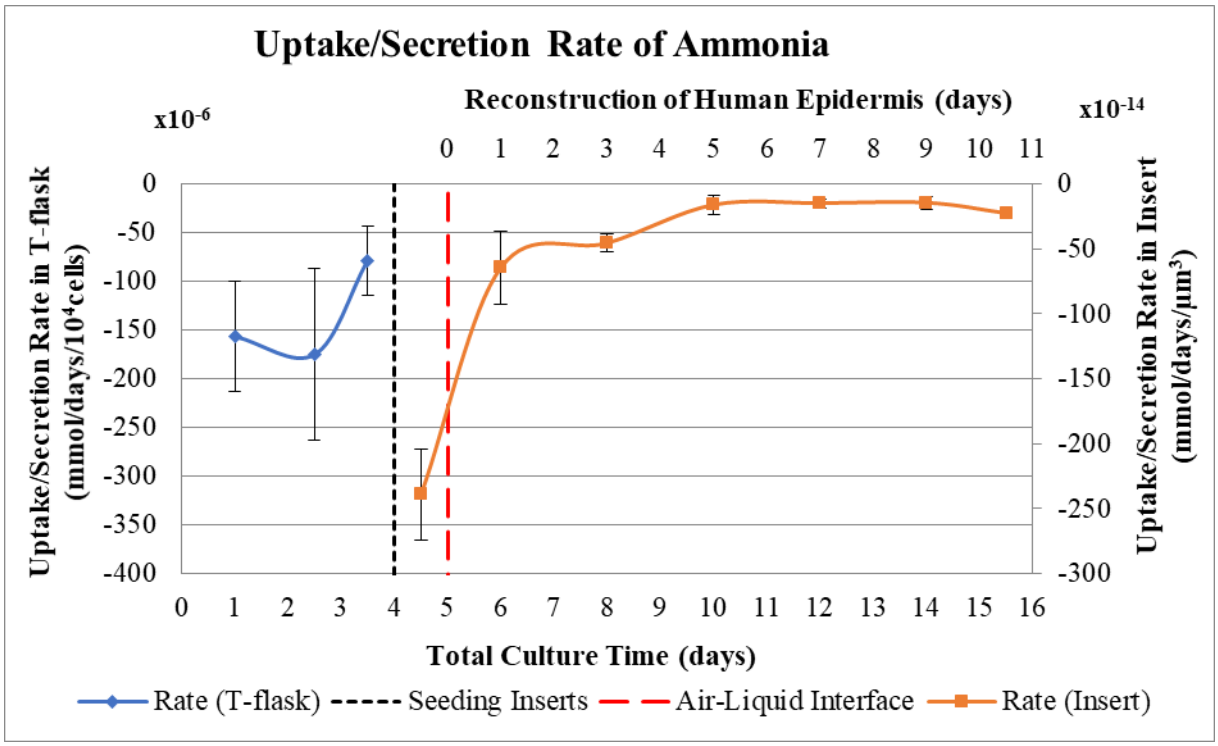

Figure 4.47 – Uptake/secretion rate of Ammonia during the keratinocyte culture in monolayer and reconstruction of human epidermis in polycarbonate filter.

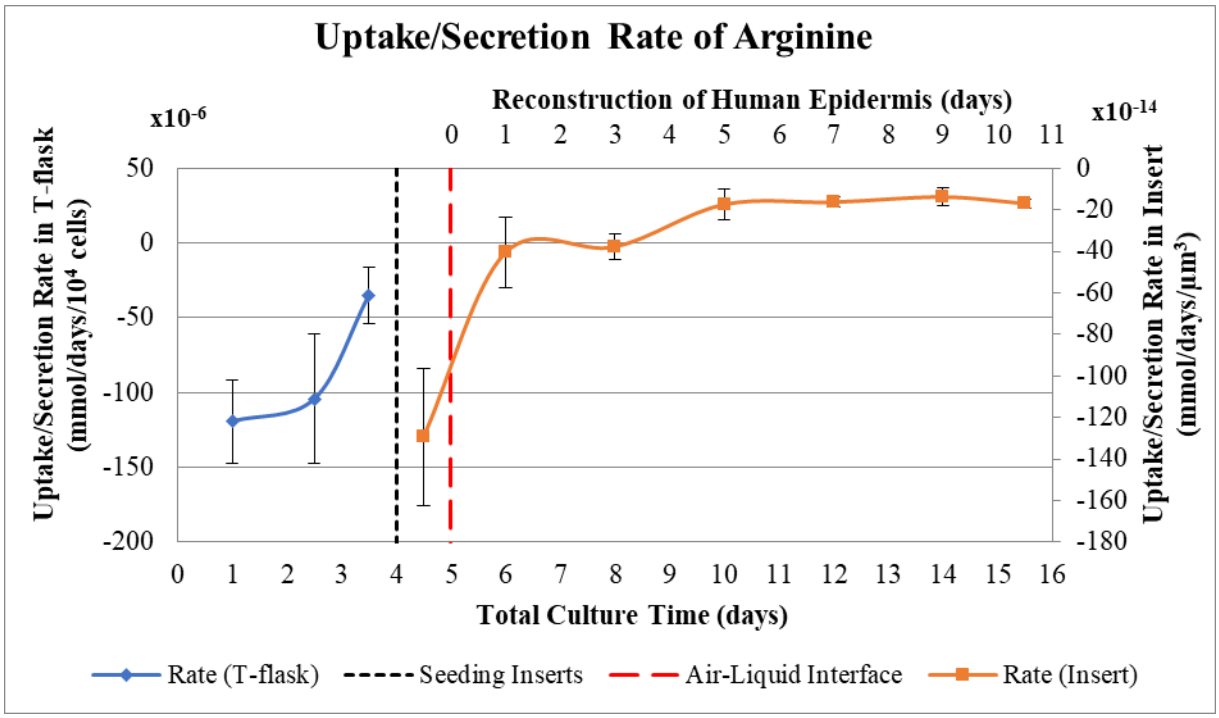

Figure 4.48 – Uptake/secretion rate of Arginine during the keratinocyte culture in monolayer and reconstruction of human epidermis in polycarbonate filter.

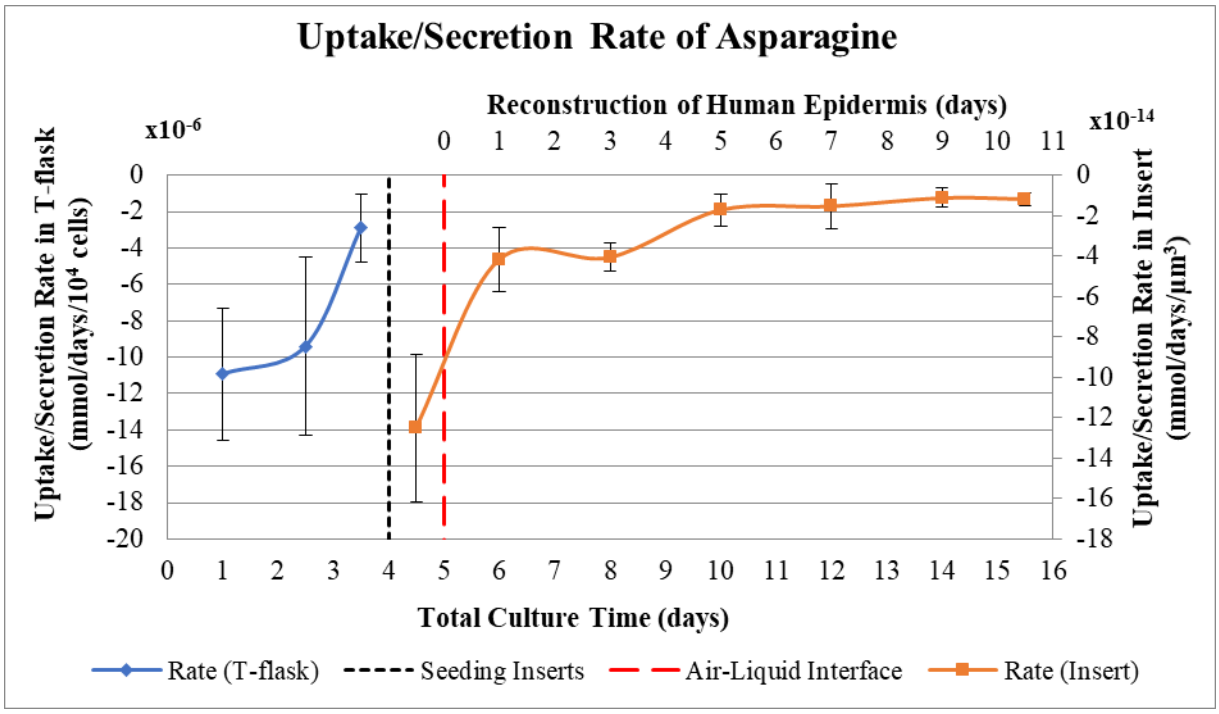

Figure 4.49 – Uptake/secretion rate of Asparagine during the keratinocyte culture in monolayer and reconstruction of human epidermis in polycarbonate filter.

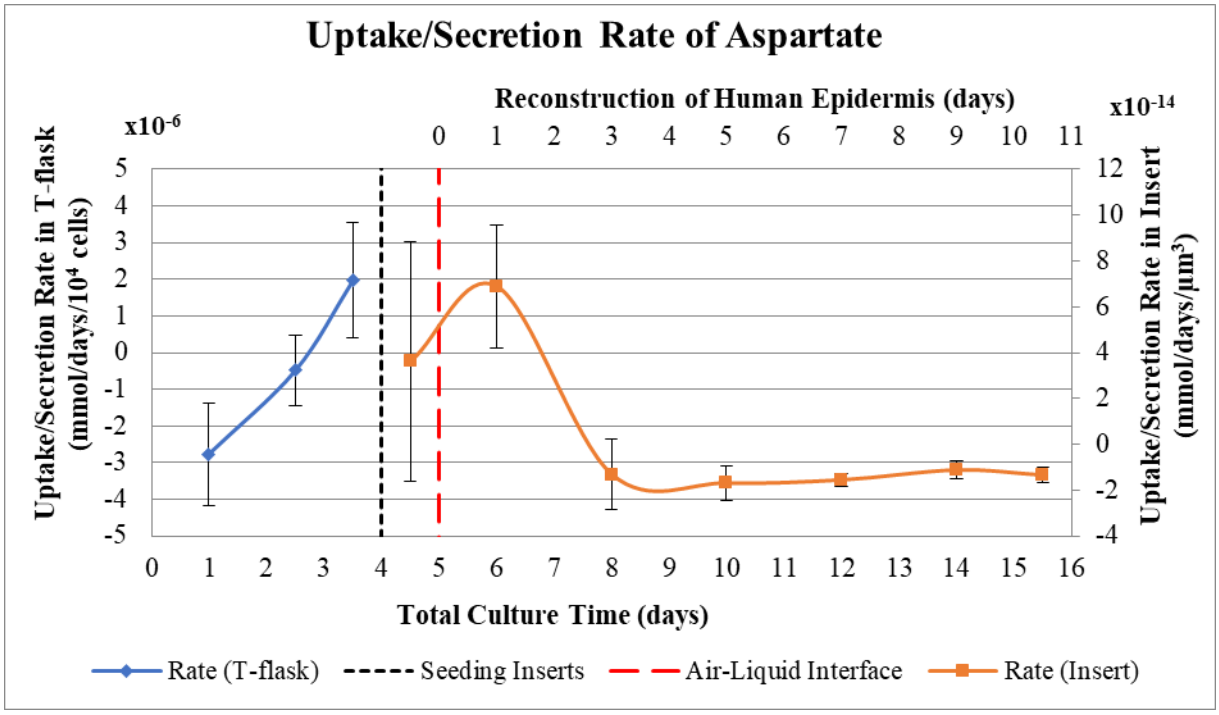

Figure 4.50 – Uptake/secretion rate of Aspartate during the keratinocyte culture in monolayer and reconstruction of human epidermis in polycarbonate filter.

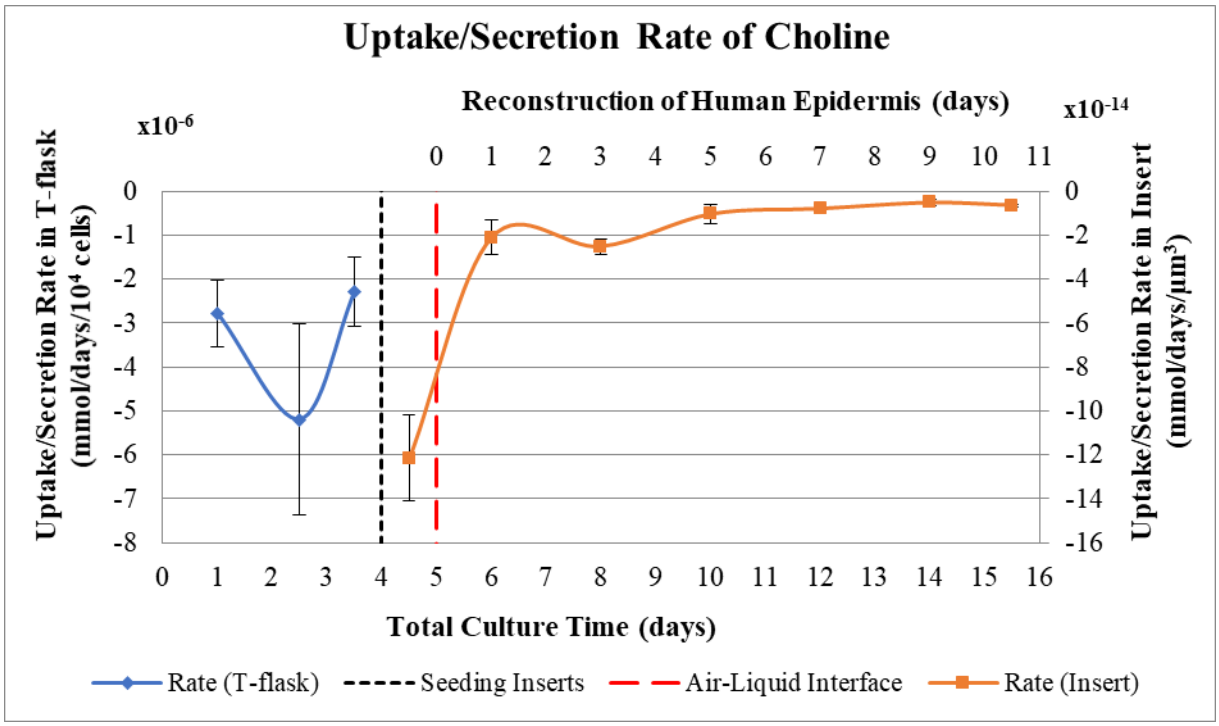

Figure 4.51 – Uptake/secretion rate of Choline during the keratinocyte culture in monolayer and reconstruction of human epidermis in polycarbonate filter.

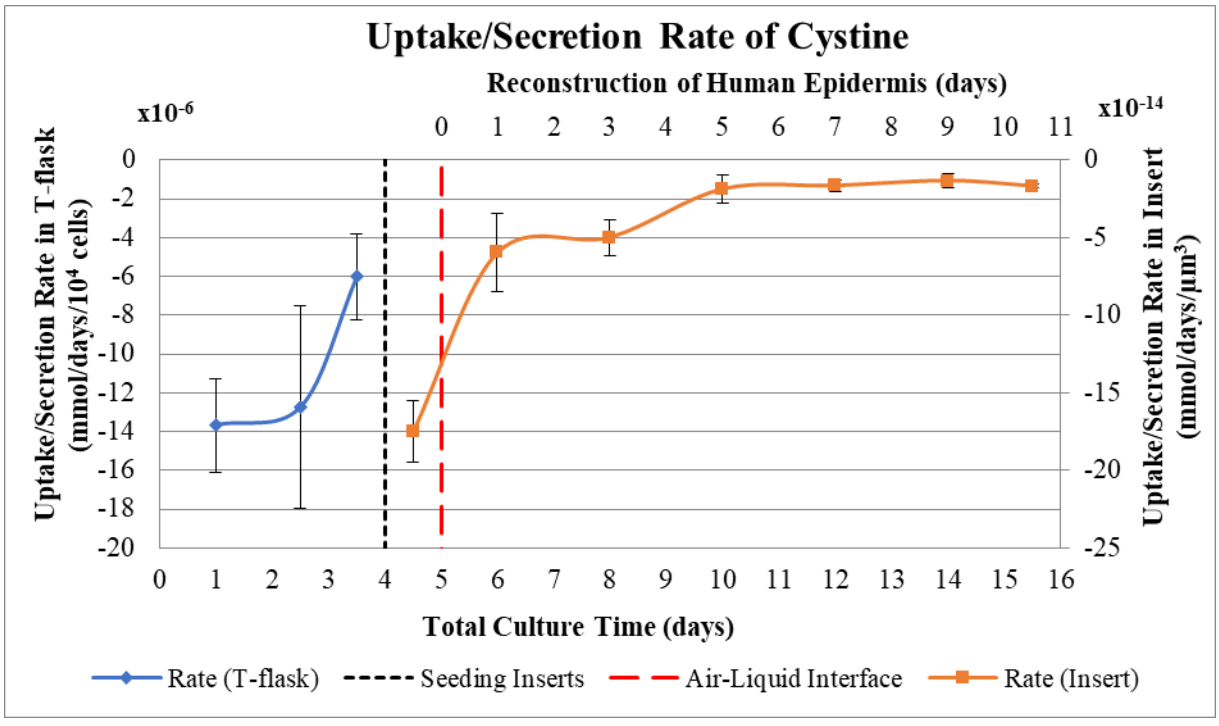

Figure 4.52 – Uptake/secretion rate of Cystine during the keratinocyte culture in monolayer and reconstruction of human epidermis in polycarbonate filter.

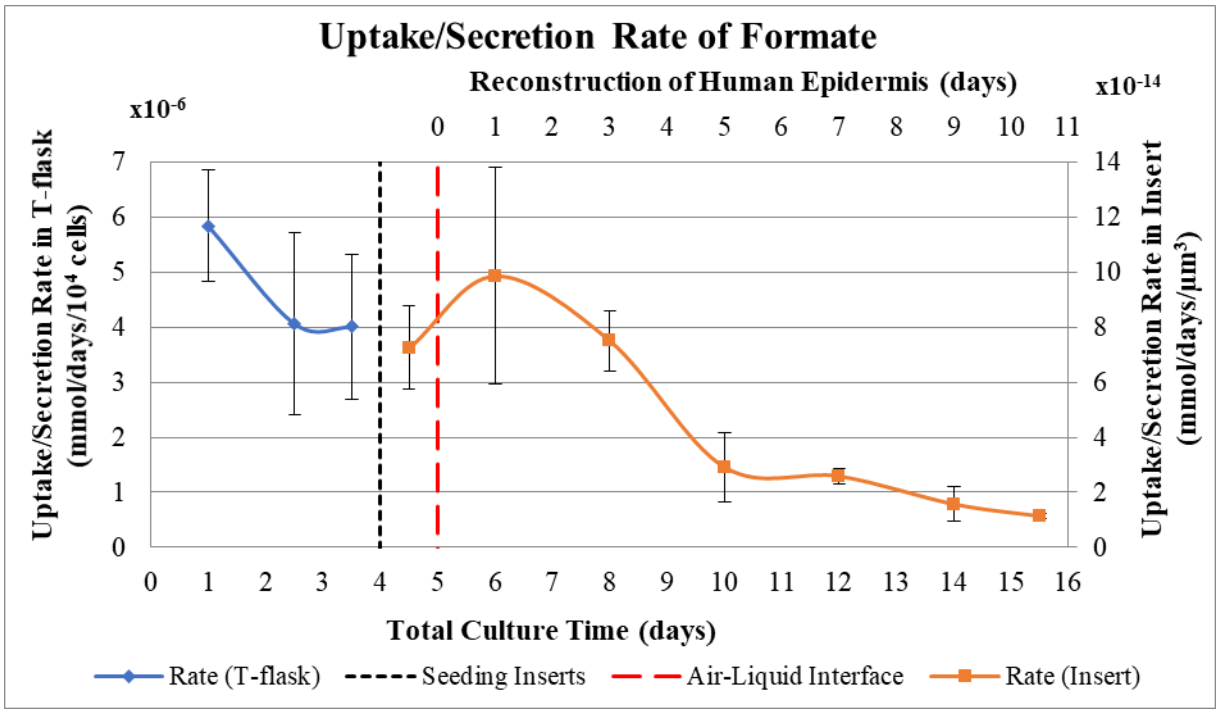

Figure 4.53 – Uptake/secretion rate of Formate during the keratinocyte culture in monolayer and reconstruction of human epidermis in polycarbonate filter.

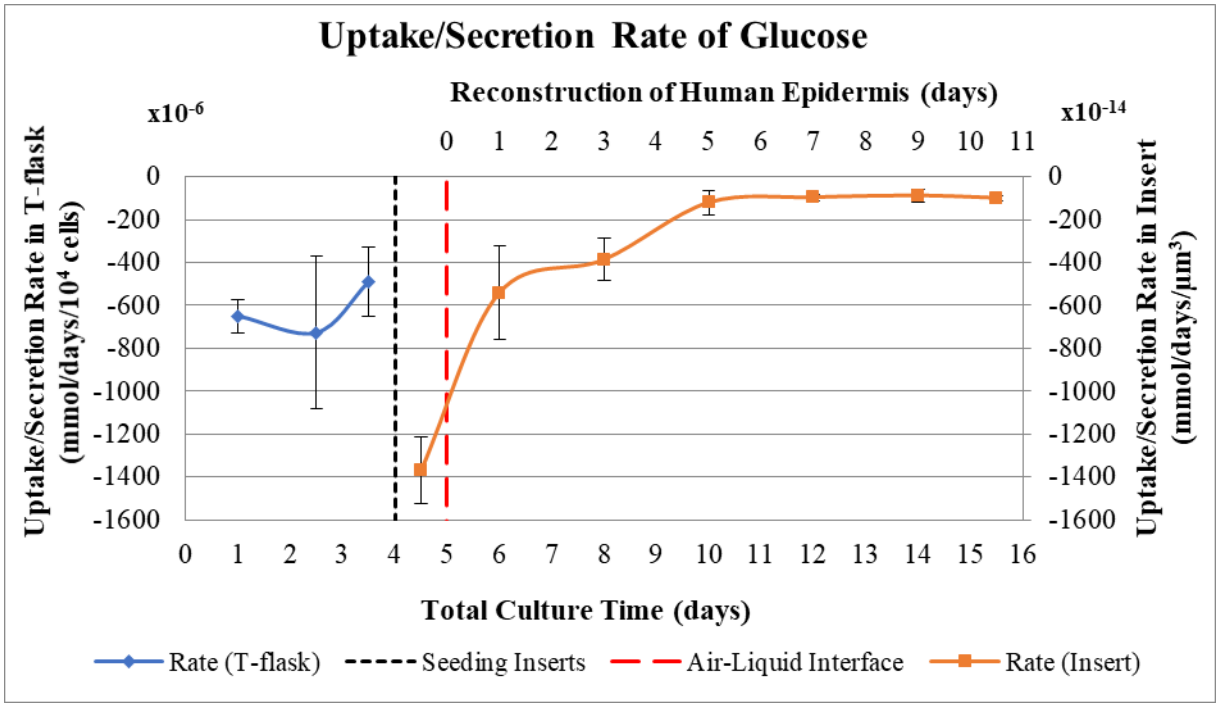

Figure 4.54 – Uptake/secretion rate of Glucose during the keratinocyte culture in monolayer and reconstruction of human epidermis in polycarbonate filter.

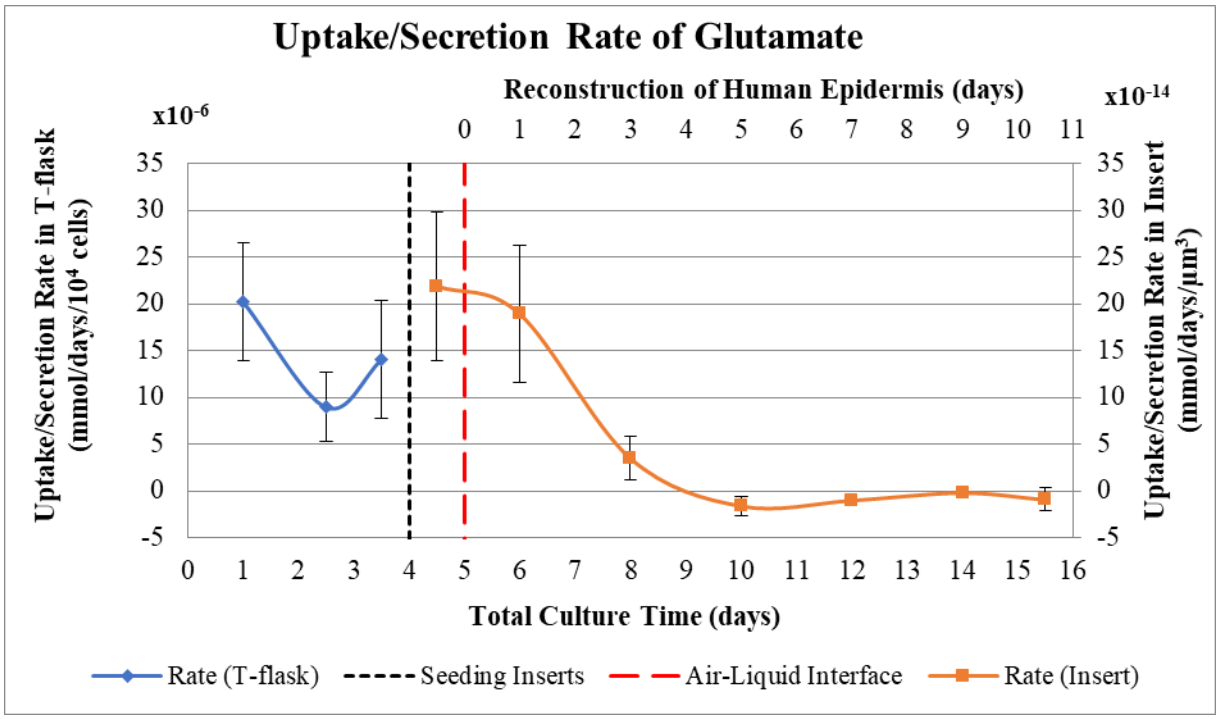

Figure 4.55 – Uptake/secretion rate of Glutamate during the keratinocyte culture in monolayer and reconstruction of human epidermis in polycarbonate filter.

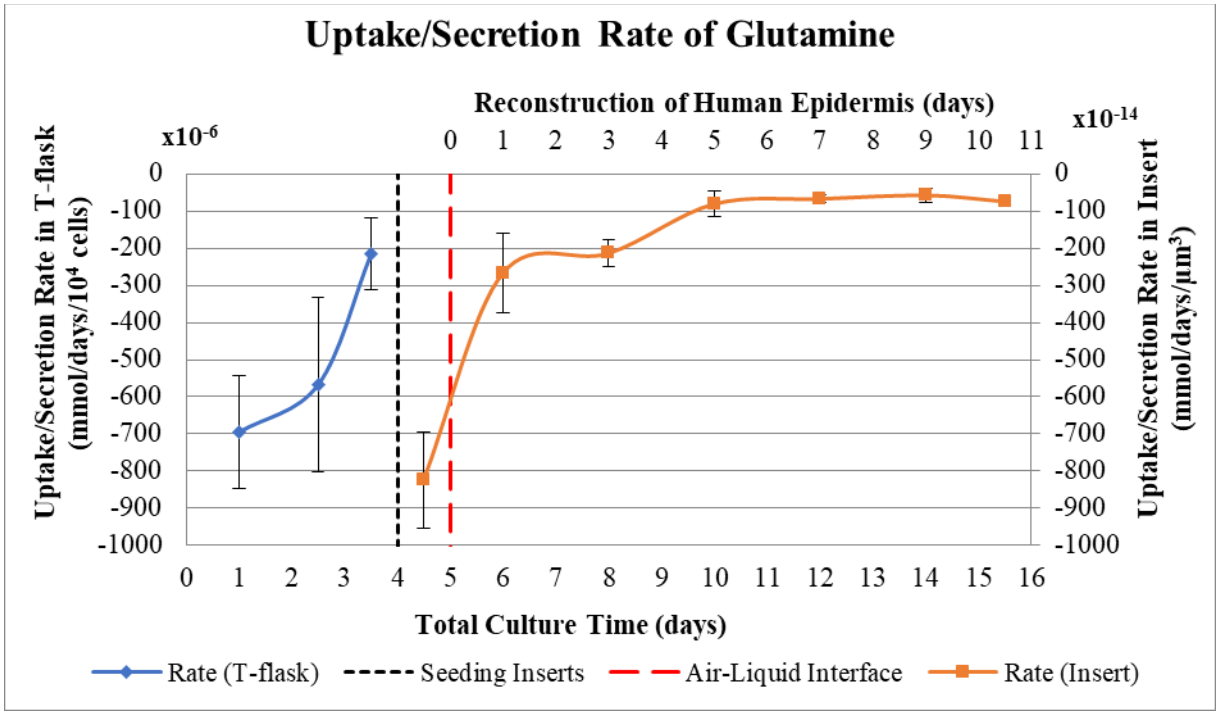

Figure 4.56 – Uptake/secretion rate of Glutamine during the keratinocyte culture in monolayer and reconstruction of human epidermis in polycarbonate filter.

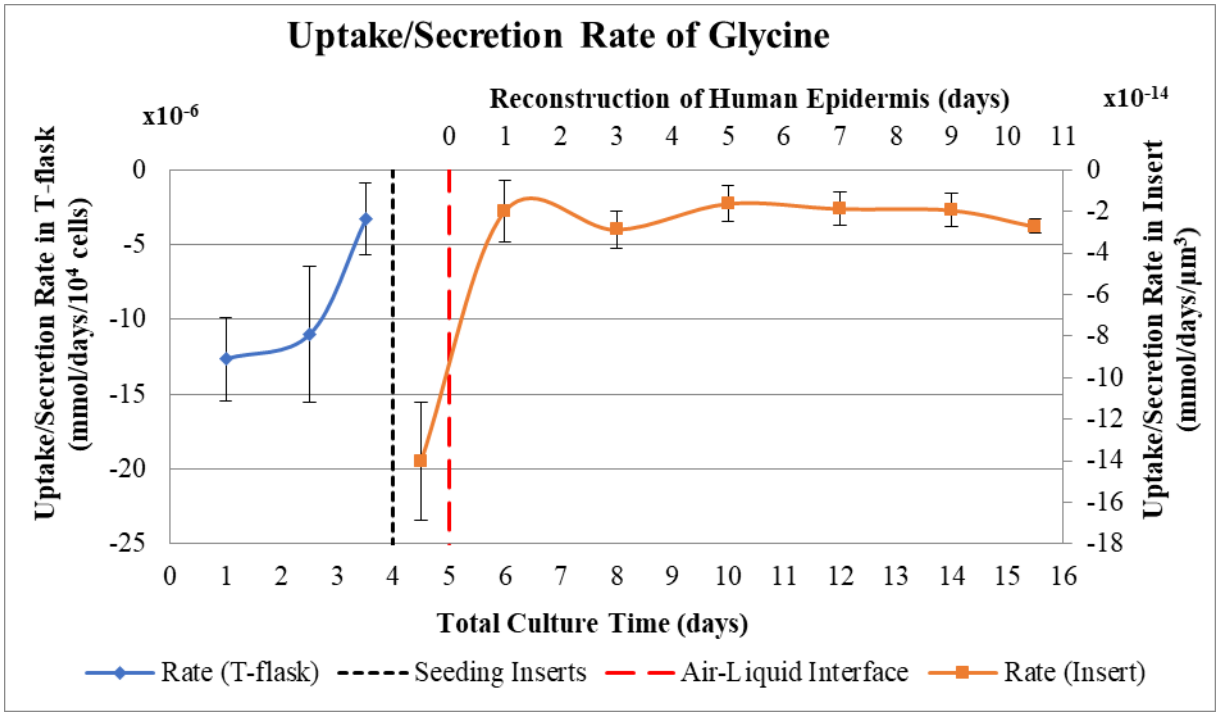

Figure 4.57 – Uptake/secretion rate of Glycine during the keratinocyte culture in monolayer and reconstruction of human epidermis in polycarbonate filter.

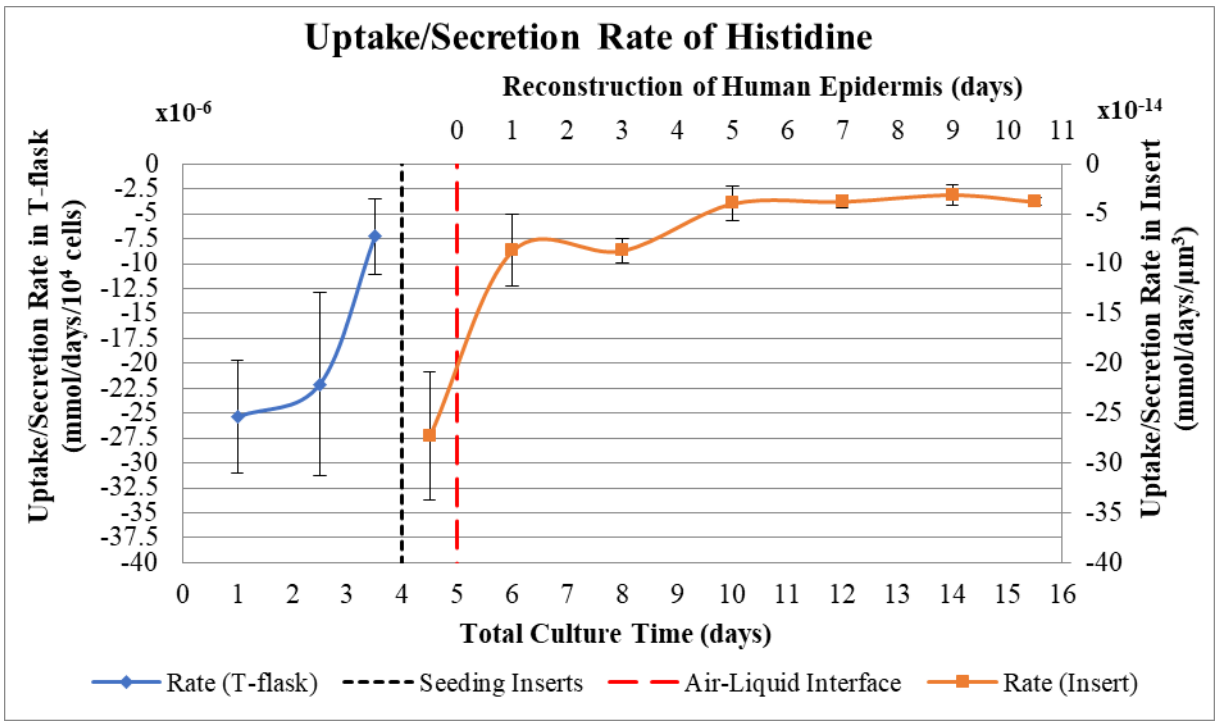

Figure 4.58 – Uptake/secretion rate of Histidine during the keratinocyte culture in monolayer and reconstruction of human epidermis in polycarbonate filter.

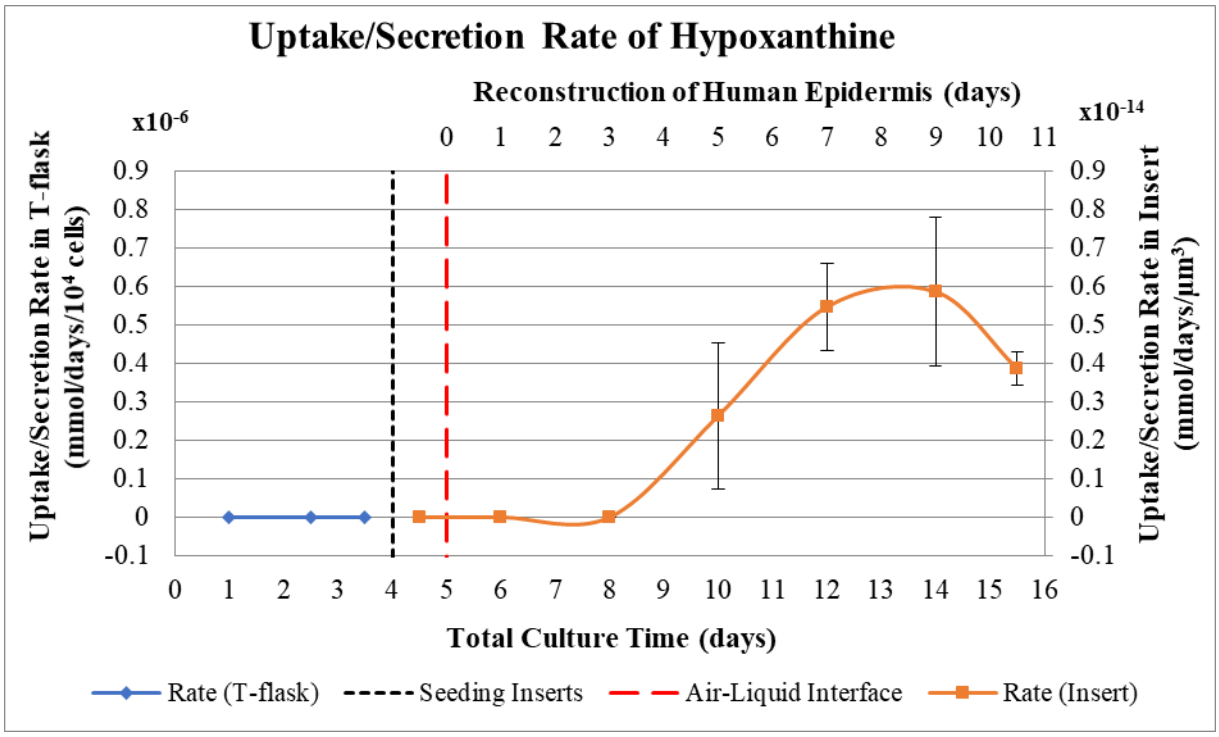

Figure 4.59 – Uptake/secretion rate of Hypoxanthine during the keratinocyte culture in monolayer and reconstruction of human epidermis in polycarbonate filter.

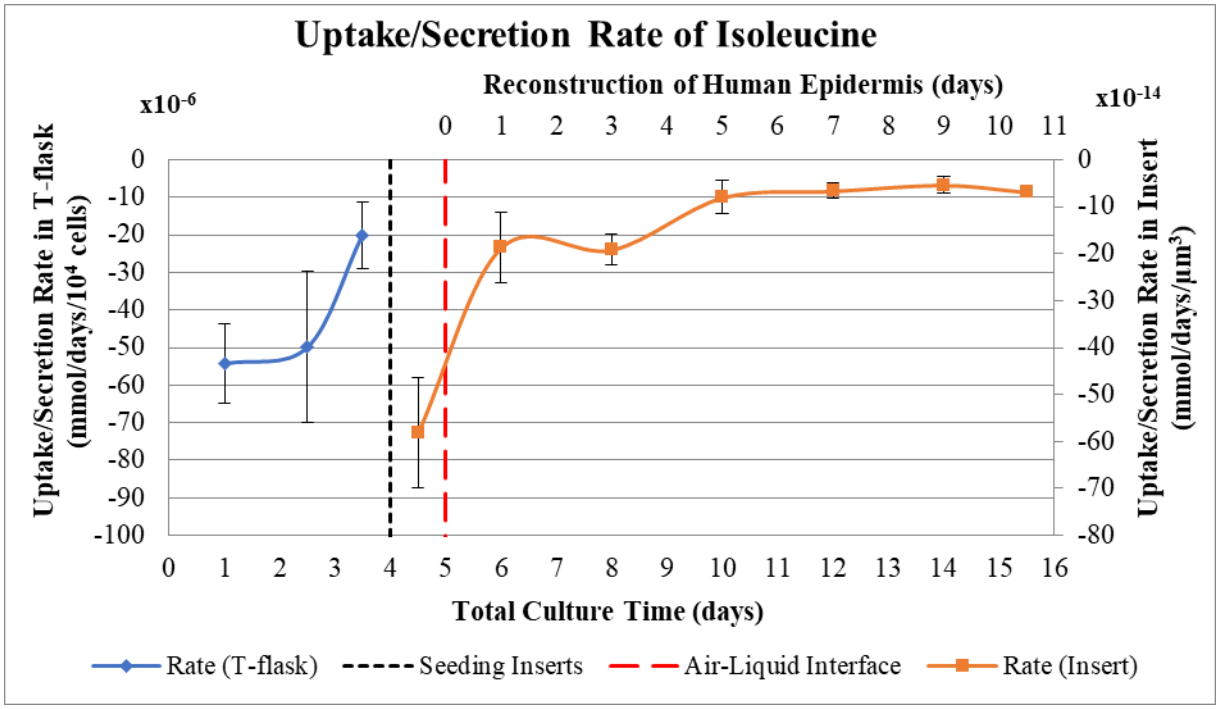

Figure 4.60 – Uptake/secretion rate of Isoleucine during the keratinocyte culture in monolayer and reconstruction of human epidermis in polycarbonate filter.

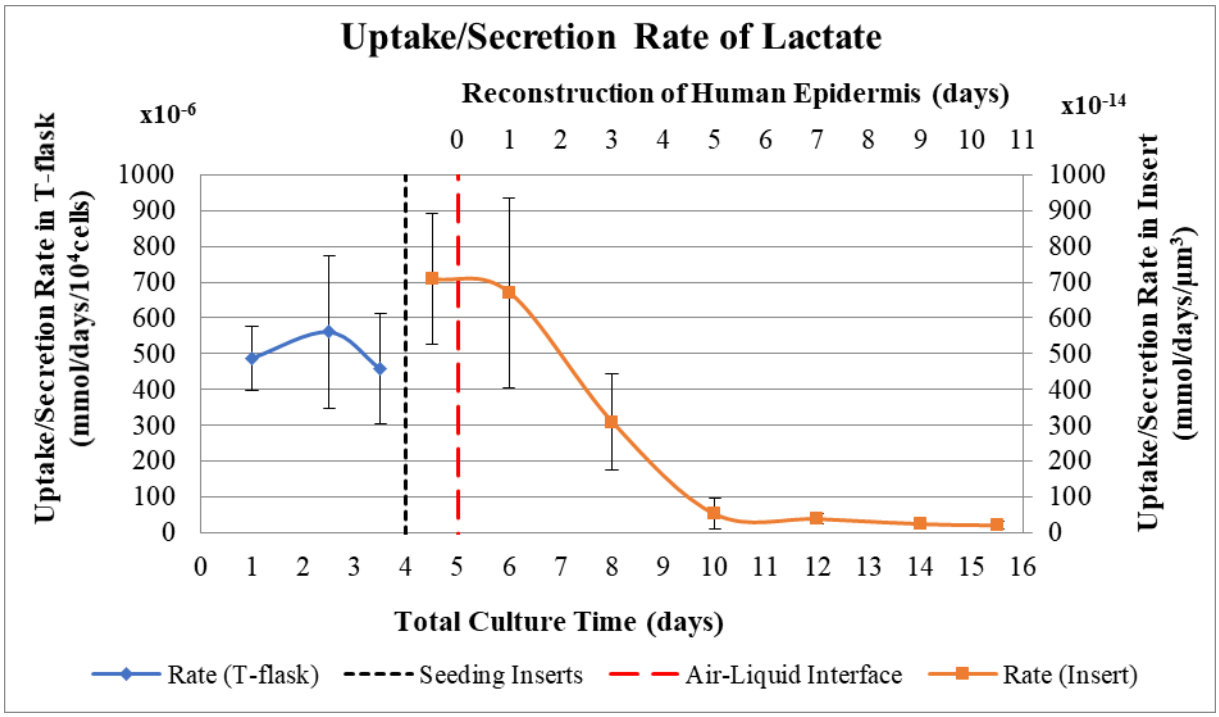

Figure 4.61 – Uptake/secretion rate of Lactate during the keratinocyte culture in monolayer and reconstruction of human epidermis in polycarbonate filter.

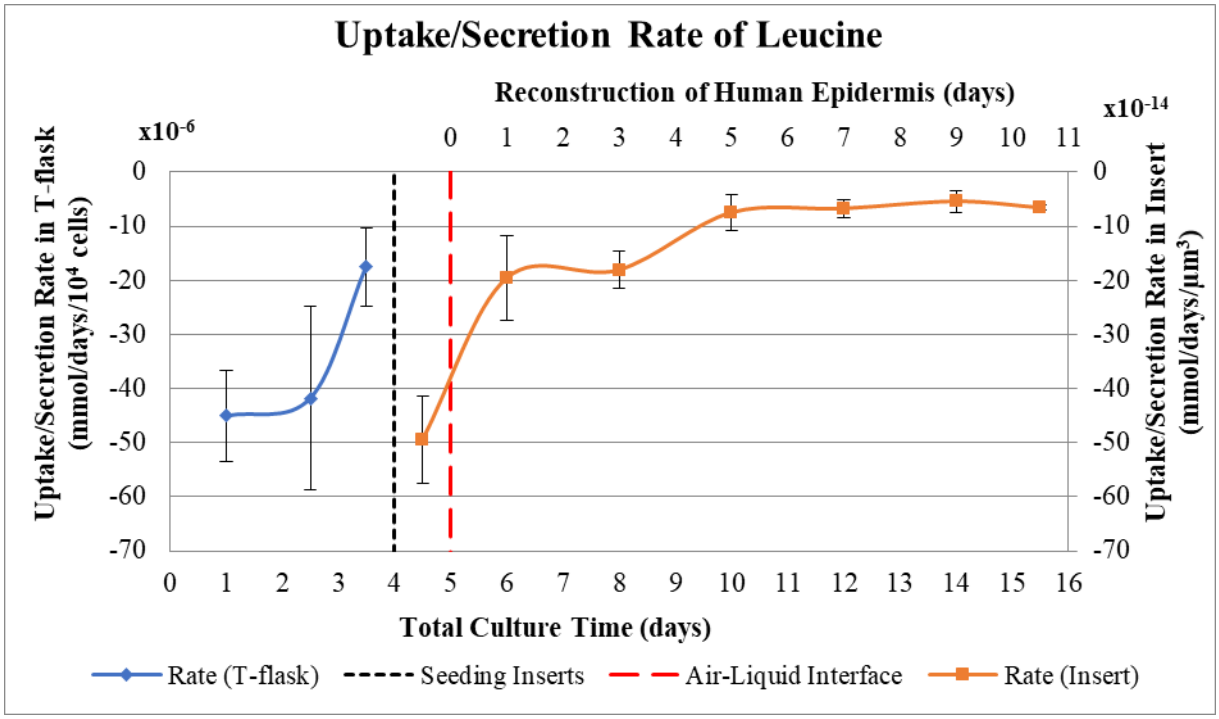

Figure 4.62 – Uptake/secretion rate of Leucine during the keratinocyte culture in monolayer and reconstruction of human epidermis in polycarbonate filter.

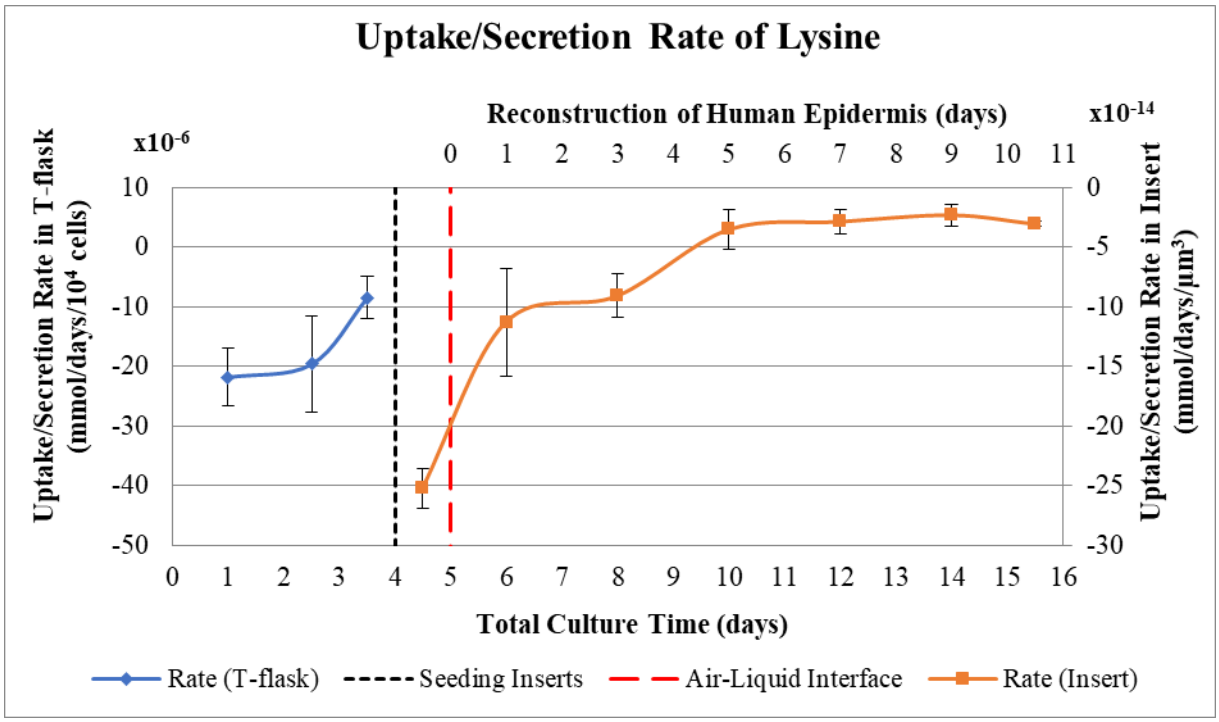

Figure 4.63 – Uptake/secretion rate of Lysine during the keratinocyte culture in monolayer and reconstruction of human epidermis in polycarbonate filter.

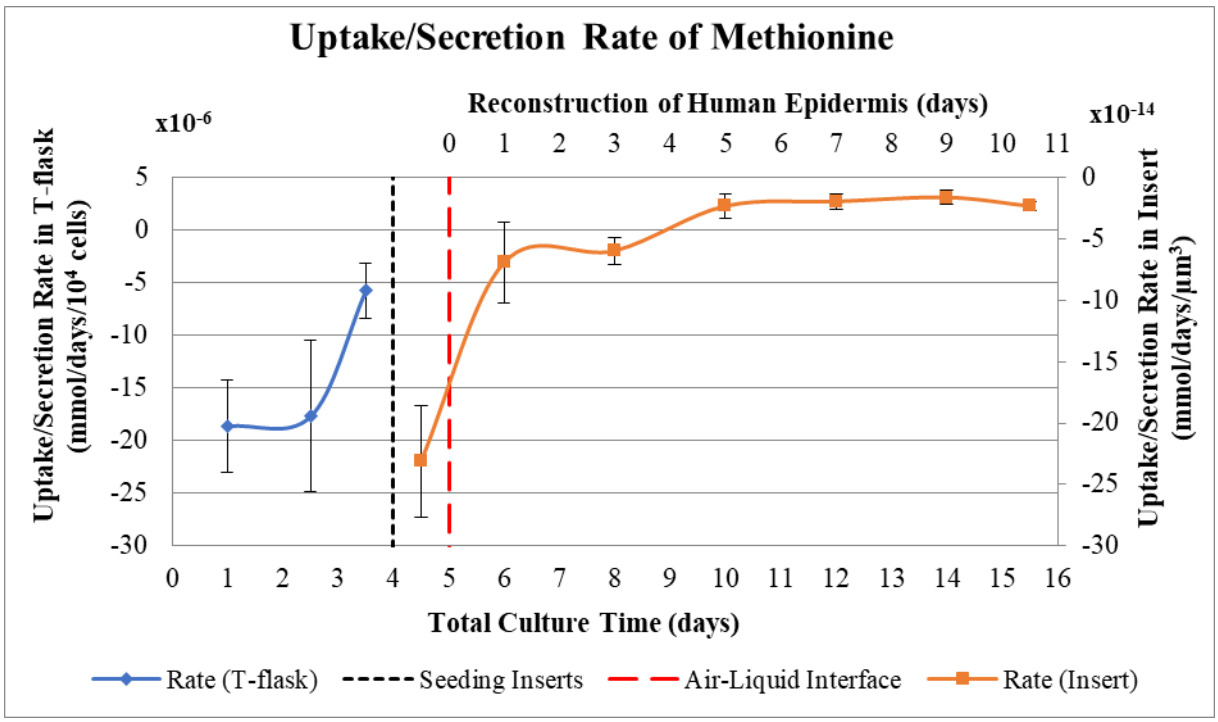

Figure 4.64 – Uptake/secretion rate of Methionine during the keratinocyte culture in monolayer and reconstruction of human epidermis in polycarbonate filter.

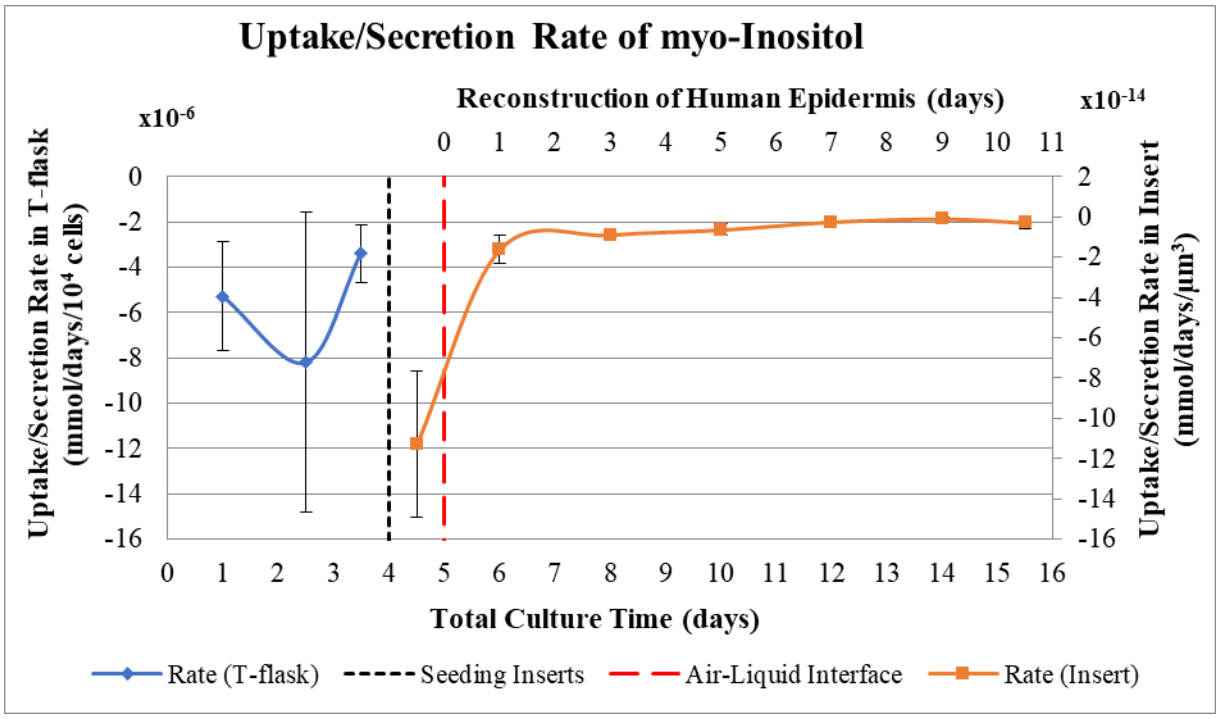

Figure 4.65 – Uptake/secretion rate of myo-Inositol during the keratinocyte culture in monolayer and reconstruction of human epidermis in polycarbonate filter.

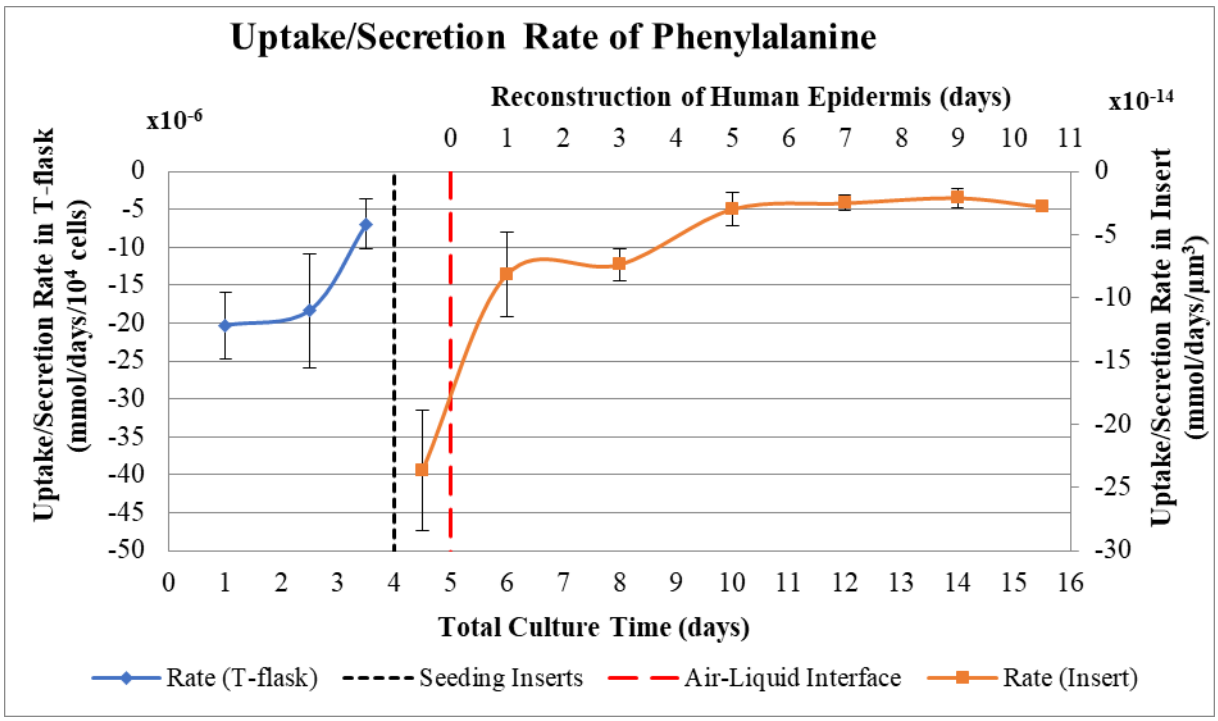

Figure 4.66 – Uptake/secretion rate of Phenylalanine during the keratinocyte culture in monolayer and reconstruction of human epidermis in polycarbonate filter.

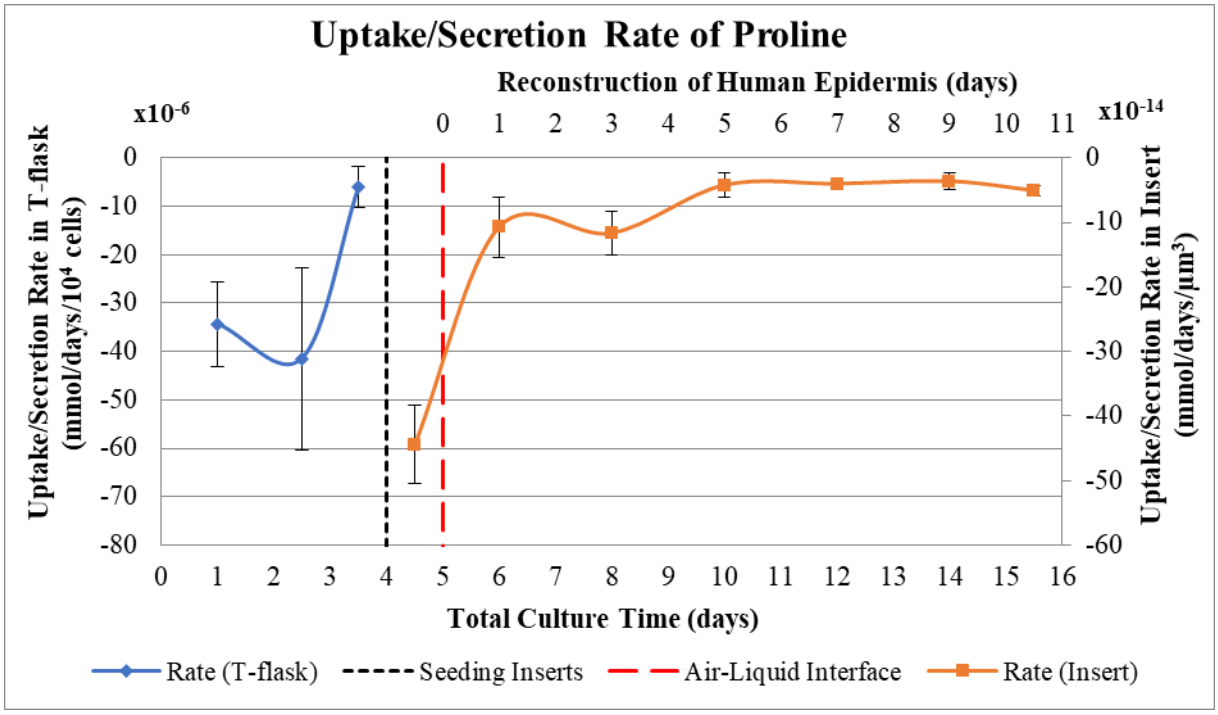

Figure 4.67 – Uptake/secretion rate of Proline during the keratinocyte culture in monolayer and reconstruction of human epidermis in polycarbonate filter.

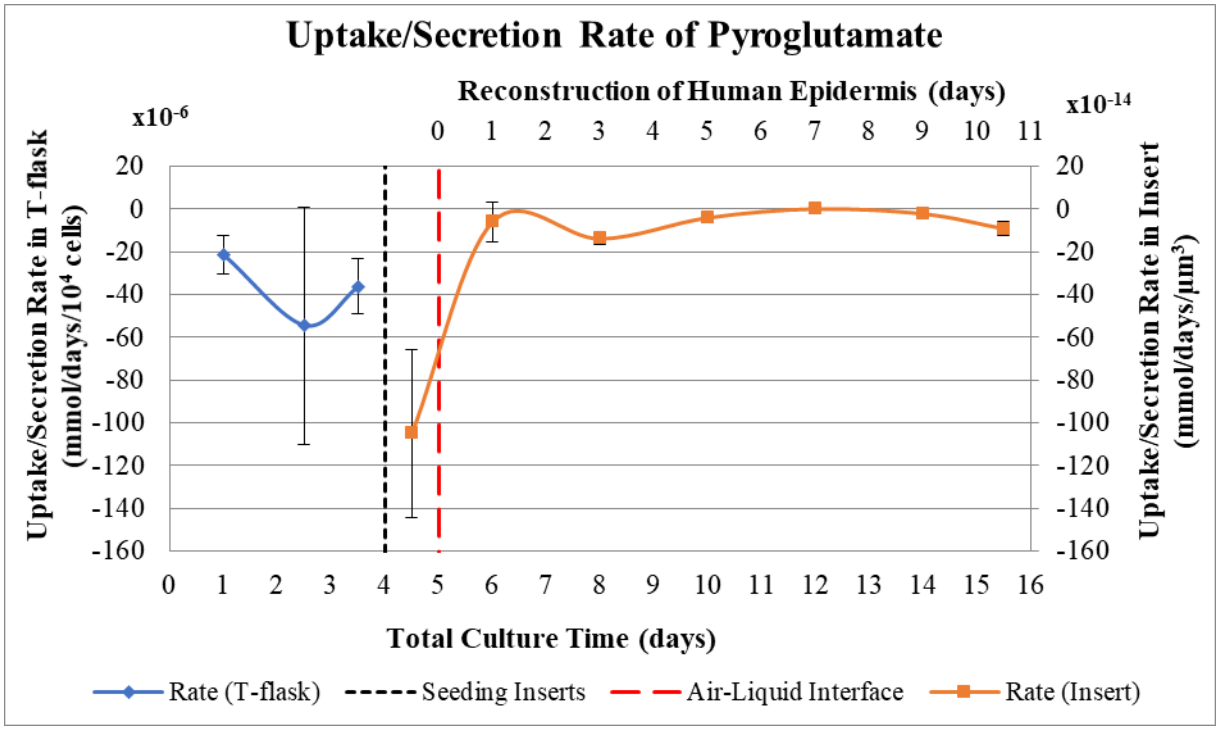

Figure 4.68 – Uptake/secretion rate of Pyroglutamate during the keratinocyte culture in monolayer and reconstruction of human epidermis in polycarbonate filter.

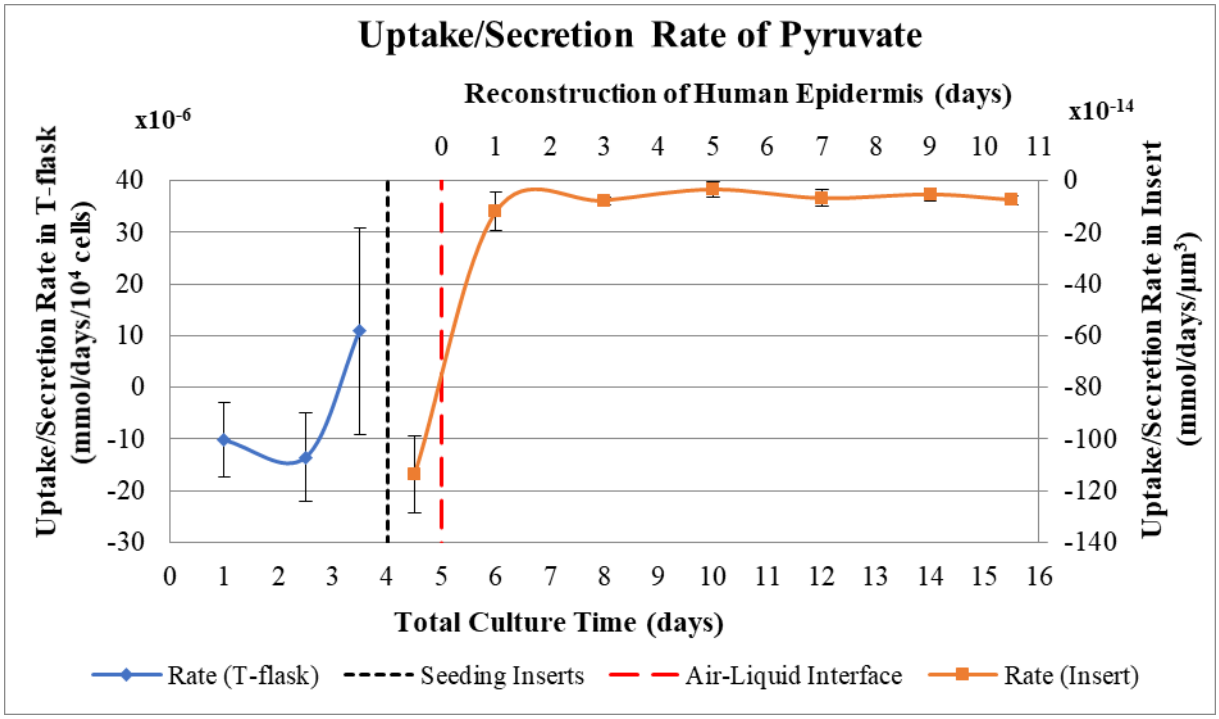

Figure 4.69 – Uptake/secretion rate of Pyruvate during the keratinocyte culture in monolayer and reconstruction of human epidermis in polycarbonate filter.

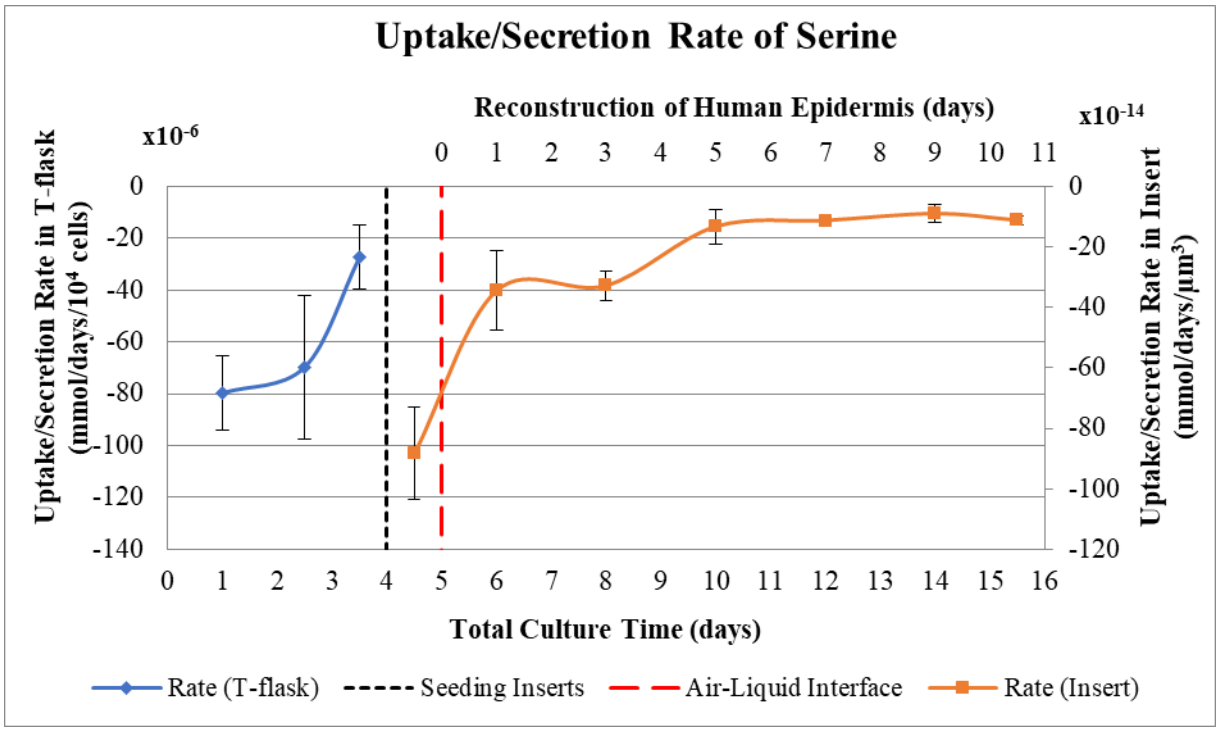

Figure 4.70 – Uptake/secretion rate of Serine during the keratinocyte culture in monolayer and reconstruction of human epidermis in polycarbonate filter.

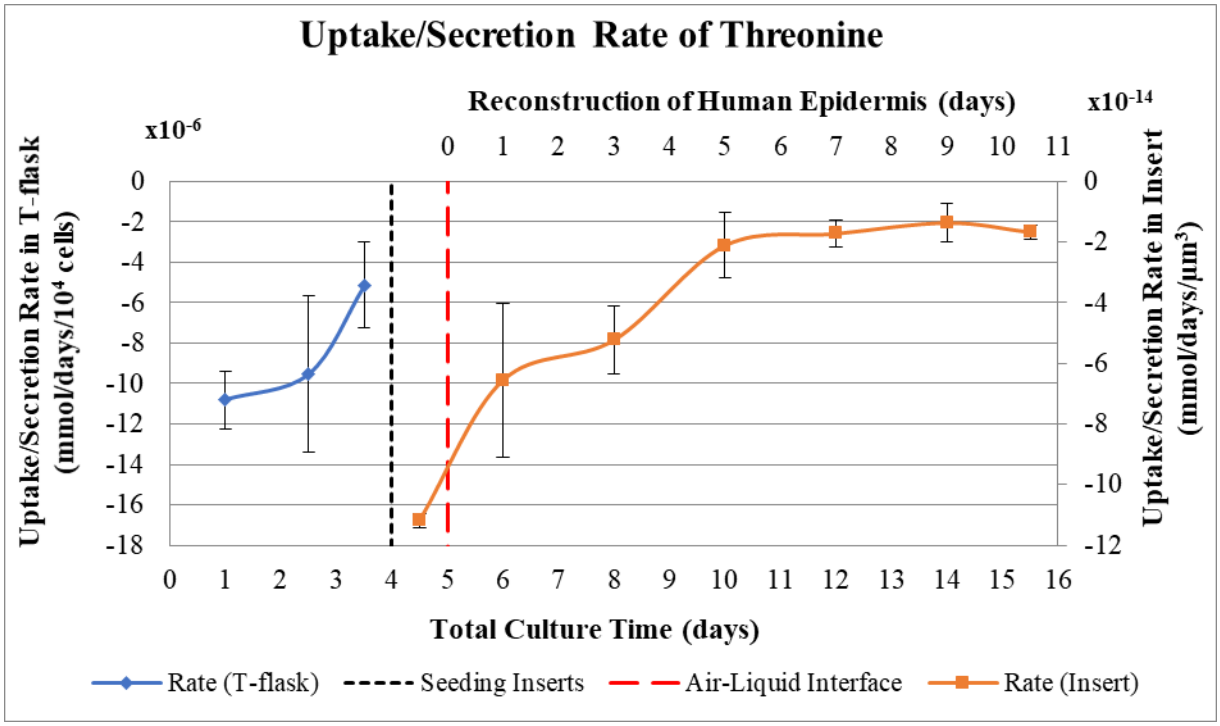

Figure 4.71 – Uptake/secretion rate of Threonine during the keratinocyte culture in monolayer and reconstruction of human epidermis in polycarbonate filter.

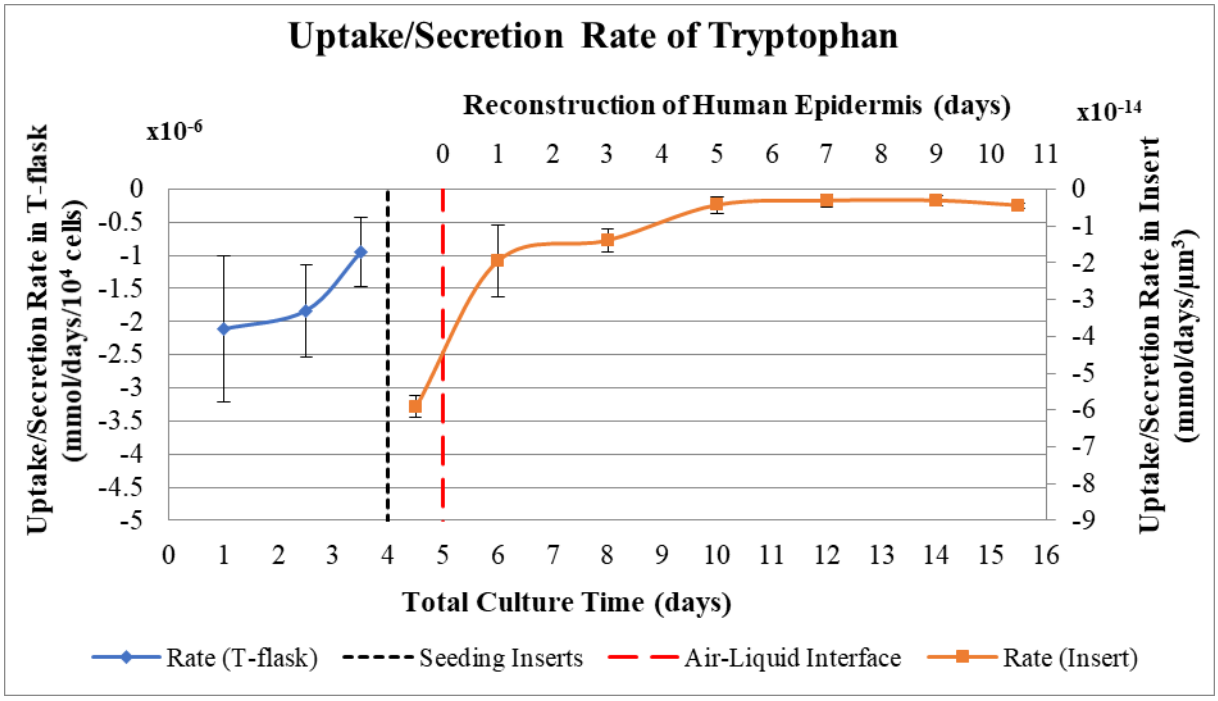

Figure 4.72 – Uptake/secretion rate of Tryptophan during the keratinocyte culture in monolayer and reconstruction of human epidermis in polycarbonate filter.

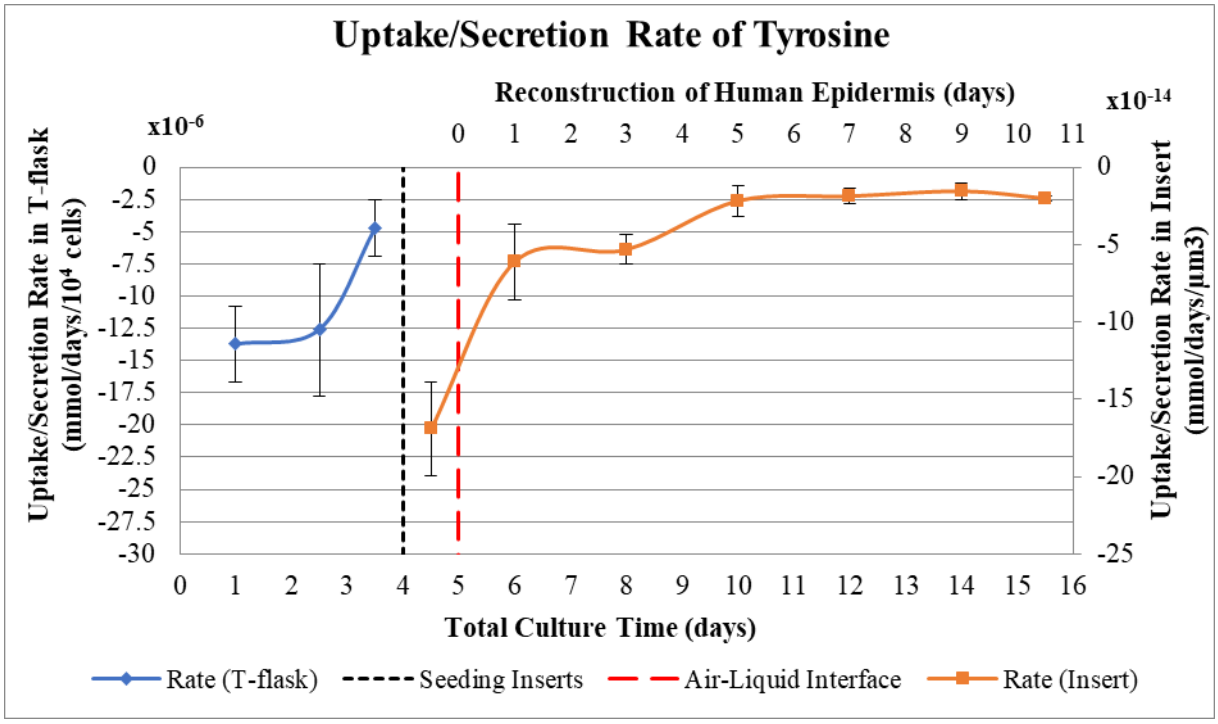

Figure 4.73 – Uptake/secretion rate of Tyrosine during the keratinocyte culture in monolayer and reconstruction of human epidermis in polycarbonate filter.

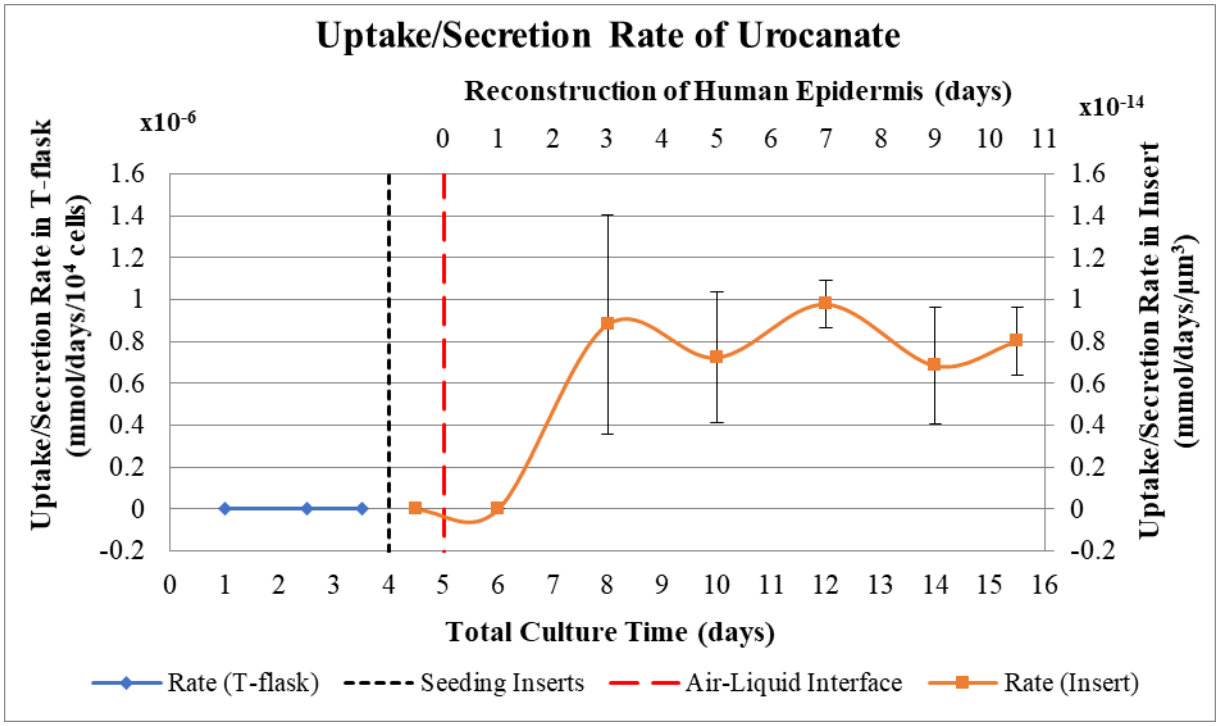

Figure 4.74 – Uptake/secretion rate of Urocanate during the keratinocyte culture in monolayer and reconstruction of human epidermis in polycarbonate filter.

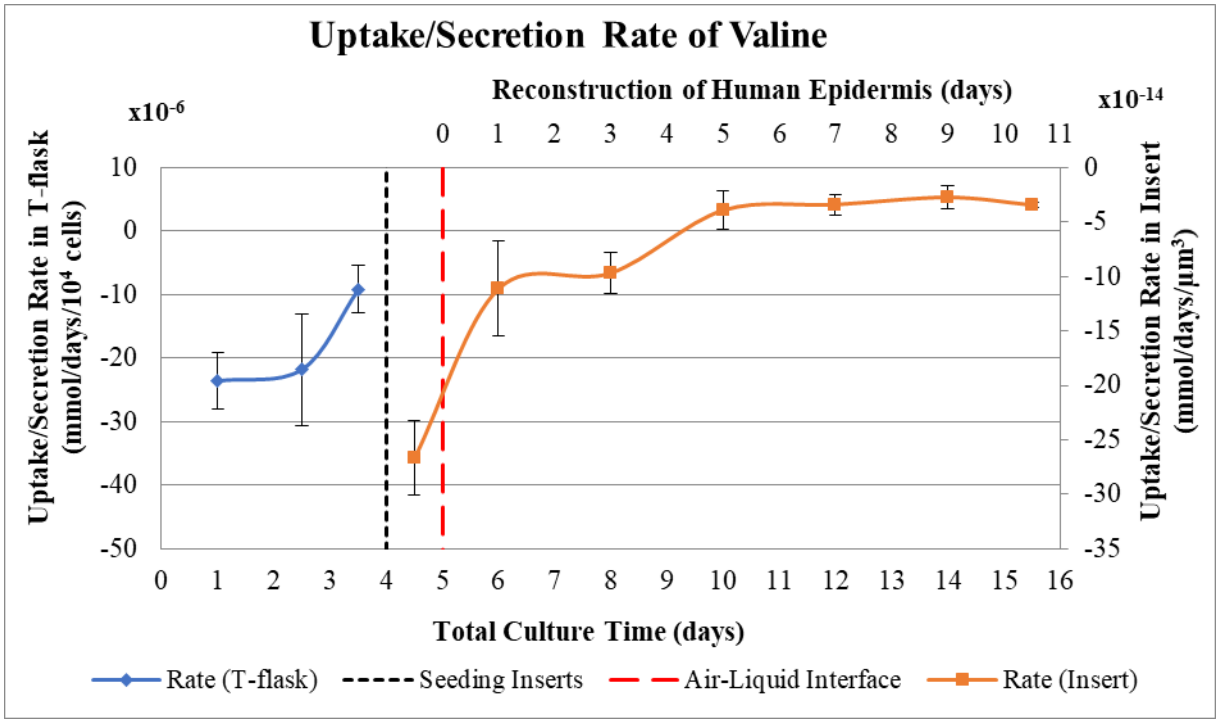

Figure 4.75 – Uptake/secretion rate of Valine during the keratinocyte culture in monolayer and reconstruction of human epidermis in polycarbonate filter.

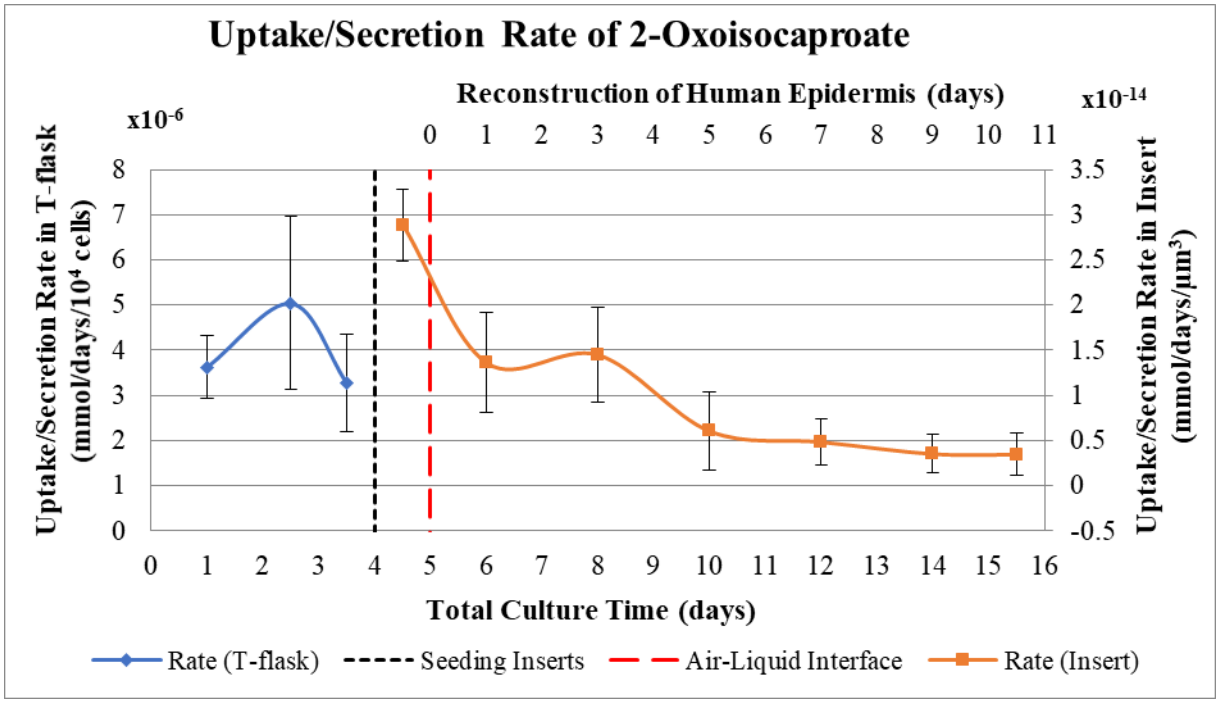

Figure 4.76 – Uptake/secretion rate of 2-Oxoisocaproate during the keratinocyte culture in monolayer and reconstruction of human epidermis in polycarbonate filter.

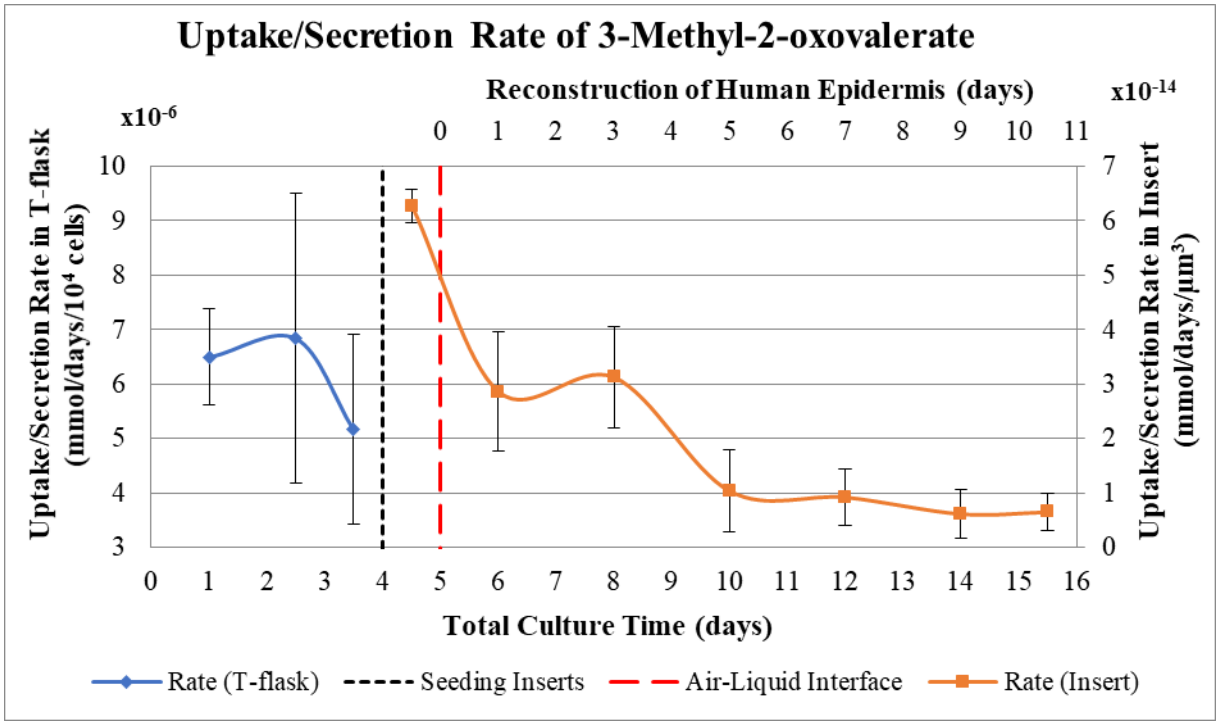

Figure 4.77 – Uptake/secretion rate of 3-Methyl-2-oxovalerate during the keratinocyte culture in monolayer and reconstruction of human epidermis in polycarbonate filter.

With the quantification of the exometabolome of the keratinocytes/epidermis and the determination of the uptake and secretion rates of the metabolites, many pertinent data were gathered about the metabolism of these cells. First, the use of ^{1}H-NMR was successful since it allowed to identify many metabolites that do not make part of the cell culture media but may appear as products of metabolism or by spontaneous reactions. These included lactate, pyroglutamate, formate, urocanate, 3-methyl-2-oxovalerate, hypoxanthine and 2-oxoisocaproate. The presence of formate indicates that there is a lack of oxygen in the cultivation process. Lactate can be produced when there is an excess of nutrients, especially glucose and amino acids, which make the cell spend more carbon sources (glucose) to produce lactic acid[47]. Its highest concentration in media is at the 2nd day of reconstruction of human epidermis on polycarbonate filter, 10 mM (see figure 4.28). Cell culture media become more acidic when the concentration of lactate exceeds its buffering capacity, which may cause growth inhibitory effects on the cells. However, studies reported that this only happens at concentrations above 25 mM[99], meaning that lactate never reached toxic levels during the proliferation of keratinocytes and the reconstruction of epidermis. Urocanate (urocanic acid) is a natural sunscreen that is formed in the *stratum corneum*. Hypoxanthine is a reaction intermediate in the metabolism of adenosine in tissues, including epidermis[100]. Pyroglutamate is a constituent of the natural moisturizing factor (NMF), a set of amino acids produced in the SC, but it was also found in samples of fresh media. This may be due to a spontaneous and non-enzymatic cyclization of glutamine in the culture media, that leads to the loss of its side-chain amide nitrogen in the form of ammonia and to the subsequent conversion of glutamine to pyroglutamate[101,102], as seen in equation 4.3:

$$(4.3)\quad \underset{\text{(Glutamine)}}{C_5H_{10}N_2O_3} \xrightarrow{-NH_3} \underset{\text{(Pyroglutamate)}}{C_5H_7NO_3}$$

As for 3-methyl-2-oxovalerate and 2-oxoisocaproate, the former is a metabolite from isoleucine[103], while the latter is an intermediate in the metabolism of leucine[104].

Regarding glucose and glutamine, both are (or can be) used for energy production, depending on the pH or the concentration of each in the media. In the case of glucose, fresh media contains approx. 6 mM, and while for the end of the culture not much is being consumed, in the beginning, and especially at day 2 of reconstruction of human epidermis, glucose is almost depleted from the media (figure 4.21). On the other hand, glutamine is at the concentration of 5 mM approx., and is not being consumed to a great extent (figure 4.23). The main role of glutamine is to provide a nitrogen source for nucleotide synthesis and to act as a precursor for protein synthesis. Energy production from glutamine is not desired, especially because one byproduct from the synthesis of nonessential amino acids from glutamine is ammonia, which is well-known to be toxic to mammalian cells[105]. However, in the case of EpiLife®, it already contains ammonia in its formulation, namely ammonium molybdate and ammonium metavanadate, and it is a metabolite that is consumed by the keratinocytes (figure 4.47). According to the literature, ammonium ions are consumed in the cytosol of the keratinocytes for production of glutamine by glutamine synthetase (GS), an enzyme abundant in the epidermis that seems to be of some importance for some functions of the skin, with deficiencies of GS resulting in early postnatal death[106,107]. Despite the possibility of it being toxic to keratinocytes at certain concentrations, the highest amount of ammonia in the media used in these studies was found to be in the fresh media, of 1.25 mM approximately, while its consumption by the cells decreases it to around 0.92 mM (figure 4.14).

Regarding the phase of reconstruction of human epidermis, besides the already mentioned glucose, the other metabolite which concentration reduces the most is the essential amino acid threonine, heavily consumed thorought the culture (figure 4.38). Other metabolites that have significant reduction of concentration include asparagine (figure 4.16), aspartate (figure 4.17), cystine (essential amino acid) (figure 4.19) and leucine (essential amino acid) (figure 4.29), as well as pyruvate (figure 4.36). As for the lipid precursors choline (figure 4.18) and myo-inositol (figure 4.32), even though they are present in media at very low concentrations (around 0.5 mM), they do not present a great variation during the culture time.

With the uptake/secretion rates it becomes easier to understand the role a certain metabolite plays in the metabolism of the cell of interest: when it is being secreted from the cell into the extracellular media, then the rate is presented with positive values above the X-axis; if instead the metabolite is being consumed, then the rate has negative values and is under the X-axis. In this study, regarding the stage of keratinocytes proliferating in T-flask, it was not possible to derive much information from the rates due to the high deviation of the results. Also, due to having different units, the rates of the keratinocytes in the T-flask, expressed in mmol/days/10^4 cells, and the rates of RHE, mmol/days/μm^3, it is also not possible to establish a direct relation between them. However, since the objective of this study was to design a new culture media to test if it would help increasing the barrier function of the skin, the focus of this analysis was the culture stage of reconstructed epidermis.

By looking at the uptake/secretion rates, it is possible to see that alanine (figure 4.46), formate (figure 4.53), glutamate (figure 4.55), hypoxanthine (figure 4.59), lactate (figure 4.61), urocanate (figure 4.74), 2-oxoisocaproate (figure 4.76) and 3-methyl-2-oxovalerate (figure 4.77) were being secreted from the cells/epidermis. On the other hand, aspartate (figure 4.50) seems to have two different profiles during the reconstruction of epidermis: it starts with a secretion profile but, in the end, it seems that the epidermal cells stopped wasting it and, instead, started consuming aspartate. As for the rest of the metabolites analyzed, they all presented an uptake profile, which was expected since many of them are essential amino acids (besides glucose). Interestingly, in all the cases where a consumption rate was detected, it is possible to observe that the cells during reconstruction of epidermis present initially a high

metabolic activity that decreases until day 5, reaching a baseline. This could seem that the reason for this to happen would be that the cells from the epidermis, at the start of the culture on the polycarbonate filter, presented a higher metabolic activity, namely the basal cells, since they are the only type of cells on the filter at the beginning of the culture. However, it is not possible to do this deduction, since keratinocytes differentiate along the epidermis, and this assumption would mean that all these different types of cells had the same metabolic activity. Day 5 is a turning point, and after it a large amount of amino acids begin to be consumed at higher rates than before. It seems that the cells are purposely directing their metabolism to glycolysis in the initial days, until the 5th, consuming high amounts of glucose and concomitantly producing high amounts of lactate to accumulate energy. Then, after day 5, an inversion of this metabolism occurs into a protein synthesis metabolism, which explains their higher rate of consumption at this stage.

4.3.2. Attempt to Improve the Barrier Function of Reconstructed Epidermis by Adopting a Clue Derived from Metabolomic Analysis

As has been said along this work, many different experiments have been performed to try to improve the permeability barrier of *in vitro* models of human epidermis, like supplementing the culture media with lipids and/or fatty acids, lowering the relative humidity, using serum-free media, adding vitamin C, reducing the incubation temperature, etc[40]. However, no epidermal equivalent capable of fully mimicking the permeability properties of native skin has yet been developed.

Therefore, a new strategy was tried based on clues derived from metabolomic analysis. An alteration was performed in the cultivation process consisting in increasing the concentration of the amino acids that were found to be more lacking in the EpiLife® culture media. As observed in the metabolomic analysis study, some amino acids were found to be reduced considerably during the reconstruction of human epidermis on polycarbonate filter, especially after the 5th day of culture at air-liquid interface. Some of these amino acids were essential amino acids, that cannot be synthesized by the cells. Others play important roles during the keratinization process, including histidine and cysteine that are constituents of proteins in the keratohyalin granules, and serine, involved in the production of sphingolipids[47]. Many of these amino acids were found to be in concentrations under 1.0 mM, even in fresh media, which may be in fact very low concentrations regarding protein synthesis and be, perhaps, causing inhibition of some vital metabolic processes. As such, the selection process was based on the consumed amino acids that were in concentrations below 1.0 mM. Additionally, all the essential amino acids were added to avoid problems of depletion. The new improved media was designed to have 3 times more the concentration of the amino acids in the EpiLife® media (see table 4.2). These concentrations were compared to those in other commercial media, to guarantee that those were not very aberrant values. The histological preparation of a skin grown in improved media can be seen in figure 4.78.

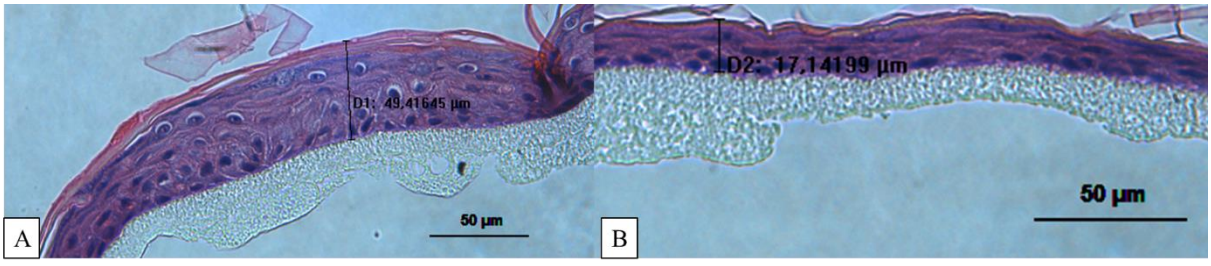

Figure 4.78 – Histology of RHE grown in improved culture media with 3 times the concentration of amino acids: (A) One replicate with approx. 49 µm thick at 11 days at air-liquid interface; (B) Another replicate with approx. 17 µm thick at 11 days at air-liquid interface. Magnification 400x.

Table 4.2 – Composition of the designed media containing 3 times the concentration of amino acids and comparison with EpiLife® media

Amino Acids	EpiLife® Media (mM)	Designed Media (mM)
Asparagine	0.0938	0.2813
Aspartate	0.0755	0.2265
Cysteine	0.1575	0.4724
Glycine	0.1183	0.3549
Histidine	0.2150	0.6451
Isoleucine	0.4243	1.2730
Leucine	0.3316	0.9947
Lysine	0.1635	0.4906
Methionine	0.1557	0.4671
Phenylalanine	0.1768	0.5304
Serine	0.6530	1.9590
Threonine	0.0773	0.2318
Tryptophan	0.0283	0.0849
Valine	0.1809	0.5426

4.3.2.1. Characterization of the Barrier Properties of Reconstructed Epidermis Cultivated with Three Times More Amino Acids

The results of the diffusion tests performed with the epidermis reconstructed in improved culture media with 3 times the concentration of amino acids were expressed as average ± standard deviation (SD) and compared to the results obtained for epidermis grown in normal conditions. These results can be found in table 4.3 and the permeability profiles for each model drug (through the skin) can also be viewed in figures 4.79 to 4.81.

Table 4.3 – Comparison of model drug permeability of reconstructed human epidermis (RHE) in improved media containing 3 times the concentration of amino acids with an RHE in normal conditions (n=5, average ± SD)

Drugs	Permeability Parameters	RHE (improved media)	RHE (normal conditions)
Hydrocortisone	Lag time (h)	0.1 ± 0.1	3.9 ± 0.7
	Q_{24} (µg/cm^2)	960.2 ± 263.1	298.7 ± 253.3
	Jmax (µg/cm^2/h)	40.6 ± 11.2	14.2 ± 12.1
Caffeine	Lag time (h)	0	1.6 ± 0.3
	Q_{24} (µg/cm^2)	58892.4 ± 6927.5	28437.8 ± 4120.3
	Jmax (µg/cm^2/h)	2447.3 ± 277.0	1222.0 ± 185.0
Tamoxifen	Lag time (h)	0	3.5 ± 1.0
	Q_{24} (µg/cm^2)	157.6 ± 57.8	140.3 ± 31.5
	Jmax (µg/cm^2/h)	10.3 ± 2.7	8.8 ± 2.0

As can be appreciated from both the Jmax and Q_{24}, the permeability of both caffeine and hydrocortisone was significantly higher ($p = 0.05$) when the epidermis was cultivated with 3 times more amino acids. For tamoxifen the differences observed were not statistically significant ($p = 0.05$). This indicates that when human epidermis was cultivated with the new culture medium the barrier was poorer.

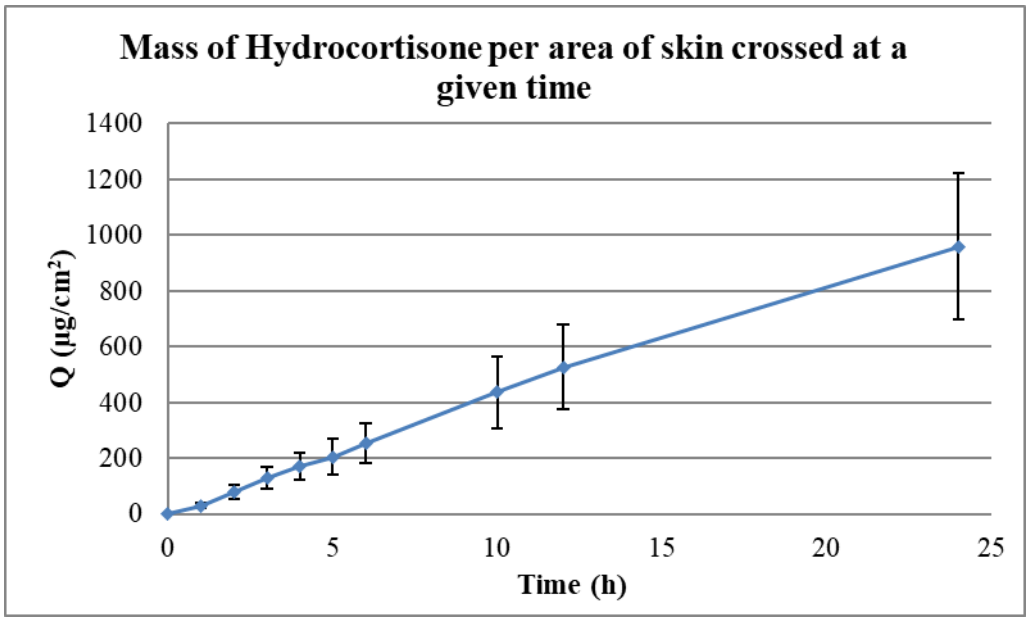

Figure 4.79 – Permeability profile of hydrocortisone in RHE grown in improved media with 3 times the concentration of amino acids during 24h (n=5, average ± SD).

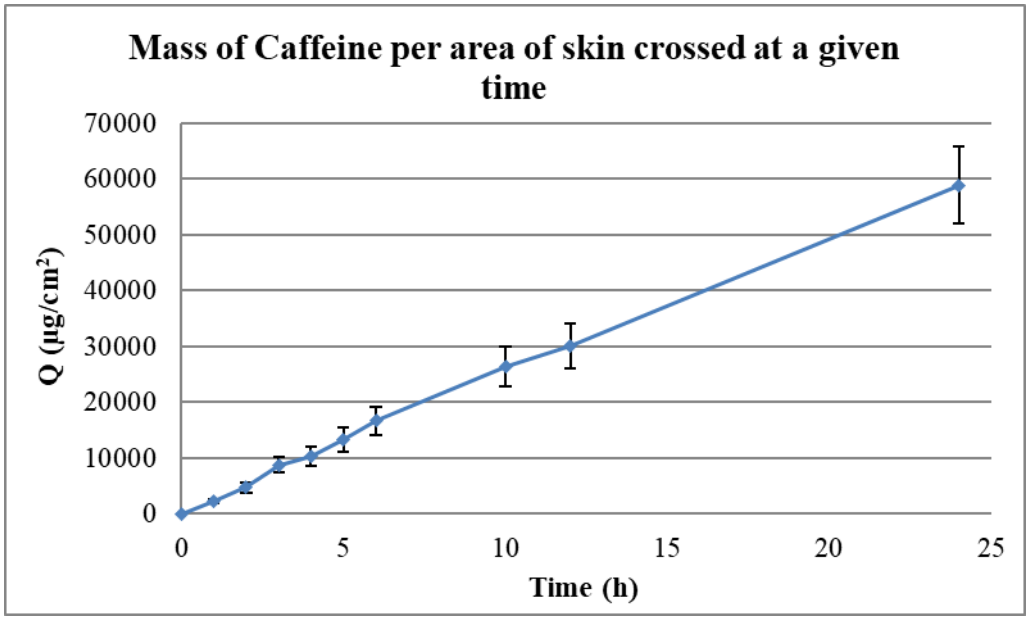

Figure 4.80 – Permeability profile of caffeine in RHE grown in improved media with 3 times the concentration of amino acids during 24h (n=5, average ± SD).

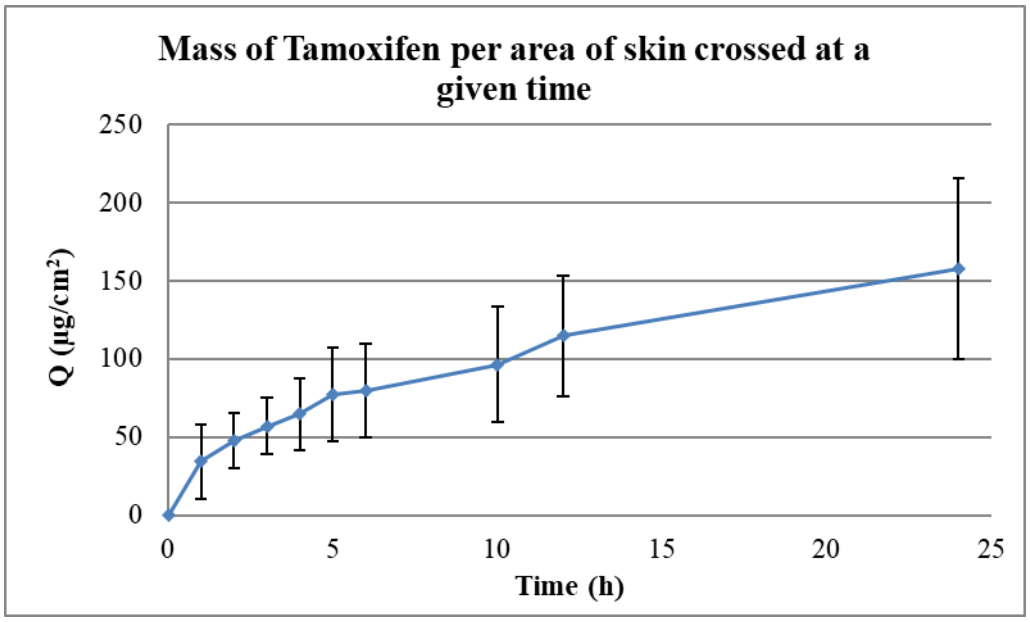

Figure 4.81 – Permeability profile of tamoxifen in RHE grown in improved media with 3 times the concentration of amino acids during 24h (n=5, average ± SD).

4.3.2.2. Total Protein Quantification of RHE Models

Due to the fact that the culture process was attempted to be improved by increasing the concentration of amino acids, which in turn can result in a different amount of proteins produced during the differentiation of the keratinocytes and tissue formation, a determination of the total protein of the tissues was performed.

The total protein obtained for reconstructed epidermis cultivated under standard conditions and with 3 times more amino acids is presented in figure 4.82 and in table 4.4.

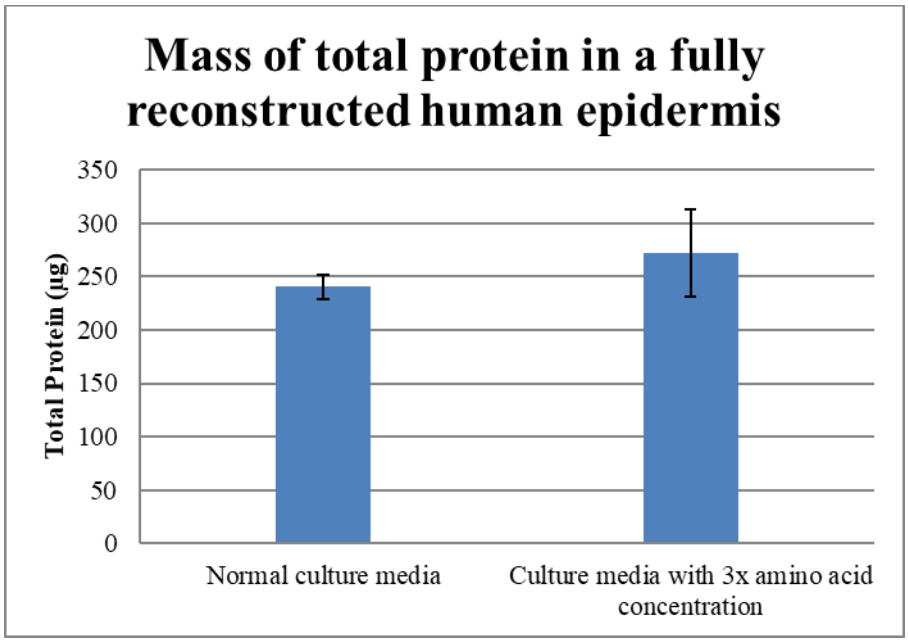

Figure 4.82 – Mass of total protein extracted from RHE grown in normal conditions with RHE in culture media with 3 times the concentration of amino acids (n=3, average ± SD).

Table 4.4 – Results of total protein extraction from the skin in normal conditions and in the improved media (n=3, average ± SD)

Total Protein extracted from the skin (µg/pellet)	
RHE (normal conditions)	**RHE (improved media)**
240.571 ± 11.508	272.412 ± 40.854

The total protein content of the reconstructed epidermis cultivated in different conditions was not statistically different ($p = 0.05$).

Even though the number of cells in an RHE is not known, it is possible to do an estimate, even if with some error. Assuming that one keratinocyte has a diameter and height of approximately 10 µm[108], then it has a volume of $7.85x10^2$ µm^3. On the other hand, an RHE with a height of 50 µm (figure 4.78) and a diameter of 1 cm has a volume of $3.93x10^9$ µm^3. The division of the volume of epidermis by the volume of one keratinocyte allows to obtain a hypothetical number of cells per insert: $5x10^6$ cells, which means that from this number of cells the total protein extracted was around 240 – 272 µg. This seems to be a very low amount of protein, when compared to what was obtained in other conditions. Work performed in the Animal Cell Technology Unit from ITQB-UNL/IBET using astrocytes showed that 258 µg of protein are obtained per 10^6 cells, which is 7 times more than what was obtained in this study. This difficulty in successfully extracting protein from the skin as well as in the dissociation of keratinocytes, may be due to the complex organization of the skin, including the fact that all proteins are crosslinked into each other and into desmosomes[109].

5. CONCLUSIONS

The reconstructed epidermis that is presently cultivated in several laboratories around the world presents morphological features similar to native skin but a deficient permeability barrier, meaning that many improvements can be performed in order to develop a more accurate model for the assessment of the toxicity of cosmetics. Also, such an improvement would be useful to use the tissues as *in vitro* models for transdermal testing.

A metabolomics study of the exometabolome of the keratinocyte culture and reconstruction of epidermis, by collecting samples from the supernatant of the cell culture and analysing them using analytical techniques like ^{1}H-NMR and HPLC, offered a better comprehension of what is happening to the metabolites in the culture media.

The media used to proliferate keratinocytes and especially the one used for reconstruction of epidermis are very rich and it seems there are no essential nutrients that deplete during the cell culture. In the reconstruction of the epidermis, the initial phase of keratinocyte proliferation that will lead to the formation of a stratified tissue (epidermis) was shown to be the most intense, in terms of metabolism, with high consumption rates of glucose and production of lactate. After the fifth day, a very high consumption of amino acids was observed. Due to this fact, a new culture media containing higher concentration of selected amino acids was tested in the production of a new batch of epidermis equivalents. Nevertheless, diffusion studies have shown that this epidermis was even more permeable than the tissues produced in standard conditions. Furthermore, the total protein content did not increase under the new culture procedure. This seems to indicate that, despite the high rates of consumption of the amino acids in the culture medium observed in the metabolomic analysis, an increase in these precursors in the culture media does not result in a reconstructed epidermis with neither more protein content, neither a better barrier function. Other yet unknown causes in the cultivation process are responsible for the poorer barrier function.

Future Studies:

Many other tests and studies can still be done. The application of multivariate analysis to the data obtained so far (for example correlating the epidermis *strata* with the uptake/secretion rates and concentrations of the metabolites) could eventually help detecting markers of the metabolic mechanism that may be occurring.

It was verified that, besides lactate, there also appears formate in the culture media, which is an indicator of anaerobic conditions, meaning that even though the culture is at air-liquid interface, the oxygen reaching the cells in the epidermis isn't enough. In the case of native skin, the vascularization of the dermis is responsible for the transportation of oxygen to the keratinocytes. Since in *in vitro* settings there are no blood vessels, it would be interesting to try to mimic it. A method very common in bacterial cell culture is the use of the orbital shaker with the objective to increase the amount of oxygen take-up into the culture media. This would be a very practical way to see if any improvement, or at least any difference, would occur. Another way would be mimicking a bioreactor, or the adaptation of the keratinocyte culture to use in a bioreactor setting, since this type of equipment can ensure that the culture media contains oxygen.

It would also be important, to perform the analysis of metabolites in media that were not possible to measure, including the lipid precursor ethanolamine.

Some cells secrete factors that may be important for the culture growth or differentiation and, as such, to avoid renovating the media in its totality, partial renovations (of, for example, only 50% of the media) could perhaps have a positive outcome. To test the addition of more glucose would also be interesting, since it was observed that it almost depletes in the first days (especially at the second) of air-liquid interface. Since the production of lactate could become a problem, a way to surpass it would be by applying the said partial renovations of media.

It could also be interesting to reduce the concentration of glutamine in the culture media, to see how it would influence the keratinocytes since it was observed that it is present in the media at high concentration (around 5 mM) and that it doesn't vary much thorought cell culture.

6. REFERENCES

1. Mathes, S. H., Ruffner, H. & Graf-Hausner, U. The use of skin models in drug development. *Adv. Drug Deliv. Rev.* **69–70,** 81–102 (2014).
2. Zhang, Z. & Michniak-Kohn, B. B. Tissue engineered human skin equivalents. *Pharmaceutics* **4,** 26–41 (2012).
3. Sun, R., Celli, A., Crumrine, D., Hupe, M., Adame, L. C., Pennypacker, S. D., Park, K., Uchida, Y., Feingold, K. R., Elias, P. M., Ilic, D. & Mauro, T. M. Lowered humidity produces human epidermal equivalents with enhanced barrier properties. *Tissue Eng. Part C. Methods* **21,** 15–22 (2015).
4. Vuyst, E. De, Charlier, C., Giltaire, S., Glas, V. De, Rouvroit, C. L. de & Poumay, Y. Reconstruction of Normal and Pathological Human Epidermis on Polycarbonate Filter. in *Methods in Molecular Biology* 191–201 (2014). doi:10.1007/7651_2013_40
5. Asbill, C., Kim, N., El-Kattan, A., Creek, K., Wertz, P. & Michniak, B. Evaluation of a human bio-engineered skin equivalent for drug permeation studies. *Pharm. Res.* **17,** 1092–1097 (2000).
6. Ponec, M., Boelsma, E., Gibbs, S. & Mommaas, M. Characterization of reconstructed skin models. *Skin Pharmacol. Appl. Skin Physiol.* **15,** 4–17 (2002).
7. Leyden, J. J. & Rawlings, A. V. *Skin Moisturization*. (Taylor & Francis, 2002).
8. Čuperlović-Culf, M., Barnett, D. A., Culf, A. S. & Chute, I. Cell culture metabolomics: Applications and future directions. *Drug Discov. Today* **15,** 610–621 (2010).
9. Blondeel, E. J. M., Ho, R., Schulze, S., Sokolenko, S., Guillemette, S. R., Slivac, I., Durocher, Y., Guillemette, J. G., McConkey, B. J., Chang, D. & Aucoin, M. G. An omics approach to rational feed: Enhancing growth in CHO cultures with NMR metabolomics and 2D-DIGE proteomics. *J. Biotechnol.* **234,** 127–138 (2016).
10. Darmon, M. & Blumenberg, M. *Molecular Biology of the Skin*. (Academic Press, 1993).
11. Jablonski, N. G. *Skin: A Natural History*. (University of California Press, 2006).
12. Aljuffali, I. A., Hsu, C.-Y., Lin, Y.-K. & Fang, J.-Y. Cutaneous delivery of natural antioxidants: the enhancement approaches. *Curr. Pharm. Des.* **21,** 2745–57 (2015).
13. Leung, D. Y. M., Boguniewicz, M., Howell, M. D., Nomura, I. & Hamid, Q. A. New insights into atopic dermatitis. *J. Clin. Invest.* **113,** 651–657 (2004).
14. Thomsen, S. F. Atopic Dermatitis: Natural History, Diagnosis, and Treatment. *ISRN Allergy* **2014,** 1–7 (2014).
15. Pappas, A. *Lipids and Skin Health*. (Springer, 2014).
16. Eaglstein, W. H. & Falanga, V. Tissue engineering and the development of Apligraf, a human skin equivalent. *Clin. Ther.* **19,** 894–905 (1997).
17. VanPutte, C. L., Regan, J. L. & Russo, A. F. *Seeley's Anatomy & Physiology*. (McGraw-Hill, 2014).
18. Sarmento, B. *Concepts and Models for Drug Permeability Studies: Cell and Tissue based In Vitro Culture Models*. (Woodhead Publishin, 2015).
19. Saladin, K. S. *Human Anatomy*. (Rex Bookstore, Inc, 2007).
20. Schachner, L. A. & Hansen, R. C. *Pediatric Dermatology*. (Elsevier Health Sciences, 2011).
21. D'Arcangelo, D., Tinaburri, L. & Dellambra, E. The role of p16inK4a pathway in human epidermal stem cell self-renewal, aging and cancer. *Int. J. Mol. Sci.* **18,** (2017).
22. Fuchs, E. Epidermal Differentiation: The Bare Essentials. *J. Cell Biol.* **111,** 2807–2814 (1990).
23. Simpson, C. L., Patel, D. M. & Green, K. J. Deconstructing the skin: cytoarchitectural determinants of epidermal morphogenesis. *Nat. Rev. Mol. Cell Biol.* **12,** 565–580 (2011).
24. Brookman, J., Chacón, J. N. & Sinclair, R. S. Some photophysical studies of cis- and trans-urocanic acid. *Photochem. Photobiol. Sci.* **1,** 327–32 (2002).
25. Chan, A. & Mauro, T. Acidification in the epidermis and the role of secretory phospholipases. *Dermatoendocrinol.* **3,** 84–90 (2011).
26. Caubet, C., Jonca, N., Brattsand, M., Guerrin, M., Bernard, D., Schmidt, R., Egelrud, T., Simon, M. & Serre, G. Degradation of Corneodesmosome Proteins by Two Serine Proteases of

the Kallikrein Family, SCTE/KLK5/hK5 and SCCE/KLK7/hK7. *J. Invest. Dermatol.* **122,** 1235–1244 (2004).
27. Ponec, M., Weerheim, A., Kempenaar, J., Mulder, A., Gooris, G. S., Bouwstra, J. & Mommaas, a M. The formation of competent barrier lipids in reconstructed human epidermis requires the presence of vitamin C. *J. Invest. Dermatol.* **109,** 348–55 (1997).
28. Fluhr, J. W., Kao, J., Jain, M., Ahn, S. K., Feingold, K. R. & Elias, P. M. Generation of free fatty acids from phospholipids regulates stratum corneum acidification and integrity. *J. Invest. Dermatol.* **117,** 44–51 (2001).
29. Ng, K. W. & Lau, W. M. Skin Deep: The Basics of Human Skin Structure and Drug Penetration. in *Percutaneous Penetration Enhancers Chemical Methods in Penetration Enhancement: Drug Manipulation Strategies and Vehicle Effects* (eds. Dragicevic, N. & Maibach, H. I.) 3–11 (2015). doi:10.1007/978-3-662-45013-0
30. Patzelt, A. & Lademann, J. The Increasing Importance of the Hair Follicle Route in Dermal and Transdermal Drug Delivery. in *Percutaneous Penetration Enhancers Chemical Methods in Penetration Enhancement: Drug Manipulation Strategies and Vehicle Effects* (eds. Dragicevic, N. & Maibach, H. I.) 43–53 (2015). doi:10.1007/978-3-662-45013-0_5
31. Promocell.com. Available at: http://www.promocell.com/fileadmin/promocell/Kapitelbilder/Keratinocytes_2.jpg. (Accessed: 22nd September 2017)
32. Pruniéras, M., Régnier, M. & Woodley, D. Methods for cultivation of keratinocytes with an air liquid interface. *J. Invest. Dermatol.* **81,** 28–33 (1983).
33. Mcheik, J. N., Barrault, C., Pedretti, N., Garnier, J., Juchaux, F., Levard, G., Morel, F., Lecron, J.-C. & Bernard, F.-X. Foreskin-isolated keratinocytes provide successful extemporaneous autologous paediatric skin grafts. *J. Tissue Eng. Regen. Med.* **10,** 252–260 (2016).
34. Biomimiq: Healthy Skin Models. Available at: http://www.biomimiq.com/science/Healthy Skin Models. (Accessed: 10th July 2016)
35. OECD. In vitro skin irritation: reconstructed human epidermis test method. 1–21 (2015). doi:10.1787/9789264242845-en
36. Guth, K., Schäfer-Korting, M., Fabian, E., Landsiedel, R. & van Ravenzwaay, B. Suitability of skin integrity tests for dermal absorption studies in vitro. *Toxicol. Vitr.* **29,** 113–123 (2015).
37. Schmook, F. P., Meingassner, J. G. & Billich, A. Comparison of human skin or epidermis models with human and animal skin in in-vitro percutaneous absorption. *Int. J. Pharm.* **215,** 51–56 (2001).
38. Ponec, M., Weerheim, A., Kempenaar, J., Mommaas, a M. & Nugteren, D. H. Lipid composition of cultured human keratinocytes in relation to their differentiation. *J. Lipid Res.* **29,** 949–961 (1988).
39. Van Gele, M., Geusens, B., Brochez, L., Speeckaert, R. & Lambert, J. Three-dimensional skin models as tools for transdermal drug delivery: challenges and limitations. *Expert Opin. Drug Deliv.* **8,** 705–720 (2011).
40. Pasonen-Seppänen, S., Suhonen, M. T., Kirjavainen, M., Suihko, E., Urtti, A., Miettinen, M., Hyttinen, M., Tammi, M. & Tammi, R. Vitamin C enhances differentiation of a continuous keratinocyte cell line (REK) into epidermis with normal stratum corneum ultrastructure and functional permeability barrier. *Histochem. Cell Biol.* **116,** 287–297 (2001).
41. Baserga, R. *Tissue Growth Factors*. (Springer Science & Business Media, 2012).
42. Mak, V. H., Cumpstone, M. B., Kennedy, A. H., Harmon, C. S., Guy, R. H. & Potts, R. O. Barrier function of human keratinocyte cultures grown at the air liquid interface. *J. Invest. Dermatol.* **96,** 323–7 (1991).
43. Boyce, S. T. & Williams, M. L. Lipid supplemented medium induces lamellar bodies and precursors of barrier lipids in cultured analogues of human skin. *J. Invest. Dermatol.* **101,** 180–4 (1993).
44. Ågren, J., Sjörs, G. & Sedin, G. Ambient humidity influences the rate of skin barrier maturation in extremely preterm infants. *J. Pediatr.* **148,** 613–617 (2006).
45. Martínez, V. S., Dietmair, S., Quek, L.-E., Hodson, M. P., Gray, P. & Nielsen, L. K. Flux balance analysis of CHO cells before and after a metabolic switch from lactate production to consumption. *Biotechnol. Bioeng.* **110,** 660–666 (2013).

46. Schneider, M., Marison, I. W. & Von Stockar, U. The importance of ammonia in mammalian cell culture. *J. Biotechnol.* **46,** 161–185 (1996).
47. Berg, J. M., Tymoczko, J. L., Gregory J. Gatto, J. & Stryer, L. *Biochemistry*. (W. H. Freeman and Company, 2015).
48. Ozturk, S. S., Riley, M. R. & Palsson, B. O. Effects of Ammonia and Lactate on Hybridoma Growth, Metabolism, and Antibody Production. *Biotechnol. Bioeng.* **39,** 418–431 (1992).
49. Glacken, M. W., Fleischaker, R. J. & Sinskey, A. J. Reduction of waste product excretion via nutrient control: Possible strategies for maximizing product and cell yields on serum in cultures of mammalian cells. *Biotechnol. Bioeng.* **28,** 1376–1389 (1986).
50. Byoung, J. K., Duk, J. O. & Ho, N. C. Limited use of Centritech Lab II centrifuge in perfusion culture of rCHO cells for the production of recombinant antibody. *Biotechnol. Prog.* **24,** 166–174 (2008).
51. Ohya, T., Hayashi, T., Kiyama, E., Nishii, H., Miki, H., Kobayashi, K., Honda, K., Omasa, T. & Ohtake, H. Improved production of recombinant human antithrombin III in Chinese hamster ovary cells by ATF4 overexpression. *Biotechnol. Bioeng.* **100,** 317–324 (2008).
52. Bradley, S. A., Ouyang, A., Purdie, J., Smitka, T. A., Wang, T. & Kaerner, A. Fermentanomics: Monitoring mammalian cell cultures with NMR spectroscopy. *J. Am. Chem. Soc.* **132,** 9531–9533 (2010).
53. CAMO Software: Multivariate statistical process monitoring and control. Available at: http://www.camo.com/multivariate_analysis.html. (Accessed: 7th September 2017)
54. Aranibar, N., Borys, M., Mackin, N. A., Ly, V., Abu-Absi, N., Abu-Absi, S., Niemitz, M., Schilling, B., Li, Z. J., Brock, B., Russell, R. J., Tymiak, A. & Reily, M. D. NMR-based metabolomics of mammalian cell and tissue cultures. *J. Biomol. NMR* **49,** 195–206 (2011).
55. Horgan, R. P. & Kenny, L. C. SAC review 'Omic' technologies: proteomics and metabolomics. *Obstet. Gynaecol.* **13,** 189–195 (2011).
56. Dunn, W. B. & Ellis, D. I. Metabolomics: Current analytical platforms and methodologies. *TrAC - Trends Anal. Chem.* **24,** 285–294 (2005).
57. Jellum, E., Kvittingen, E. A. & Stokke, O. Mass spectrometry in diagnosis of metabolic disorders. *Biol. Mass Spectrom.* **16,** 57–62 (1988).
58. Sauter, H., Lauer, M. & Fritsch, H. Metabolic profiling of plants: a new diagnostic technique. *ACS Symp. Ser. Am. Chem. Soc.* 288–299 (1991).
59. Omasa, T., Furuichi, K., Iemura, T., Katakura, Y., Kishimoto, M. & Suga, K. I. Enhanced antibody production following intermediate addition based on flux analysis in mammalian cell continuous culture. *Bioprocess Biosyst. Eng.* **33,** 117–125 (2010).
60. Sá, J. V., Duarte, T. M., Carrondo, M. J. T., Alves, P. M. & Teixeira, A. P. Metabolic Flux Analysis: A Powerful Tool in Animal Cell Culture. in *Animal Cell Culture* **9,** 521–539 (2015).
61. Ma, N., Ellet, J. A., Okediadi, C., Hermes, P., McCormick, E. & Casnocha, S. A single nutrient feed supports both chemically defined NS0 and CHO fed-batch processes: Improved productivity and lactate metabolism. *Biotechnol. Prog.* **25,** 1353–1363 (2009).
62. Martinez, V., Gerdtzen, Z. P., Andrews, B. A. & Asenjo, J. A. Viral vectors for the treatment of alcoholism: Use of metabolic flux analysis for cell cultivation and vector production. *Metab. Eng.* **12,** 129–137 (2010).
63. Chong, W. P. K., Reddy, S. G., Yusufi, F. N. K., Lee, D. Y., Wong, N. S. C., Heng, C. K., Yap, M. G. S. & Ho, Y. S. Metabolomics-driven approach for the improvement of Chinese hamster ovary cell growth: Overexpression of malate dehydrogenase II. *J. Biotechnol.* **147,** 116–121 (2010).
64. Vinayavekhin, N. & Saghatelian, A. Untargeted metabolomics. *Curr. Protoc. Mol. Biol.* 1–24 (2010). doi:10.1002/0471142727.mb3001s90
65. Exarchou, V., Krucker, M., Van Beek, T. A., Vervoort, J., Gerothanassis, I. P. & Albert, K. LC-NMR coupling technology: Recent advancements and applications in natural products analysis. *Magn. Reson. Chem.* **43,** 681–687 (2005).
66. Khoo, S. H. G. & Al-Rubeai, M. Metabolomics as a complementary tool in cell culture. *Biotechnol. Appl. Biochem.* **47,** 71–84 (2007).
67. BRUKER. AVANCE - Beginners Guide. (2002).
68. Kwan, A. H., Mobli, M., Gooley, P. R., King, G. F. & MacKay, J. P. Macromolecular NMR

spectroscopy for the non-spectroscopist. *FEBS J.* **278,** 687–703 (2011).
69. Council, N. R., Sciences, D. on E. and P., Astronomy, B. on P. and, Committee, S. S. S. & Science, C. on O. in H. M. F. *Opportunities in High Magnetic Field Science*. (National Academies Press, 2005).
70. Avance II+ - 500 MHz | cermax.itqb.unl.pt. Available at: http://cermax.itqb.unl.pt/SiTe_d/?q=node/48. (Accessed: 11th September 2017)
71. Van, Q. N., Issaq, H. J., Jiang, Q., Li, Q., Muschik, G. M., Waybright, T. J., Lou, H., Dean, M., Uitto, J. & Veenstra, T. D. Comparison of 1D and 2D NMR spectroscopy for metabolic profiling. *J. Proteome Res.* **7,** 630–639 (2008).
72. Hamilton, R. J. *Lipid Analysis in Oils and Fats*. (Springer Science & Business Media, 1998).
73. Du, F., Zhou, H., Chen, L., Zhang, B. & Yan, B. Structure elucidation of nanoparticle-bound organic molecules by 1H NMR. *TrAC - Trends Anal. Chem.* **28,** 88–95 (2009).
74. King, G. F. & Kuchel, P. W. Theoretical and Practical Aspects of NMR Studies of Cells. *Immunomethods* **4,** 85–97 (1994).
75. Kelly, A. E., Ou, H. D., Withers, R. & Dotsch, V. Low-Conductivity Buffers for High-Sensitivity NMR Measurements. *J. Am. Chem. Soc.* **124,** 12013–12019 (2002).
76. Tredwell, G. D., Bundy, J. G., De Iorio, M. & Ebbels, T. M. D. Modelling the acid/base 1H NMR chemical shift limits of metabolites in human urine. *Metabolomics* **12,** 1–10 (2016).
77. Wishart, D. S. Quantitative metabolomics using NMR. *TrAC - Trends Anal. Chem.* **27,** 228–237 (2008).
78. Yanase, H., Torishima, H. & Yamamoto, R. United States Patent [19]. **143,** (1998).
79. Poumay, Y., Dupont, F., Marcoux, S., Leclercq-Smekens, M., Hérin, M. & Coquette, A. A simple reconstructed human epidermis: Preparation of the culture model and utilization in in vitro studies. *Arch. Dermatol. Res.* **296,** 203–211 (2004).
80. Recombinant Human KGF/FGF-7 Protein 251-KG-010: R&D Systems. Available at: https://www.rndsystems.com/products/recombinant-human-kgf-fgf-7-protein_251-kg. (Accessed: 17th September 2017)
81. Lo-Laboroptik – UK manufacturers of blood counting chambers. Available at: http://www.lo-laboroptik.com/#Bürker. (Accessed: 12th September 2017)
82. Nexcelom.com - Counting Mammalian Cells Using a Hemacytometer- Manual Cell Counting. Available at: http://www.nexcelom.com/Applications/cc-04-counting-mammalian-cells-using-a-hemacytometer.php.
83. Minner, F., Herphelin, F. & Poumay, Y. Study of Epidermal Differentiation in Human Keratinocytes Cultured in Autocrine Conditions. in *Epidermal Cells* **585,** 71–82 (2010).
84. Kim, N., El-Khalili, M., Henary, M. M., Strekowski, L. & Michniak, B. B. Percutaneous penetration enhancement activity of aromatic S,S-dimethyliminosulfuranes. *Int. J. Pharm.* **187,** 219–229 (1999).
85. Moss, G., Gullick, D. & Wilkinson, S. *Predictive Methods in Percutaneous Absorption*. (Springer, 2015).
86. Brodin, B., Steffansen, B. & Nielsen, C. U. Passive diffusion of drug substances: the concepts of flux and permeability. *Mol. Biopharm. Asp. drug characterisation, drug Deliv. Dos. form Eval.* 135–151 (2010). doi:10.1200/JCO.2003.10.116
87. Thermo Fisher Scientific. NanoDrop 2000/2000c Spectrophotometer - User Manual. (2009). doi:ONLINE
88. Holmgaard, R. & Nielsen, J. B. Dermal absorption of pesticides – evaluation of variability and prevention. (2009).
89. Duarte, T. M., Carinhas, N., Silva, A. C., Alves, P. M. & Teixeira, A. P. 1H-NMR Protocol for Exometabolome Analysis of Cultured Mammalian Cells. in *Animal Cell Biotechnology: Methods and Protocols* **1104,** 237–247 (2014).
90. Chenomx NMR Suite 8.3. Available at: http://www.chenomx.com/support/nmrsuite/8.3/#?noticesAndTrademarks. (Accessed: 11th September 2017)
91. Jansen, J. F. a, Backes, W. H., Nicolay, K. & Kooi, M. E. 1H MR spectroscopy of the brain: absolute quantification of metabolites. *Radiology* **240,** 318–332 (2006).
92. Waters Corporation. AccQ-Fluor Reagent Kit care and use manual. 1–5 (2008).

93. Burden, D. W. Guide to the homogenization of biological samples. *Random Prim.* 1–14 (2008). doi:10.1111/j.1474-9726.2006.00237.x
94. De Corte, P., Verween, G., Verbeken, G., Rose, T., Jennes, S., De Coninck, A., Roseeuw, D., Vanderkelen, A., Kets, E., Haddow, D. & Pirnay, J. P. Feeder layer- and animal product-free culture of neonatal foreskin keratinocytes: Improved performance, usability, quality and safety. *Cell Tissue Bank.* **13,** 175–189 (2012).
95. Al-Refu, K. General Methods in Preparation of Skin Biopsies for Haematoxylin & Eosin Stain and Immunohistochemistry. in *Skin Biopsy - Perspectives* 19–30 (2011).
96. Corporation, W. The Successful Use of UV Detection with the AccQ-Tag Method. 1–2 (1996).
97. Gray, N. & Plumb, R. A Validated Assay for the Quantification of Amino Acids in Mammalian Urine. 1–8
98. Hamann, M. J. Irreversible oxidation of protein cysteine residues. *Retrosp. Theses Diss.* (2002).
99. Hassell, T., Gleave, S. & M, B. Growth Inhibition in Animal Cell Culture. *Appl. Biochem. Biotechnol.* **30,** 29–41 (1991).
100. Koizumi, H., Iizuka, H., Aoyagi, T. & Miura, Y. Adenosine deaminase in human epidermis from healthy and psoriatic subjects. *Arch. Dermatol. Res.* **275,** 310–314 (1983).
101. Kumar, A. & Bachhawat, A. K. Pyroglutamic acid: Throwing light on a lightly studied metabolite. *Curr. Sci.* **102,** 288–297 (2012).
102. Purwaha, P., Silva, L. P., Hawke, D. H., Weinstein, J. N. & Lorenzi, P. L. An artifact in LC-MS/MS measurement of glutamine and glutamic acid: In-source cyclization to pyroglutamic acid. *Anal. Chem.* **86,** 5633–5637 (2014).
103. 3-Methyl-2-oxovaleric acid. Available at: http://www.hmdb.ca/metabolites/HMDB00491. (Accessed: 17th September 2017)
104. Ketoleucine. Available at: http://www.hmdb.ca/metabolites/HMDB0000695. (Accessed: 18th September 2017)
105. Xie, L. & Wang, D. I. C. Stoichiometric analysis of animal cell growth and its application in medium design. *Biotechnol. Bioeng.* **43,** 1164–1174 (1994).
106. Adeva, M. M., Souto, G., Blanco, N. & Donapetry, C. Ammonium metabolism in humans. *Metabolism.* **61,** 1495–1511 (2012).
107. Danielyan, L., Zellmer, S., Sickinger, S., Tolstonog, G. V., Salvetter, J., Lourhmati, A., Reissig, D. D., Gleiter, C. H., Gebhardt, R. & Buniatian, G. H. Keratinocytes as depository of ammonium-inducible glutamine synthetase: Age- and anatomy-dependent distribution in human and rat skin. *PLoS One* **4,** (2009).
108. Barrandon, Y. & Green, H. Cell size as a determinant of the clone-forming ability of human keratinocytes. *Proc. Natl. Acad. Sci. U. S. A.* **82,** 5390–5394 (1985).
109. Candi, E., Schmidt, R. & Melino, G. The cornified envelope: a model of cell death in the skin. *Nat. Rev. Mol. Cell Biol.* **6,** 328–340 (2005).
110. Zsila, F., Matsunaga, H., Bikádi, Z. & Haginaka, J. Multiple ligand-binding properties of the lipocalin member chicken α1-acid glycoprotein studied by circular dichroism and electronic absorption spectroscopy: The essential role of the conserved tryptophan residue. *Biochim. Biophys. Acta - Gen. Subj.* **1760,** 1248–1273 (2006).
111. Harika, M. & Kumar, G. S. Simultaneous UV-spectrophotometric estimation of hydrocortisone acetate and sulphacetamide sodium in combined dosage form. *Int. J. Pharm. Sci. Res.* **4,** 1901–1904 (2013).
112. Bhawani, S. A., Fong, S. S. & Ibrahim, M. N. M. Spectrophotometric Analysis of Caffeine. *Int. J. Anal. Chem.* **2015,** 1–7 (2015).

7. APPENDIX

APPENDIX A – EpiLife® Formulation

Table 7.1 – EpiLife® Formulation.

		Concentration in MCDB 153 (mM)[78]
Amino Acids	Glycine	0.1
	L-Alanine	0.1
	L-Arginine HCl	1
	L-Asparagine.H_2O	0.1
	L-Aspartic Acid	0.03
	L-Cysteine	0.24
	L-Glutamic Acid	0.1
	L-Glutamine	6
	L-Histidine HCl.H_2O	0.08
	L-Isoleucine	0.015
	L-Leucine	0.5
	L-Lysine HCl	0.1
	L-Methionine	0.03
	L-Phenylalanine	0.03
	L-Proline	0.3
	L-Serine	0.6
	L-Threonine	0.1
	L-Tryptophan	0.015
	L-Tyrosine	0.015
	L-Valine	0.3
Vitamins	Choline Chloride	0.1
	D-Pantothenic Acid	0.001
	Folic acid	0.0018
	myo-Inositol	0.1
	Niacinamide	0.0003
	Pyridoxal HCl	0.0003
	Riboflavin	0.0001
	Thiamine HCl	0.001
	Vitamin B_{12}	0.003
	d-Biotin	0.00006

Table 7.1 (Continuation) – EpiLife® Formulation. NE – Does not exist in MCDB 153 Media.

		Concentration in MCDB 153 (mM)[78]
Other Components	Adenine.HCl	0.18
	D-Glucose (Dextrose)	6
	DL-alpha-Lipoic Acid	0.001
	Ethanolamine	NE
	HEPES	28
	O-Phosphorylethanolamine	NE
	Phenol Red	0.0033
	Putrescine 2HCl	0.001
	Sodium Pyruvate	0.5
	Thymidine	0.003
Inorganic Salts	Ammonium Molybdate ($(NH_4)_6Mo_7O_{24}.4H_2O$)	0.000001
	Ammonium metavanadate (NH_4VO_3)	0.000005
	Cupric sulfate ($CuSO_4.5H_2O$)	0.000011
	Ferric sulfate ($FeSO_4.7H_2O$)	0.005
	Magnesium Chloride ($MgCl_2.6H_2O$)	0.6
	Manganese Sulfate ($MnSO_4.H_2O$)	0.000001
	Nickelous Chloride ($NiCl_2.6H_2O$)	0.0000005
	Potassium Chloride (KCl)	1.5
	Sodium Bicarbonate ($NaHCO_3$)	14
	Sodium Chloride (NaCl)	130
	Sodium Meta Silicate ($Na_2SiO_3.9H_2O$)	0.0005
	Sodium Phosphate dibasic ($Na_2HPO_4.7H_2O$)	2
	Sodium Selenite (Na_2SeO_3)	NE
	Tin Chloride ($SnCl_2.2H_2O$)	0.0000005
	Zinc sulfate ($ZnSO_4.7H_2O$)	0.0005
	Calcium Chloride	0.15

Table 7.2 – Human Keratinocyte Growth Supplement Formulation.

Components	**Concentration**
Bovine pituitary extract (BPE)	0.2 % v/v
Recombinant human insulin-like growth factor-I	5 µg/mL
Hydrocortisone	0.18 µg/mL
Bovine transferrin	5 µg/mL
Human epidermal growth factor	0.2 ng/mL

APPENDIX B – Skin Permeability Tests

Table 7.3 – Franz Cells Dimensions.

Franz Cells	Internal Diameter (mm)		Volume of Receptor Chamber (mL)
	Donor Chamber	Receptor Chamber	
1	14.36	13.60	13.90
2	14.21	13.59	12.60
3	13.86	14.10	13.20
4	14.15	13.81	13.70
5	14.43	14.31	14.30

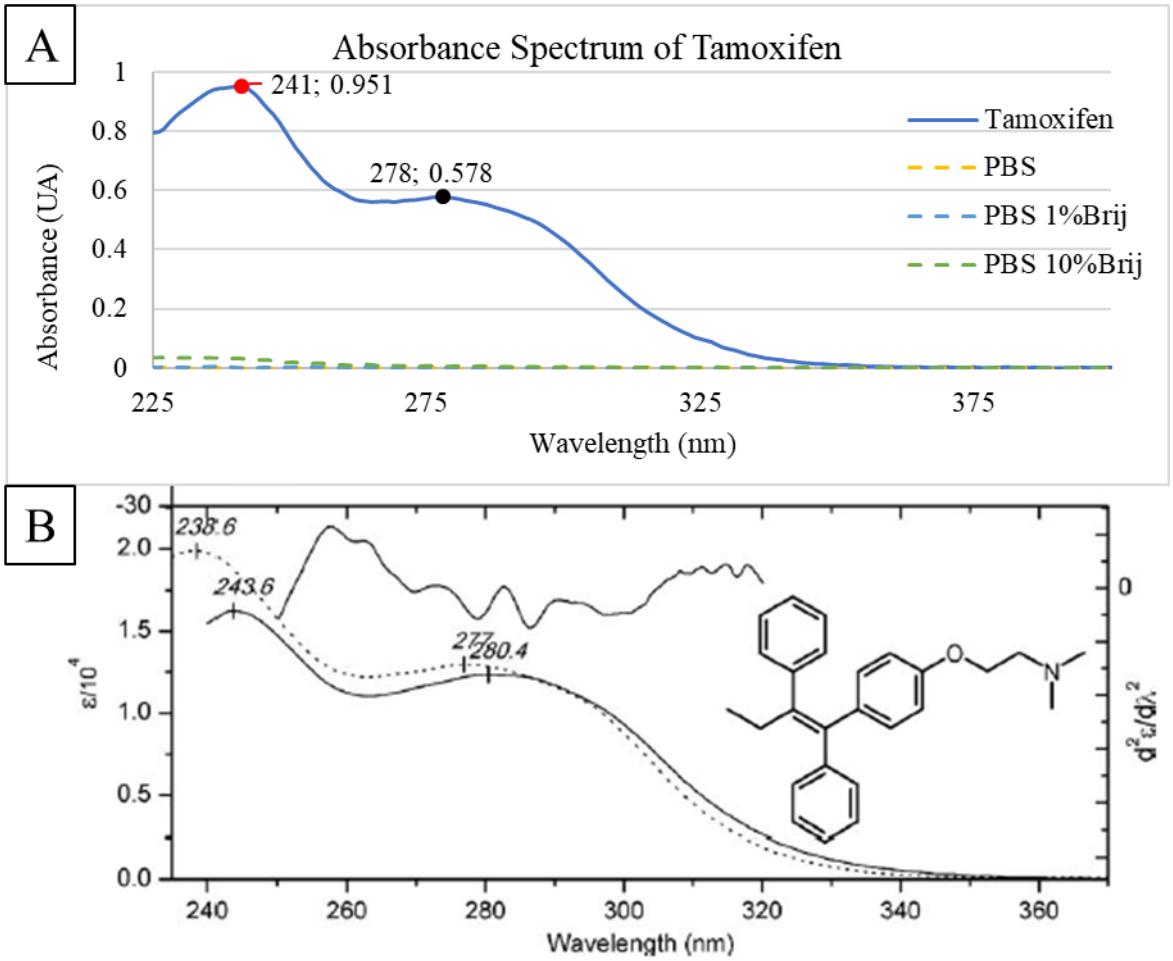

Figure 7.1 – (A) Comparison of the absorbance spectra of tamoxifen (full line in blue), PBS (yellow dashed line), PBS with 1 % of Brij-58® (blue dashed line) and PBS with 10 % of Brij-58® (green dashed line). The highest absorbance peak of tamoxifen was at λ=278 nm, with an absorbance value of 0.578 (concentration of tamoxifen was 0.2 mg/mL); (B) Absorbance spectra of tamoxifen citrate in ethanol (dashed line, λ=277 nm) and with cAGP (chicken α1-acid glycoprotein, full line, λ=280.4 nm) in buffer solution (pH 7.4 sodium phosphate buffer at 25°C[110]). Given that the absorption of tamoxifen is similar in both the spectra here represented (A and B), and in ref.[5] where it is referred that the absorbance of tamoxifen was at λ=277 nm), it is possible to say that the conditions have been gathered to safely perform diffusion studies with this model drug.

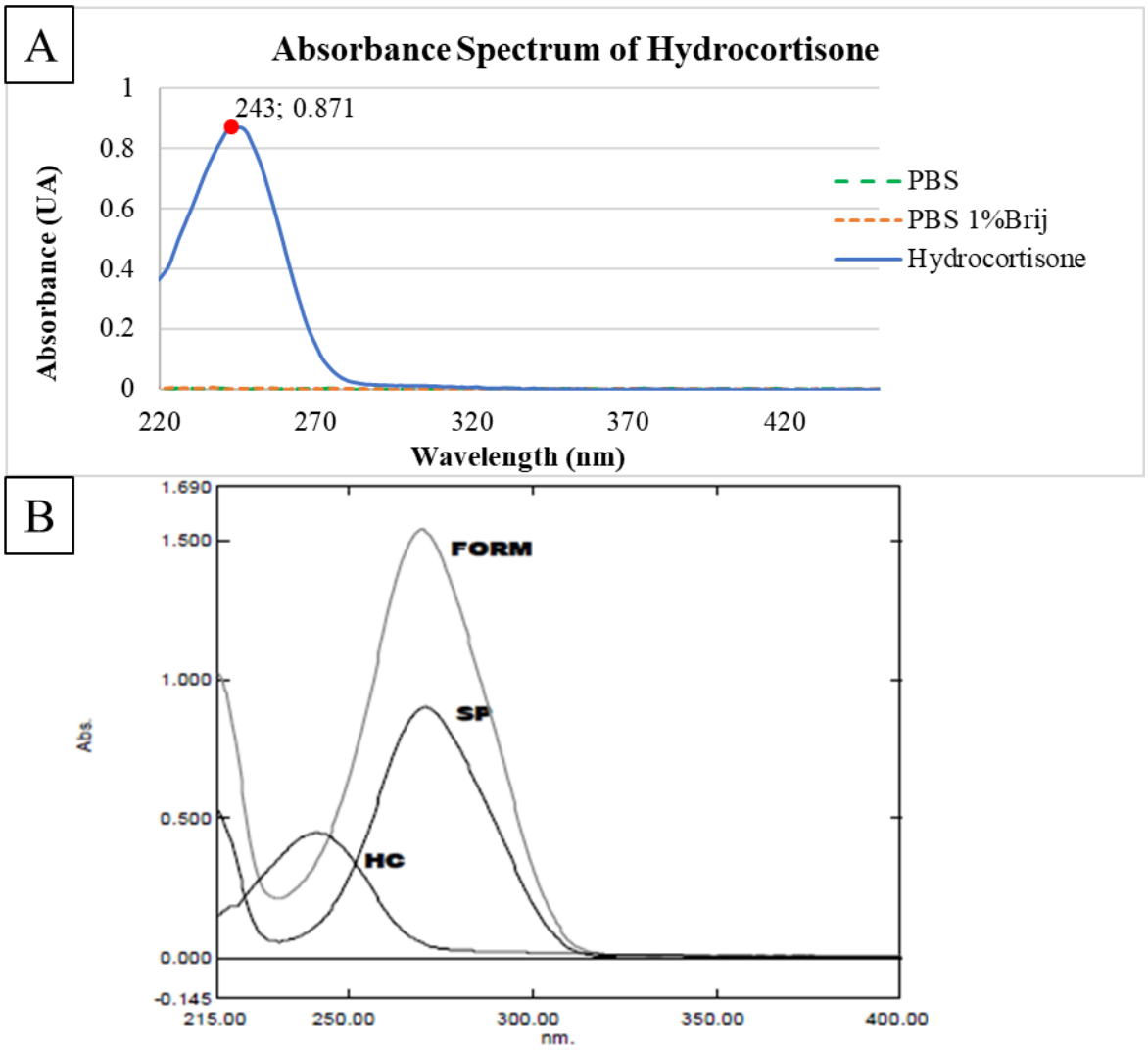

Figure 7.2 – (A) Comparison of the absorbance spectra of hydrocortisone (full line in blue), PBS (green dashed line) and PBS with 1 % of Brij-58® (orange dashed line). The highest absorbance peak of hydrocortisone was at λ=243 nm, with an absorbance value of 0.871 (concentration of hydrocortisone was 0.22 mg/mL); (B) Absorbance spectra of hydrocortisone acetate (HC) in ethanol at λ=241.5 nm (other substances measured were sulphacetamide sodium (SP) and a combination of both SP and HC (Form)[111]). Given that the absorption of hydrocortisone is similar in both the spectra here represented (A and B), and in ref.[5] where it is referred that the absorbance of hydrocortisone was at λ=242 nm, it is possible to say that the conditions have been gathered to safely perform diffusion studies with this model drug.

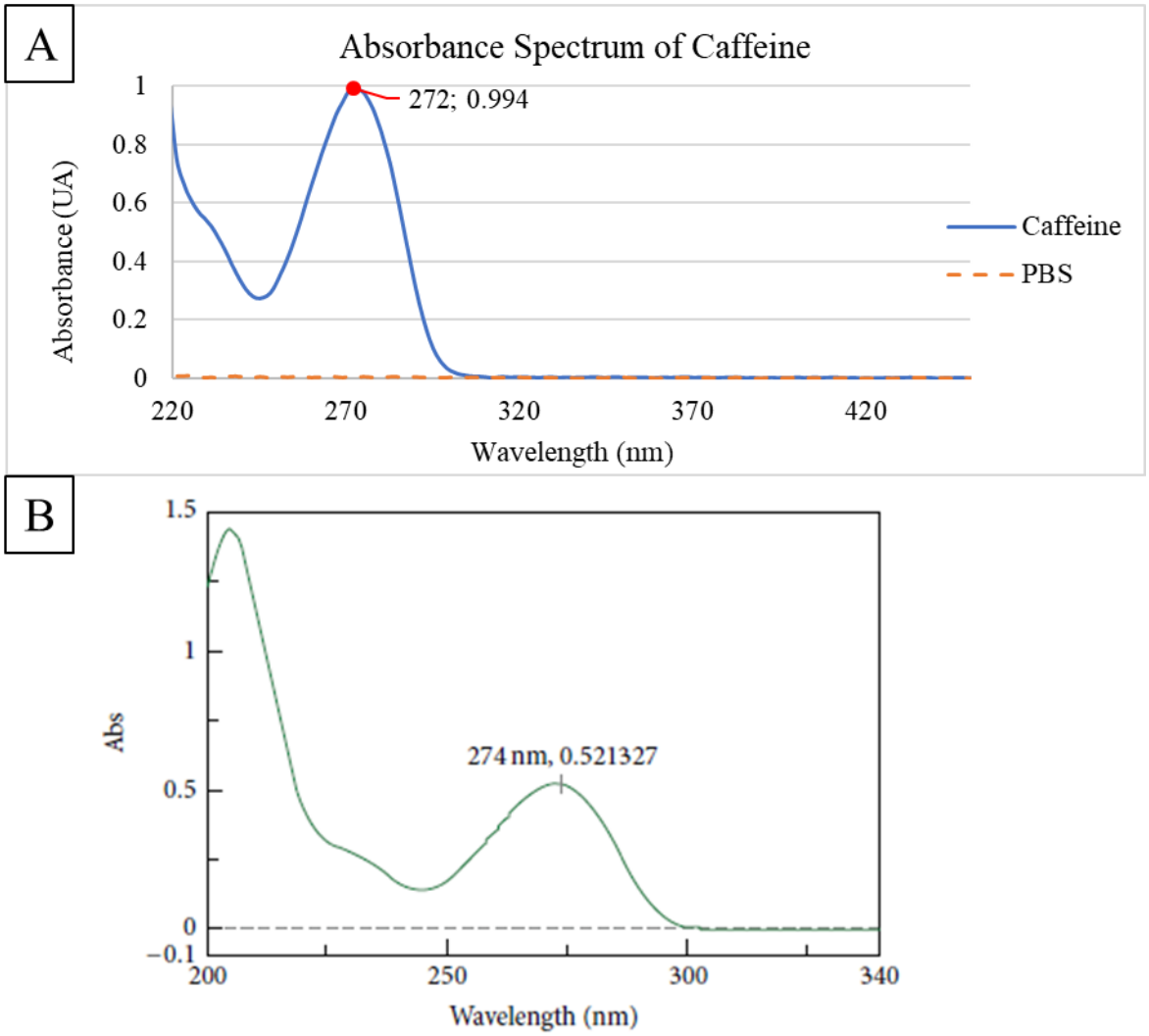

Figure 7.3 – (A) Comparison of the absorbance spectra of caffeine (full line in blue) and PBS (orange dashed line). The highest absorbance peak of caffeine was at λ=272 nm, with an absorbance value of 0.994 (concentration of caffeine was 0.20475 mg/mL); (B) Absorbance spectra of caffeine in distilled water (λ=274 nm)[112]. Given that the absorption of caffeine is similar in both the spectra here represented (A and B), and in ref.[5] where it is referred that the absorbance of caffeine was at λ=270 nm, it is possible to say that the conditions have been gathered to safely perform diffusion studies with this model drug.

APPENDIX C – Metabolomic Analysis

Table 7.4 – Keratinocyte (3rd Passage) growth over time during culture in monolayer (n=3, average ± SD).

Days	Number of live cells (10^4 cells/cm^2)
0	0.25 ± 0.00
1	0.28 ± 0.14
2	0.33 ± 0.17
2.5	0.43 ± 0.19
3	0.79 ± 0.28
3.5	0.97 ± 0.22
4	1.66 ± 0.32

Table 7.5 – Epidermis (4th Passage) thickness over time during culture in air-liquid interface (n=20, average ± SD).

Days	Skin thickness (µm)
0	6.04 ± 3.16
1	12.66 ± 4.85
2	17.19 ± 4.15
3	14.66 ± 4.23
4	20.63 ± 3.26
5	68.67 ± 4.47
6	49.21 ± 8.17
7	53.54 ± 3.63
8	61.52 ± 5.32
9	37.07 ± 8.31
10	86.09 ± 5.25
10.5	80.05 ± 7.85
11	71.64 ± 3.43

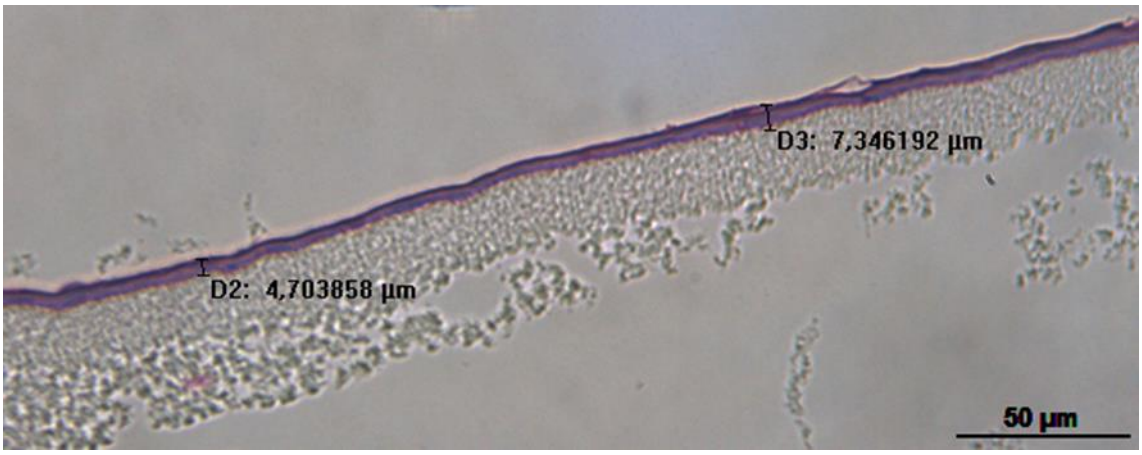

Figure 7.4 – 4th passage RHE at 0 days at air-liquid interface. Magnification 400x.

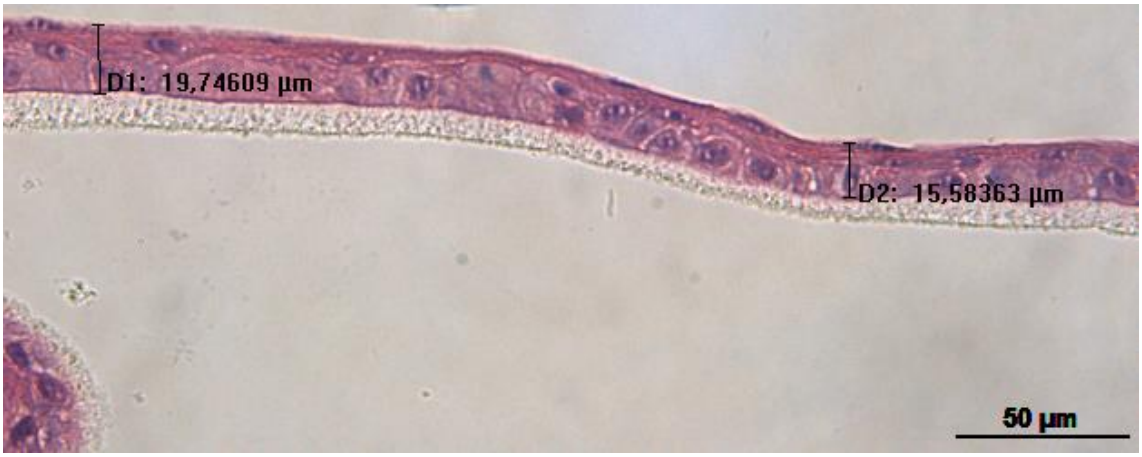

Figure 7.5 – 4th passage RHE at 1 day at air-liquid interface. Magnification 400x.

Figure 7.6 – 4th passage RHE at 2 days at air-liquid interface. Magnification 400x.

Figure 7.7 – 4th passage RHE at 3 days at air-liquid interface. Magnification 400x.

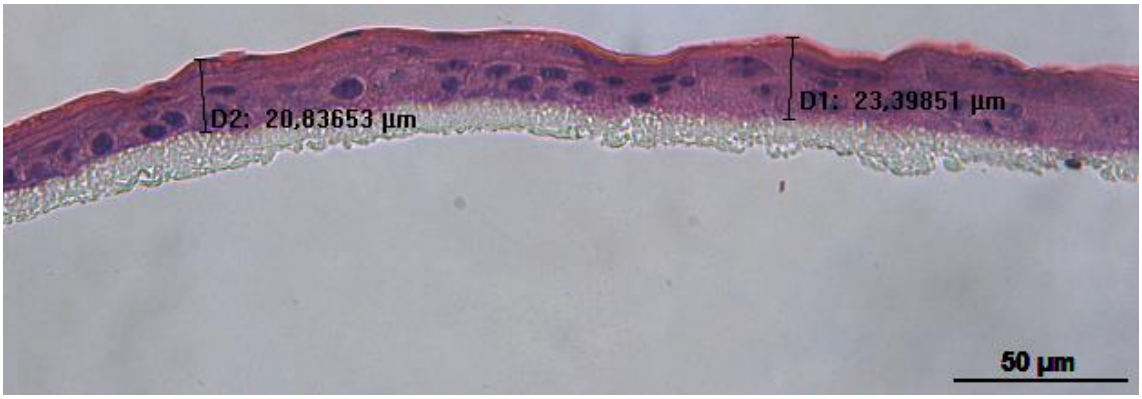

Figure 7.8 – 4th passage RHE at 4 days at air-liquid interface. Magnification 400x.

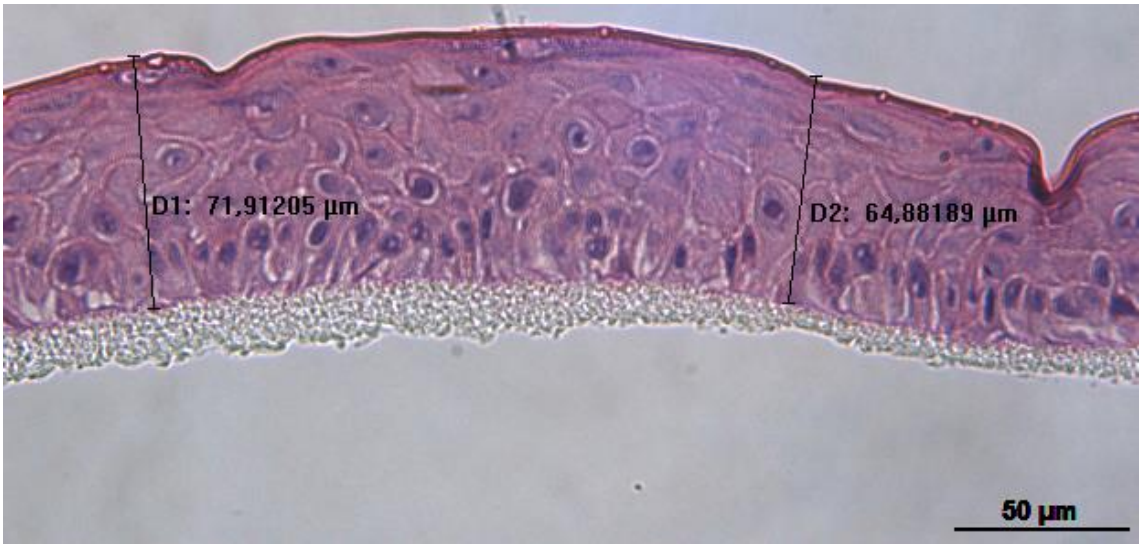

Figure 7.9 – 4th passage RHE at 5 days at air-liquid interface. Magnification 400x.

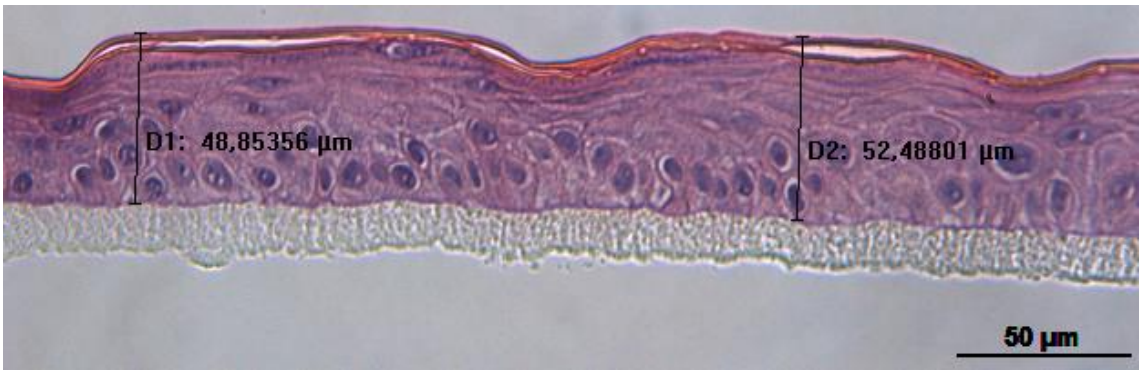

Figure 7.10 – 4th passage RHE at 6 days at air-liquid interface. Magnification 400x.

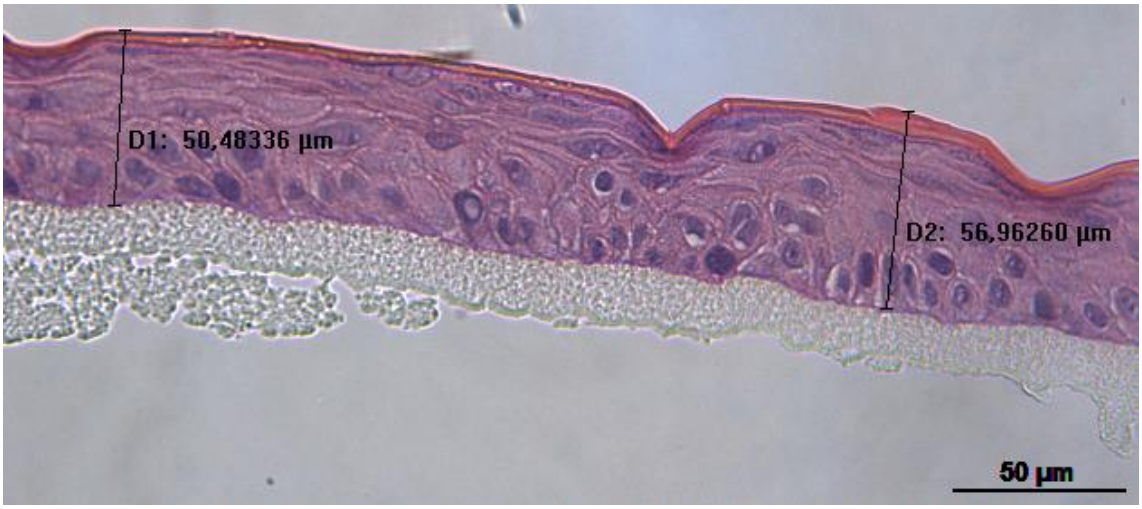

Figure 7.11 – 4th passage RHE at 7 days at air-liquid interface. Magnification 400x.

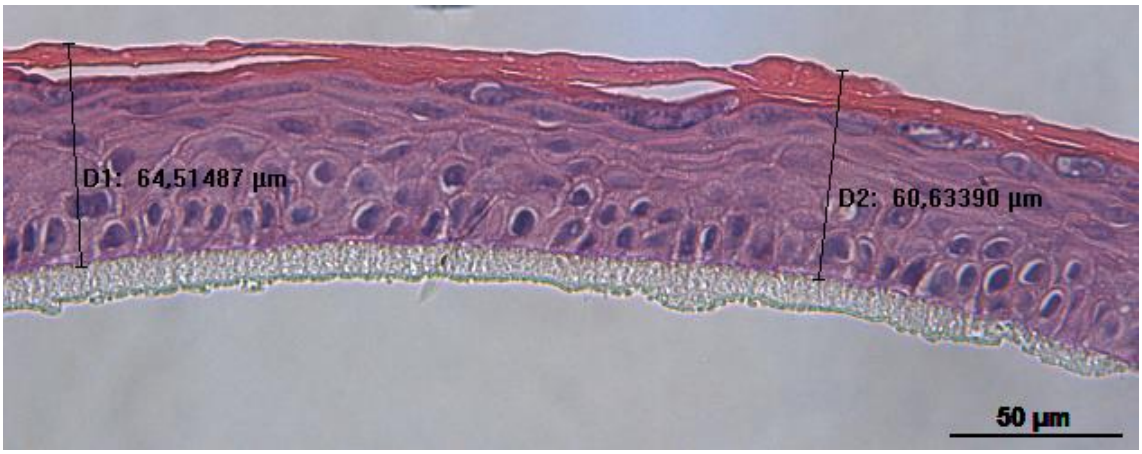

Figure 7.12 – 4th passage RHE at 8 days at air-liquid interface. Magnification 400x.

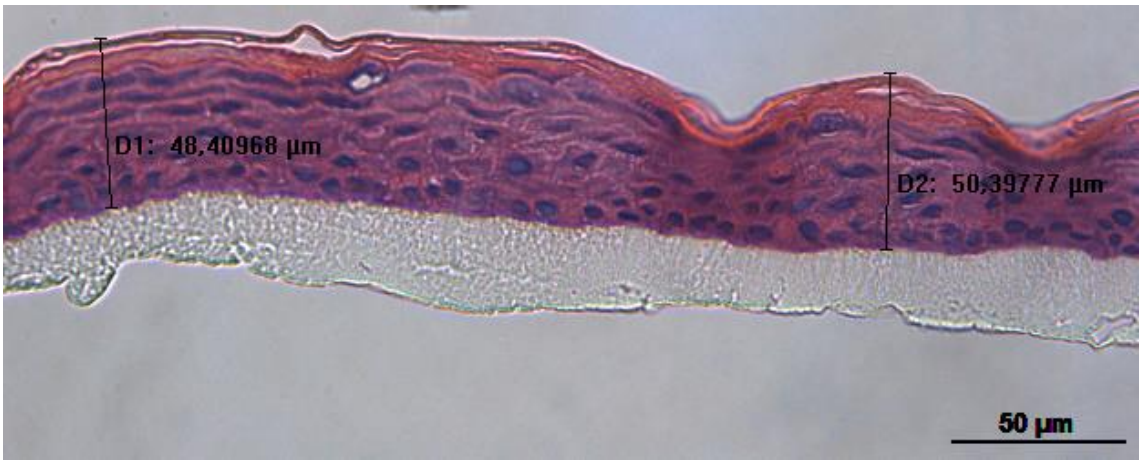

Figure 7.13 – 4th passage RHE at 9 days at air-liquid interface. Magnification 400x.

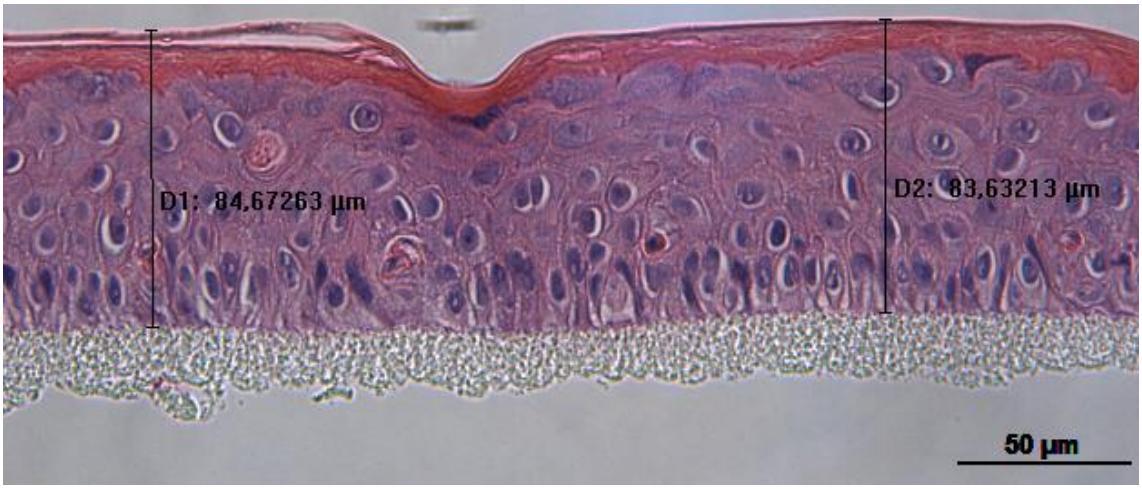

Figure 7.14 – 4th passage RHE at 10 days at air-liquid interface. Magnification 400x.

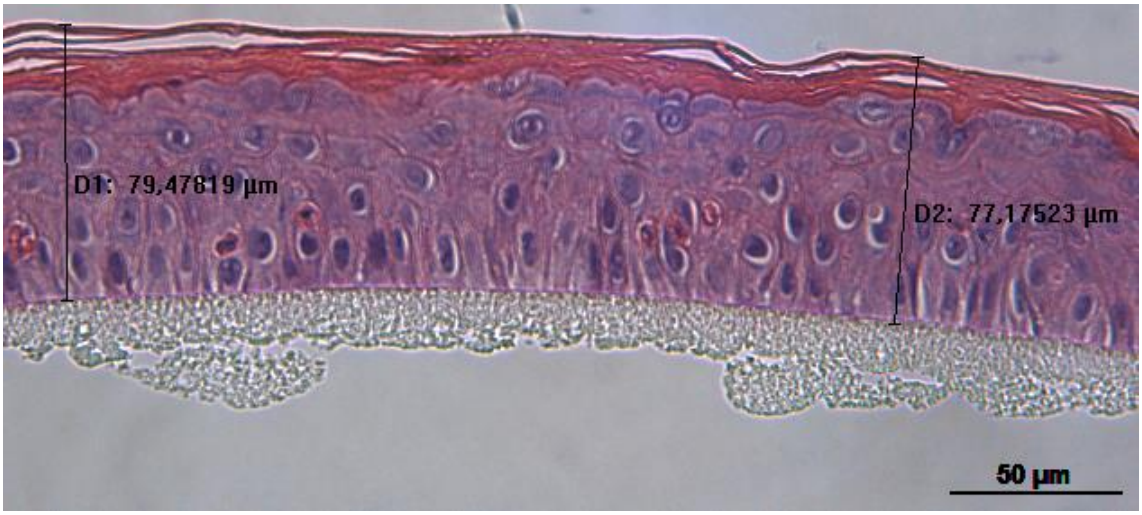

Figure 7.15 – 4th passage RHE at 10.5 days at air-liquid interface. Magnification 400x.

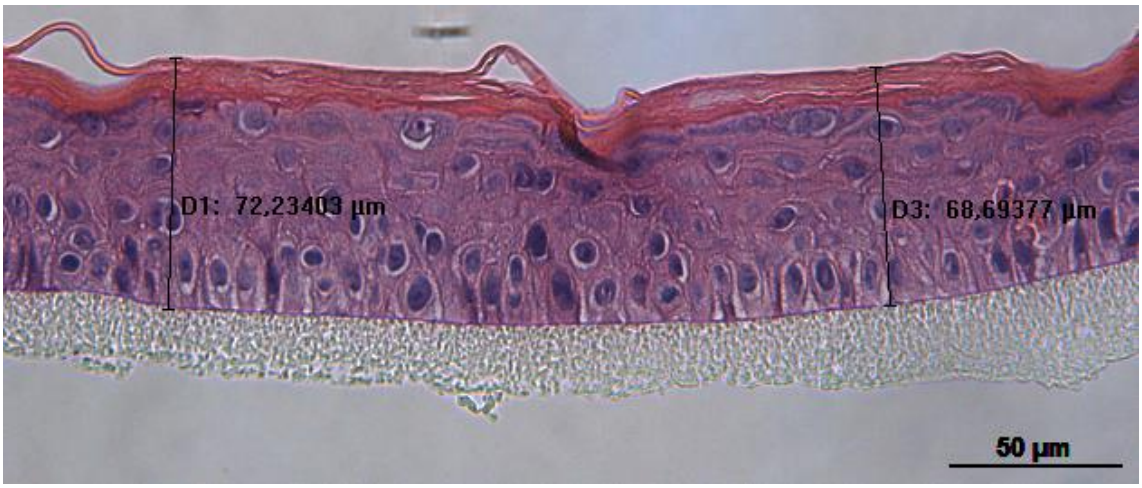

Figure 7.16 – 4th passage RHE at 11 days at air-liquid interface. Magnification 400x.